

Flexibility in heat demand at the TU Delft campus smart thermal grid with phase change materials

Master of Science Thesis E.H.A. van Vliet

Date: February 14th 2013

Process & Energy Department
Mechanical, Maritime and Materials Engineering
Delft University of Technology

Committee members:

Delft University of Technology:

Prof.dr.ir. B.J. Boersma

Dr.ir. M.J.B.M. Pourquoi

Dr.ir. W.P. Breugem

Deerns:

Ir. A.J. Nagtegaal

Abstract

Plans have been made to change the current district heating grid at the TU Delft to a smart thermal grid. New heat suppliers will be connected to the grid including a geothermal well and waste heat from the Schie area. The heating grid will change from a demand driven grid to a combination of demand and supply driven heating grid. Demand side flexibility will improve the potential for a smart thermal grid as more favourable heat production units can be used on the TU Delft grid. This project focuses on the potential for phase change materials to increase the thermal buffer capacity. A building simulation model (the 'Low Energy Architecture' model developed by Deerns) is used to model three buildings connected to the TU Delft district heating grid. A module for phase change material has been developed and two configurations for the passive use of phase change materials (PCM) are simulated with the LEA model. The PCM used as suspended ceiling tiles and as PCM fins both show a very small potential for phase change materials. The heat transfer to the PCM is too small to show significant diurnal heat storage in the phase change materials due to the low heat transfer coefficient and the small temperature difference between the air in the building and the phase change material.

Nomenclature

Variable	Unit	Description
A	m^2	Area
Bi	-	Biot number
C_p	J/kg	Specific heat at constant pressure
c_f	-	Convection factor, part of heat transferred via convection
D_h	m	Hydraulic diameter
g	m/s^2	Gravitational constant
F	-	View factor
Fo	-	Fourier Number
h	J/kg	Enthalpy
h	rad	Height of the sun
h_{PCM}	m	Height of PCM fin
h	$W/m^2 K$	Heat transfer coefficient
g	m/s^2	Gravitational constant
k	$W/m K$	Thermal conductivity
L	m	Length
m	kg	Mass
Nu	-	Nusselt number
Pr	-	Prandtl number
Q	Wh, J	Thermal energy, heat
Q̇	W	Heat transfer
q̇	W/m^2	Heat transfer
R_c	$m^2 K/W$	Total conductive heat transfer resistance of wall
Ra	-	Rayleigh number
Re	-	Reynolds number
SGF	-	Solar gain factor (Dutch: ZTA) the ratio of the entering solar radiation to the total solar radiation
T	$°C, K$	Temperature
t	s	Time
U	$W/m^2 K$	Overall heat transfer coefficient
U	m/s	Velocity
U_∞	m/s	Wind speed uninfluenced by building
V	m^3	Volume
w_{PCM}	m	Width between PCM
x	m	Length
x	$g/kg_{dry air}$	Absolute humidity of air
α	m^2/s	Thermal diffusivity
β	-	Liquid fraction
β	T^{-1}	Thermal expansion coefficient
γ_w	-	Window fraction
ε	-	Emissivity
η	-	Efficiency
η	-	Dimensionless spatial coordinate
θ	-	Dimensionless temperature
λ	J/kg	Latent heat
λ	-	Eigenvalue

Variable	Unit	Description
μ	kg/ms	Dynamic viscosity
ν	m^2/s	Kinematic viscosity
ρ	kg/m^3	Density
ρ_{env}	-	Reflectivity of the surrounding environment
σ	W/m^2K^4	Stefan-Boltzmann constant ($5.67e - 8 W/m^2K^4$)
Ψ	-	Prandtl number relation

Subscript	
<i>a</i>	Air
<i>AHU</i>	Air handling unit
<i>bot</i>	Bottom (floor façade)
<i>c</i>	Convective
<i>ceil</i>	Ceiling
<i>conc</i>	Concrete
<i>d</i>	Demand
<i>dif</i>	Diffuse
<i>dir</i>	Direct
<i>env</i>	Environment
<i>f</i>	Fluid
<i>fac</i>	Façade
<i>fl</i>	Internal floors in building
<i>hr</i>	Heat recovery
<i>in</i>	In the building
<i>inf</i>	Infiltration
<i>inst</i>	Installations

Subscript	
<i>int</i>	Internal
<i>ld</i>	Local demand
<i>m</i>	Mush
<i>max</i>	Maximum
<i>mech</i>	Mechanical
<i>min</i>	Minimum
<i>nat</i>	Natural
<i>out</i>	Outside
<i>PCM</i>	Phase change materials
<i>r</i>	Radiative
<i>refl</i>	Reflective
<i>s</i>	Solid
<i>sup</i>	Supply
<i>tr</i>	Transition
<i>v</i>	Ventilation
<i>win</i>	Window

Contents

Abstract.....	1
Nomenclature	3
1. Introduction	7
1.1. Energy use in the built environment.....	7
1.2. The TU Delft campus heating grid.....	7
1.3. The project	8
2. Heat demand reduction options.....	11
2.1. Heat demand.....	11
2.1. Influencing the total heat demand	12
2.2. Heat demand flexibility.....	13
2.3. Other heat demand lowering measures	17
2.4. Cold demand reduction options	17
2.5. Overview of the heat demand reduction options	18
3. The LEA model	19
3.1. Building heat balance.....	19
3.2. Heat production from people, installations and lighting.....	21
3.3. Solar radiation.....	21
3.4. Heat transfer to the environment	23
3.5. Floor heat balance	26
3.6. Ventilation.....	38
3.7. Review on the model	40
3.8. Changes to the LEA model	40
4. PCM module.....	43
4.1. Phase change materials use.....	43
4.2. PCM modelling approach / method.....	44
4.3. PCM model.....	45
4.4. Choice of PCM and PCM characteristics	49
4.5. Configuration of PCM modules.....	51
5. Simulation of TU Delft buildings with the LEA model.....	55
5.1. Buildings	55
5.2. Simulations and results.....	57
5.3. Increasing the convective heat transfer coefficient	69
5.4. Thin PCM	74

6. Conclusions	75
7. Discussion and recommendations	77
8. References	79
9. Appendix	81
9.1. Building data	81

1. Introduction

1.1. Energy use in the built environment

Energy used in the built environment accounts for 35% of the primary energy use in the Netherlands [3]. In the built environment energy is used for heating, cooling and electricity. A large potential for energy saving in the built environment is available via the reduction of heat demand.

As a result of the growth of renewable electricity suppliers at the electricity grid the smart electricity grids are developed, because the dynamics and flexibility of these new electricity suppliers differ from the gas-fired, coal-fired and nuclear power plants. In the field of heat supply via district heat grids similar developments are started. Heat supply units with different characteristics are used or will be used in the near future like seasonal heat and cold storage, usage of waste heat, solar thermal boilers and geothermal heat. When these new suppliers are connected to the grid together with traditional sources, like gas-fired boilers and combined heat and power units, the dynamics of the district heating systems will change. A simple demand driven approach for the district heating grid will no longer suffice.

1.2. The TU Delft campus heating grid

1.2.1. Current heating grid at TU campus

The district heating grid at the TU Delft campus covers the majority of the heat demand at the TU Delft campus. The culture centre and some of the student housing are not connected and the buildings 3mE (Faculty of Mechanical, Maritime and Materials Engineering), EWI (Faculty Electrical Engineering, Mathematics and Computer Science) and the university library are partially heated (and cooled) by aquifer thermal energy storage. The buildings using the district heating system are connected to one or two of the total of four different tracks of the district heating grid. An overview of the TU Delft district heating grid is given in Figure 1.1.

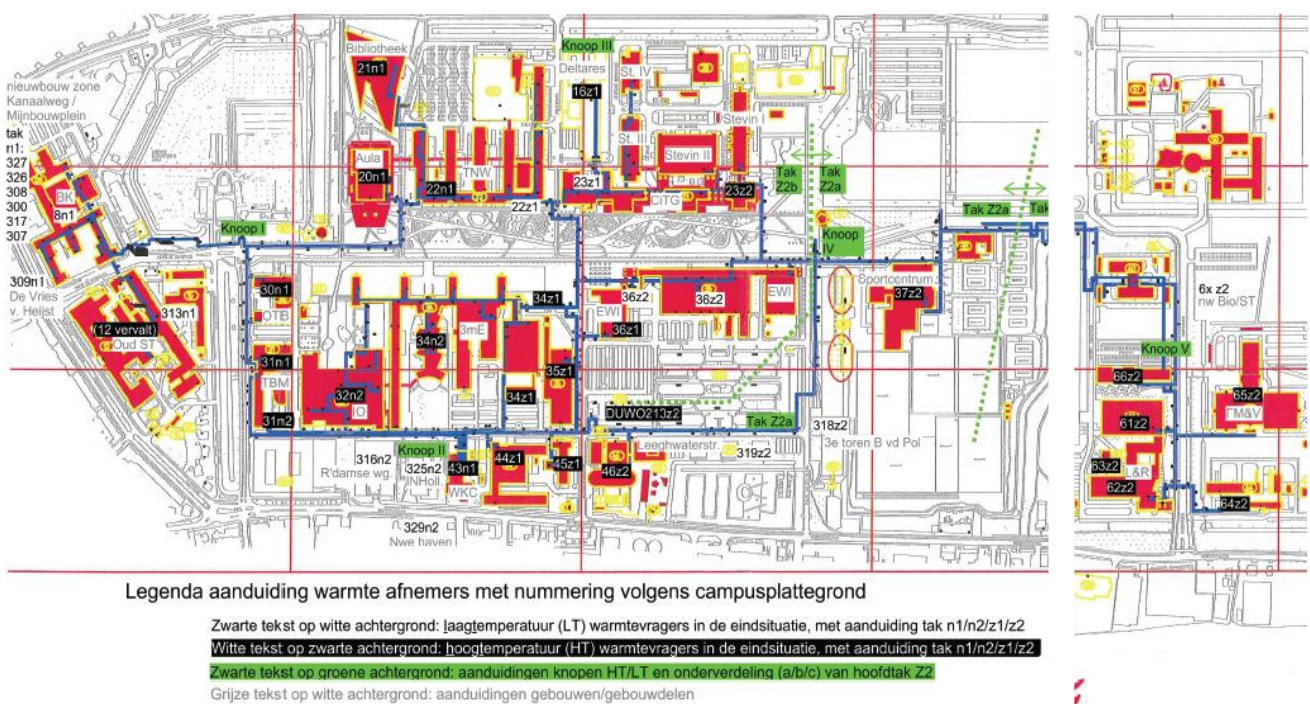


Figure 1.1 District heating grid at the TU Delft campus connecting the combined heat and power plant to the TU Delft buildings

The heat is supplied to the heating grid by two 1.85 MW_{th} (and 1.85 MW_e) gas engines and 3 gas boilers (15, 30 and 35 MW_{th}) for peak demand. The gas engines also produce a large part of the electricity used at the university. The electricity produced by the gas engines is less expensive for the university and therefore the gas engines are preferred over the gas boilers for heat production.

1.2.2. IPIN project, the smart thermal grid at the TU Delft Campus

The IPIN ('Innovatieprogramma Intelligente Netten') project is initiated and aims to change the TU Delft district heating system to a smart thermal grid. The goals of the project are to supply the smart thermal grid with heat from renewable sources, to create a more efficient heating system and to start the transition from a high temperature (130 – 80°C) to a low temperature district heating grid (70 – 40°C).

The IPIN project is a pilot project to show the possibilities for smart thermal grids. The IPIN project is subsidized by the Dutch government (via Agentschap NL) and is executed by 5 companies / institutions: Imtech, Deerns, Deltares, Priva and the Delft University of Technology (TU Delft). The TU Delft is the operator, owner and client for the heating grid. Through this combination the heating grid can be approached from a point in which the main interests are all with the same party

Within the IPIN project several new heat sources are studied for its applicability at the TU Delft heating grid. The options covered include a geothermal well and waste heat from the industry near the Schie. While in the current situation the heating grid is completely demand driven, the result of the IPIN project will be a heating grid controlled by a smart control system taking both the demand and supply side into consideration.

1.3. The project

In this research project the demand side of the smart thermal grid will be approached. The goal of the project will be to study opportunities to adapt the heat demand in the smart thermal grid to the heat supply. The benefit of the heat demand measures will be found by using the most favourable (renewable) sources maximally and operating the district heating grid with a minimum of installed heating capacity.

Maximizing the use of the most favourable sources via demand side measures will mean that an ideal situation will have constant heat demand throughout the day. The reduction of the installed capacity via demand side measures will mean that a reduction of the peak heat demand is the main goal. The most important goals are:

- Reduction of peak heat demand
- More constant heat demand

In this project the heat demand for several buildings at the TU Delft campus will be simulated with the 'Low Energy Architecture' (LEA) model. The LEA model is a model developed for the calculation of heat and cold demand by Deerns and is described in chapter 3. Some options for the reduction of peak heat demand and a more constant heat demand will be described. The reduction measures considered to reach the goals as stated above are the use of phase change materials and the application of different heating strategies.

“Can (the combination of) Phase Change Materials and heating strategies lower the peak heat demand and create a more flexible heat demand within the future smart thermal grid?”

1.3.1. Application for in other district heating grids

Via a smart thermal grid more sustainable resources could be used and the total heat supply can be more efficient. Opportunities for smart thermal grids are particularly interesting when a single organization is in control of (the major part of) the heat users. In the Netherlands most of the Universities have a campus with multiple buildings connected to a single grid and could thus benefit from a smart thermal grid. About 350 universities exist throughout Europe of which, many of these universities have a district heating system on which this project could be applied. Other interesting locations could be industrial areas where a single company operates multiple buildings, for examples the Schiphol airport area.

2. Heat demand reduction options

Chapter 2 covers the heat demand for buildings and the possibilities to lower the peak and the total heat demand.

2.1. Heat demand

The heat demand of a building is determined by building properties, the use of a building, the control characteristics and the weather.

The building properties determine the heat loss to the environment through the outer shell, the solar heating through windows and the type of heating used in the buildings. Another important building property is the thermal inertia of the building which determines how fast a building can be heated or cooled.

The use of the building determines the occupancy of persons in the building spread over the day and night. The presence of people in the building determines whether or not the rooms must be kept at comfort levels. The presence of people also results in heat production by the persons present, by lighting and by running installations in the buildings like computers, et cetera.

The main goal of the control system of the heating, ventilation and air conditioning (HVAC) system of the building is to keep climate in the rooms comfortable. This is done by controlling the keeping the temperature and humidity levels within a set range and supplying fresh air to the rooms. The control system can adjust the slope of heating before the first people arrive at the building to obtain the set goals more easily. The control settings of the heating system are chosen based on the building properties like the thermal inertia of the building and the thermal insulation of the building.

The weather conditions have a large impact on the heat and cold demand of the building. The outside temperature determines the heat loss to the environment or the heat gain from the environment. The solar radiation supplies extra heat to the building lowering the heat demand and increasing the cold demand.

The total heat demand of a building is

$$Q_{demand} = Q_{leak} - Q_{production} \quad (2.1)$$

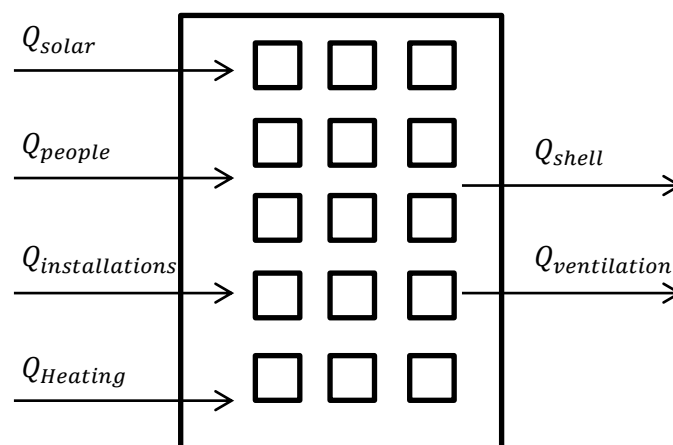


Figure 2.1 Schematic of basic heat balance in building

In which the leaking heat is determined by the heat leaking through the outer shell of the building and the heat lost via the air ventilation system. The heat production is equal to the heat produced by presence of people, the heat produced by the installations in the building (lighting, computers, etc.) and the heat from solar radiation.

2.1.1. Objectives

As stated in the introduction the objective is to reduce the peak heat demand and to create a more constant heat demand, while the total heat demand will decrease or only increase slightly. In this chapter the reduction options for both objectives are listed and briefly explained. The working principle of these options will be described and their potential to achieve the objectives. Some of the options will benefit to one objective and will negatively influence the other objective; the developed model will be able to quantify these contributions to the objectives.

2.1. Influencing the total heat demand

2.1.1. Increase of building insulation

The amount of heat that has to be supplied to the building is equal to the amount of heat lost through the bounds of the building minus the heat produced within the building by persons and installations and the solar heat. The total heat demand could thus be reduced by reducing the heat lost to the environment. The potential for extra insulation is thus determined by the current leaking of heat from the building which is largely determined by the current insulation. New buildings have a higher level of insulation compared to old buildings and will benefit less from extra insulation. The insulation of old buildings however could be improved up to a level comparable to newly built buildings.

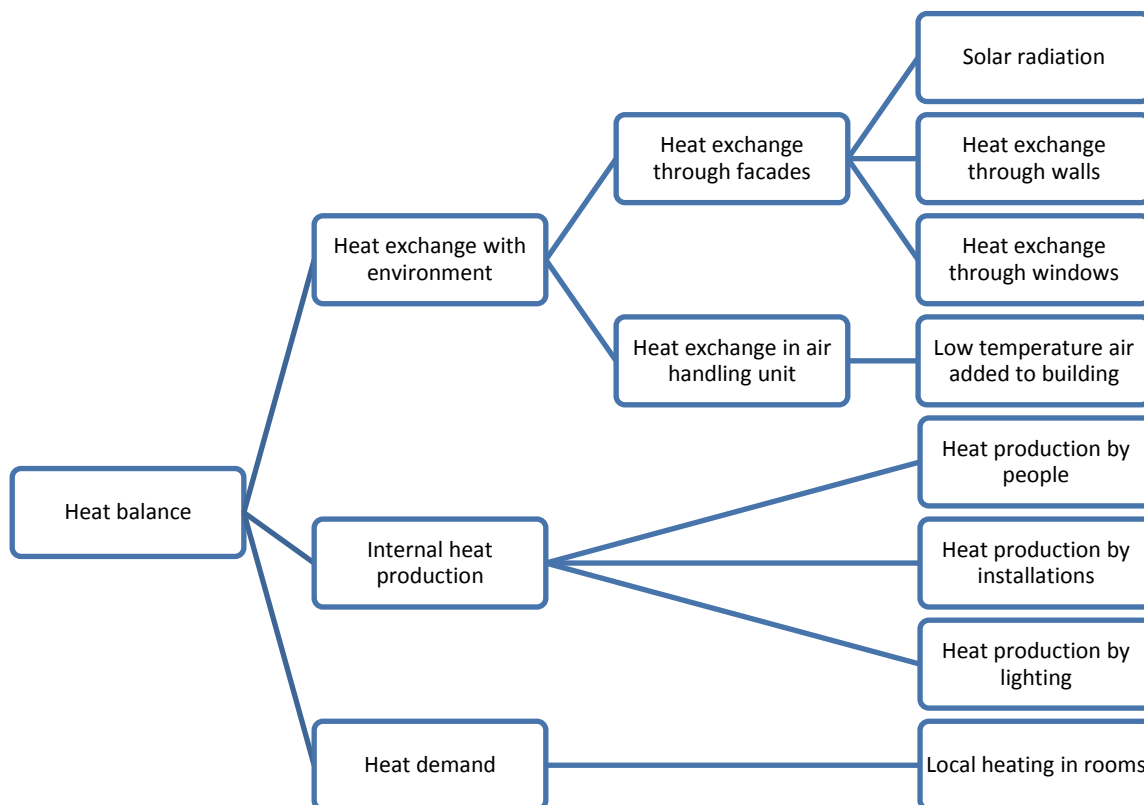


Figure 2.2 Overview of heat balance for buildings

Insulation can be increased on all parts of the shell: window insulation, wall insulation, floor insulation and roof insulation. Usually the largest portion of heat is lost via the windows, this loss can be reduced by HR, HR+ or HR++ glass. The heat transfer through the walls can be reduced via different measures depending on the current wall. Possibilities are insulation on the inside of the wall, insulation on the outside of the wall or insulation inside a cavity wall. Floor insulation is particularly interesting for buildings with an open parking area below the building, for buildings with regular basements or closed parking areas the floor insulation has a smaller impact. Roof insulation is possible in two generic ways, by placing regular insulation on top of the roof and by using a 'green roof' which also buffers water drainage and filters dust from the air.

During cold periods the extra insulation reduces the heating demand. During hot days when the outside temperature is higher than the inside temperature, the extra insulation will decrease the cold demand. At intermediate temperatures the increased insulation could cause the produced heat to become larger than the leaked heat and as a result a change from heat demand to cold demand will occur.

The effects of increased insulation for the flexibility of heat demand are moderate. The heat lost to the environment is decreased so the morning peaks will also be lowered. The total heat demand profile will be lowered, but the effect on the cold demand is uncertain. The reduction of heat demand that can be obtained and the price that has to be paid is very much dependent on the properties of the building. The effect on the peak heat demand is limited and a side effect of the total heat demand reduction. The increased insulation is not considered in this study as such, however since several buildings are simulated with the model, the effect of different levels of insulation can be indicated in the result.

2.1.2. Low temperature heating system

Most new offices are equipped with a low temperature heating systems. The low temperature heating systems operate at 55 – 30 °C. Low temperature heating has only small effects on the total heat demand, but offers a range of possible installations and equipment unavailable for high temperature heating system. These include the use concrete core activation, floor heating and heat pumps in combination thermal energy storage.

2.2. Heat demand flexibility

As indicated in Figure 2.3 the heat demand varies during the day and over the week with peak values in the morning and a low heat demand during the night. The heat demand of the buildings is lower during the night and during the weekends when the buildings are not used by people, but in the morning the buildings are reheated back to a comfortable temperature. During opening hours extra heat is produced by lighting, appliances and people and extra heat is lost to the environment via ventilation. As a result the heat production differs during the day, with a peak heat demand when the building opening hours start. The total heat production will be less efficient because during peak periods the heat production will be delivered by less favourable production units and ramping up and down of the gas engines or gas boilers decrease its efficiency.

Regulations prescribe the installed capacity has to be high enough to cover the peak demand for a cold day even when the largest production unit will be out of service, the n-1 rule. If the peak

demand could thus be reduced by spreading the heat demand equally over the day, the installed capacity could also be smaller.

In this subchapter measures to reduce the peak demand will be introduced. Some of the peak demand reduction measures will lead to an increase in the total demand. The ratio between the two parameters will differ with the building characteristics and will be calculated with the model.

2.2.1. Night heating (heat strategy)

The peak heat demand is reached in the morning; this peak is reached only a few hours after the heat demand trough during the night. During the night the set point for the temperature is lowered a few degrees Celsius to decrease the total heat demand. As a result the heat demand drops for the building and in a network configuration this will happen for most of the buildings at the same time. If the night heating inside the buildings would be increased the peak during the morning would be flattened.

A few options are possible to increase the night heat demand and decrease the morning peak demand:

- Increase the night temperature set point with a few degrees Celsius.
- Increase the night temperature up to the day temperature to flatten the heat demand during the day. The resulting heat demand profile will show a higher heat demand during the night than during the day because of colder ambient temperature and smaller internal heat production
- Use base load heat demand during the night. Decrease the depth of the trough by a constant heat demand during the night, as a result the morning heat demand peak will be lowered. The size of the constant heat demand can be chosen such that the favourable source is completely used. Another option is to size the night heat demand based on predictions for the morning heat demand in such a way that the morning peak is completely removed. The second option will require an intelligent control system.

2.2.2. Successive heating of buildings during nights

In the TU Delft campus heating grid the building level control systems all run without any communication with any of the other buildings. Most of the buildings demand heat at the same time in the morning, by which the peak heat demand for the CHP plant is increased. If the heat demand of some of the buildings could be shifted in time the campus peak demand could be lowered.

To calculate the results of successive heating of the different buildings a grid level simulation should be performed. The LEA model however is not equipped to model and simulate different buildings with individual heating characteristics. However if simulations for different buildings are performed with different heating periods during the night, the results could be added up to indicate results for peak heat demand and total heat demand.

2.2.3. Phase change materials

When the temperature in the building is higher than the minimum temperature in the building heat is accumulated in the buildings thermal mass. A temperature profile for a building during one week is given in Figure 2.3, which show the possibilities to store heat during a period marked with “A” to reduce heat demand during a period marked with “B”. Part of the heat is stored in the buildings own

thermal mass, the building materials and objects in the building. By increasing the thermal mass of the building at the minimum temperature during the opening hours the total heat demand can be lowered. Also the temperature fluctuations in the building are mitigated and the building will cool down less during the night, which spreads the heat demand more equally over the day.

Phase change materials use the latent heat of a phase change of a material to store heat. The advantage of latent heat compared to sensible heat is the large thermal capacity at a small temperature range. PCMs can save a substantial amount of energy used for heating and cooling applications when heating is necessary during in the morning and cooling in the afternoon. The PCMs can be passively used when the ambient night temperature is below the temperature set point. The use of PCMs will have an impact on the total energy used for heating applications and the on the peak heat demand. [4, 5].

2.2.3.1. PCMs in vessels

Phase change materials can be installed either as a buffer vessel supplying heat and cold when demanded or as part of the building envelope. When the PCMs are used in a buffer vessel the heat or cold demand can be shifted from the peak demand. The heat and cold can be supplied during low demand moments and when favourable sources are available. PCMs in a buffer vessel are basically a small heat and cold storage with a high thermal storage density. PCMs in vessels will not be studied as such, but long term thermal energy storage is considered in the form of Aquifer Thermal Energy Storage systems (see chapter 0).

2.2.3.2. PCMs as part of the building envelope

PCMs as part of the building envelope aim to increase the building thermal mass. The PCMs can be integrated in the building walls, roofs and floors and will temper the climate in the rooms. In periods when daytime cooling is necessary the PCMs melt during the day while absorbing heat from the building. During the night the PCMs solidify and release heat (and thus demand cold) which will be used again next day (see Figure 2.4). This cold can be supplied off the (electricity) peak during the night reducing peak demand. Also the amount of energy

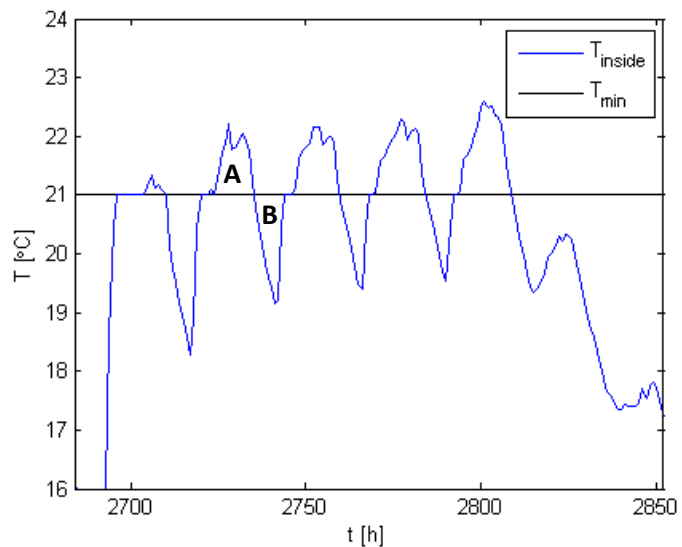


Figure 2.3 Potential for heat storage in phase change materials. When the temperature in the building exceeds the minimum temperature in the building for opening hours, heat can be stored to reduce heat demand for later.

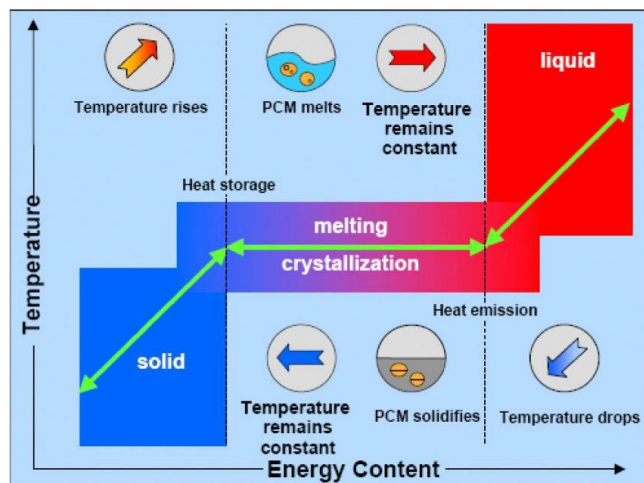


Figure 2.4 PCM working principle (<http://www.energyball.ch/pcm/wissenswertes>)

needed is lower since the ambient air has a lower temperature and thus needs less cooling before entering the building.

2.2.3.3. PCM in heating

PCMs are not heat demand reducing measure during the winter period for buildings since during the heating periods the PCMs don't change their phase. However the PCMs can have an impact on the peak heat demand. As the buildings thermal mass increases the internal temperature will show smaller fluctuations. As a result it will be easier to shave peak heat demand when PCMs are applied. The PCMs can reduce heat demand outside of the cold winter periods when during daytime the temperature in the building exceeds the minimum set temperature. This daytime heat can be stored and released during daytime when heat is demanded.

Thermal simulation by Heim [6] showed that a significant reduction of heat demand could be achieved in autumn by applying phase change materials for storing heat.

2.2.3.4. Choice of PCM

The choice of the PCM depends on its application and the operating temperature range. For all applications good PCMs have a large latent heat, a high heat transfer coefficient and a suitable transition range. Much research has been done on the properties of phase change materials [4].

For a PCM system in the building envelope a PCM has to be chosen with a melting temperature within the comfort temperature level.

2.2.4. Concrete core activation

Concrete core activation (CCA) uses the thermal mass to mitigate temperature fluctuations. During the construction phase a long tube is embedded in the concrete floors. This tube can be fed with warm water to heat the surrounding concrete or with cold water to cool the concrete depending up the demand. Similar to phase change materials (PCMs) the heat demand peaks can be shaved, but the total heat demand will remain constant. The total cooling demand however can be greatly reduced by using the night cold to activate the concrete core with low temperature coolant.

A large difference compared to PCM is that CCA is an active part of the heating and cooling system, while PCM, as described in the previous subchapter, can be used as a passive system. Concrete core activation demands low temperature heat and high temperature cold system.

Concrete core activation is an embedded tube in the concrete core which means that the tube has to be constructed during the building phase. CCA is thus only realistically applicable to new built buildings and thus not applicable to the current TU Delft buildings. The CCA will not be considered further in this project, though CCA could be interesting for lowering the peak heat demand for future buildings.



Figure 2.5 Concrete core activation system

2.2.5. Long term thermal energy storage

During the winter heat has to be supplied to the building, while during the summer heat has to be extracted from the building. If the extracted heat in the summer could be used to heat the building in the winter and vice versa a large amount of heat and cold use could be saved. Long term thermal energy storage should thus be able to buffer heat for half a year.

A common method for long term energy storage is via energy storage in the aquifers in the earth soil, which is called Aquifer Thermal Energy Storage (ATES). Aquifers are located between 20 and 300m below the ground. The ATES system uses a warm and cold aquifer to store extract heat in winter and store heat in summer. The aquifers need to be balanced over the year, if more heat than cold is extracted or the other way around, the ATES system loses its capacity. The heat or cold that can't be extracted from the aquifer needs to be produced with alternative heating or cooling equipment.

ATES systems are regularly used in new buildings in The Netherlands, thousands of ATES systems are in operation in the Netherlands [7], and on the TU Delft campus three buildings are currently cooled and (partly) heated via an ATES system (3mE, TU Library and EWI). An ATES system however can only be used in buildings with a low temperature heating system. So buildings with high temperature heating will need investments in the heating systems to be able to use an ATES system.

Via the application of an ATES system the heat (and cold) demand of a building will not change, only the supply from the heating grid will drop. The amount of heat needed from the district heating will mainly depend on the size of the ATES system and the rate of heat and cold demand. If the ATES system would be designed to be able to supply the complete cold demand, the heat demand will only depend on the rate of heat and cold demand, because the heat and cold supplied by the ATES will have to be equally sized. The rate of heat and cold demand will depend on the heat leaking from the building and the internal heat production.

The ATES system would only have a minor impact on the heat demand in the building since only the heat and cold supply changes. In terms of the flexibility on the district heating grid, the ATES system could shift heat demand by using the district heat when total heat demand (on the campus) is low and the ATES heat when total demand is high.

2.3. Other heat demand lowering measures

Besides the heat demand reduction as described other small buildings specific measures could be taken to further reduce the heat demand. This could be anything from insulation of piping, using more energy efficient installations, change room heating installations, increase heat recovery from ventilation air, decreasing the ventilation rate et cetera. These options will not be modelled because they have either only small effect or are too specific for the use in a generic model.

2.4. Cold demand reduction options

Although the reduction of cold is not the objective of the model, some options will be listed below. The model will give calculate the change in cold demand from the heat reduction options, since some options will show a large change in cold demand and thus total energy demand.

Options for the reduction of cold could later be added to the model as these options lower the total energy demand of the building. These options include daylight-dependent lighting control en blinds.

Daylight-dependent lighting control reduces the electricity use by measuring the solar the daylight and only supplying the extra light needed in the office. Blinds reduce the entrance of sunlight in the building and reduce the heat production from solar radiation. By using blinds in the summer the cold demand is reduced.

2.5. Overview of the heat demand reduction options

The explored options are rated on their ability to reduce the peak heat demand of a building. The increased insulation effect is visible when different buildings with different insulation levels are modelled, but since (increasing) the insulation of buildings is unique for every building it is not rational to model. Increased insulation will reduce the total heat demand and the peak heat demand.

The low temperature heating system has little effect on both the peak and the total heat demand. However the low temperature heating system is necessary for the application of some other measures like concrete core activation and aquifer thermal energy storage. The concrete core activation is only suited for use in newly built buildings, while this research focuses on existing buildings. Aquifer thermal energy storage systems create an external buffer for the building, but the building heat (and cold) demand are unaffected only the demand at grid level is affected.

This study focuses on the use of phase change materials and different heating strategies to reduce the peak heat demands of buildings in a smart grid. The model calculates the total heat demand and the heat demand flexibility compared with the original situation. The effect of several heating strategies in combination with phase change materials on the building heat demand can give interesting results for the reduction of the peak heat demand.

	Peak heat demand reduction	Total heat demand reduction	Applicable to existing buildings	Used in the developed model
Increased building insulation	+	++	+	-
Low temperature heating system	0	0	0	-
Base load night heating	+	-	++	+
Heating 24/7	+	-	++	+
Successive heating of buildings	+	-	++	+
Phase change materials	+	+	++	+
Concrete core activation	+	0	--	-
Aquifer thermal energy storage	0	0	0	-

Table 2.1 Overview of the heat demand reduction options

3. The LEA model

The LEA (Low Energy Architecture) model models the heat demand for buildings based on weather data, building characteristics, the building use profile and the indoor climate settings. The indoor climate preferences are prescribed by a maximum and minimum indoor temperature (and relative humidity), by the heating curve for the air supplied by mechanical ventilation and the mechanical ventilation rate. Heat transfer to and from the environment as a result of a temperature difference and solar radiation is calculated for all facades. The main model output is hourly data for heat demand, cold demand and the inside temperature for the modelled building.

The heat transfer to the environment per façade is modelled in two parts: a window part and a closed wall part. The closed walls are modelled as 1D convective heat transfer through a wall with a supplied thermal conductive resistance. The windows are modelled similar to the walls with the addition of the solar radiation which has a convective and a radiative part. Properties of the facades are given as an average over the façade; if necessary a façade can be split to supply different properties.

The accumulation of heat in the building consists of two parts, the accumulation of heat in the air and the accumulation of heat in the building structure. All heat accumulated in the building structure is modelled via one-dimensional heat transfer to the floors and ceiling which are modelled as being symmetrical.

The model is developed primarily for buildings with an office use and assumes uniformity in the building. The model assumes uniformity throughout the building in air temperature and humidity, in presence of people, installations and lighting, in thermal mass, et cetera. The model assumes uniformity per façade in heat transfer coefficients for walls and windows, type and size of windows, solar blinds, et cetera.

The LEA model is a discrete model and uses a constant time step of 2 minutes. If the simulation is unstable the time step is decreased for the entire simulation. The LEA model is written in Matlab code.

Chapter 3 describes the LEA model as created by Deerns and assumptions made in the LEA model on heat transfer in and to the buildings are reviewed and compared with literature.

3.1. Building heat balance

To keep the building within the desired temperature range heat or cold has to be supplied to the building to compensate for the heat transfer to the environment, the internal heat production and the heat transfer to the floors and ceilings. The air temperature T_a change in the building if no heat would be added to the building can be calculated via equation (3.1) from the heat entering from the environment \dot{Q}_{env} , the heat produced internally and the heat transferred to the floor \dot{Q}_{fl} and the specific heat capacity of air $C_{p,a}$, the density of the air ρ_a and the volume of the air in the building V_a

$$\frac{dT_a}{dt} = \frac{\dot{Q}_{env} + \dot{Q}_{int} - \dot{Q}_{fl}}{C_{p,a}\rho_a V_a} \quad (3.1)$$

The internal heat production is a sum of the heat production from people \dot{Q}_{people} , from appliances and installations \dot{Q}_{inst} and from lighting \dot{Q}_{light} . The heat entering from the environment is

calculated from the heat entering through the façade \dot{Q}_{fac} , the solar heat \dot{Q}_{solar} and the heat from ventilation \dot{Q}_{vent} .

If the temperature as a result of the heat balance in equation (3.1) will be outside of the temperature boundaries, the local heat demand can be calculated as follows:

$$\dot{Q}_{ld} = \dot{Q}_{env} - \dot{Q}_{int} - \dot{Q}_{fl} - \frac{\Delta T}{\Delta t} c_{p,a} \rho_a V_a \quad (3.2)$$

The local heat demand will be zero when the temperature will be within the allowed range set by T_{max} and T_{min} . T_{max} and T_{min} are determined by the operating set points and are time-dependent. The operating set points are the input maximum and minimum temperature with a ramp up instead of a step when the night values change to daytime values. The size of the correction ramp is determined by an input of the model representing the time necessary to heat the building.

The total amount of heat supplied to the building is calculated by adding all positive values of the hourly heat demand as calculated in equation (3.2) and the heat supplied to the air in the air handling unit. The cold demand is calculated similarly with the negative values of the local and the air handling unit heat supply.

$$Q_d = Q_{ld} + Q_{AHU} \quad (3.3)$$

Where the heat transfer to the floor Q_{fl} can be calculated from the temperature difference between the air and the floor and the overall heat transfer coefficient of the floor U_{fl} and the area of the floor A_{fl} :

$$Q_{fl} = U_{fl} A_{fl} (T_a - T_{fl}) \quad (3.4)$$

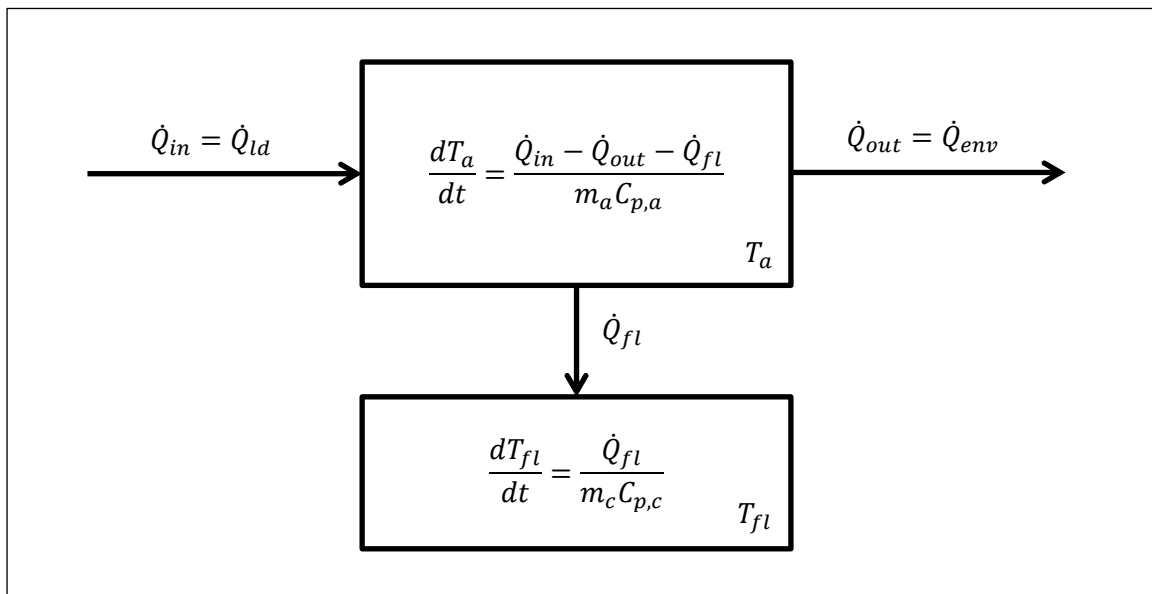


Figure 3.1 Basic building heat balance for the temperature of the air and the concrete floors in the buildings with heat transfer with the environment, local heat supplied and heat transfer with the floors.

So the overall system of equation could be written as:

$$d \begin{bmatrix} \bar{T}_a \\ T_{fl} \end{bmatrix} / dt = \begin{bmatrix} -\frac{h_c A_{fl} + U_{fac} A_{fac}}{m_a C_{p,a}} & \frac{h_c A_{fl}}{m_a C_{p,a}} \\ \frac{h_c A_{fl}}{m_{conc} C_{p,conc}} & -\frac{h_c A_{fl}}{m_{conc} C_{p,conc}} - \dot{Q}_{acc}(T_{fl}) \end{bmatrix} \begin{bmatrix} \bar{T}_{air} \\ T_{fl} \end{bmatrix} + f(t, T_{outside}, \dots) \quad (3.5)$$

Equation (3.5) is discretized with a fixed time step in a Matlab model. If the time step in the model will create an unstable simulation the time step is decreased to obtain a stable situation.

The model is based on a building level simulation in which the total heat demand of the building is calculated from the heat lost and gained. The heat demand is calculated on a building level and not on a room level. So local changes in the building caused for instance by solar radiation on the south side of the building or higher local heat production is not taken is not calculated.

3.2. Heat production from people, installations and lighting

The amount of people present in the building is an input for the model and is calculated per hour of the day. The heat production per person is assumed to be 80 Watt.

The heat production of the appliances and the lighting in the building is given as an input for the model in Watt per square meter. Depending on the input the heat production from installations is considered either a continuous heat source or only a heat source during opening hours. The lighting can be modelled in three ways; as lighting which is always turned on, as lighting which is only turned on during opening hours or as daylight dependent lighting.

The internal heat production from people, installations and lighting is split in a convective and a radiative part. The ratio of the convective part is determined by the convection factor given as a separate input for people, installations and lighting, the convection factor is equal to one minus the emissivity. The convective part is transferred to the air in the building and the radiative part is transferred to the floor and ceilings via radiation. So the heat transfer to the air \dot{Q}_{int} is equal to the total convective load $\dot{Q}_{c,load}$ which is the convective part of the heat production of the people \dot{Q}_{people} , installations \dot{Q}_{inst} and lighting \dot{Q}_{light} . The convective part of these heat loads is determined by the convection factor c_f of the source. This convection factor is defined as one minus the emissivity ϵ of the source.

$$\dot{Q}_{int} = \dot{Q}_{c,load} = \dot{Q}_{people} c_{f,people} + \dot{Q}_{inst} c_{f,inst} + \dot{Q}_{light} c_{f,light} \quad (3.6)$$

$$\dot{Q}_{r,load} = \dot{Q}_{pers}(1 - c_{f,pers}) + \dot{Q}_{inst}(1 - c_{f,inst}) + \dot{Q}_{light}(1 - c_{f,light}) \quad (3.7)$$

$$c_f = 1 - \epsilon \quad (3.8)$$

3.3. Solar radiation

The solar radiation is modelled with a direct part, a diffuse part and a reflective part. Hourly data for direct and diffuse solar radiation is supplied in the climate file (see chapter 3.3.1). The direct solar radiation is given for the plane normal to the solar angle. The direct solar radiation on the facades is calculated with the values in the climate file and the angle between the position of the sun and the direction of the façade. The direct solar radiation is corrected for the shade created by the window

frame and the submergence of window in the façade. However shade created by other parts the building or by neighbouring buildings is not taken into account. The position of the sun in the sky with respect to the building is calculated for every hour with the user supplied latitude and longitude of the modelled building.

Hourly data for the heat from diffuse solar radiation from the sky is supplied with the climate file as input. For all facades the diffuse solar radiation is calculated from its surface area and the view factor to the sky.

The heat transfer from the reflection of solar radiation on the earth \dot{q}_{refl} is calculated per façade from the reflectivity ρ_{env} of the surrounding environment and its view factor to the ground F , the heat from direct \dot{q}_{dir} and diffuse solar radiation \dot{q}_{dif} and height of the solar position h in rad.

$$\dot{q}_{refl} = \rho_{env} F (\dot{q}_{dif} + \sin(h) \dot{q}_{dir}) \quad (3.9)$$

The total amount of heat from solar radiation entering the building is partially entering via radiation and partially via convection. The amount of heat entering the building is calculated by adding the heat transferred through each façade. The heat transferred through a façade determined by the solar gain factor SGF of the window, the facades window fraction γ_w and the surface area of the façade A_{fac} . The solar gain factor gives the rate of solar radiation which is passed through the window as heat. The rate of the convective part to the total is determined by the convection factor c_f of the window or of the combined window and blinds system when blinds are switched on. The convective heat transfer \dot{Q}_c and the radiative heat transfer \dot{Q}_r are calculated via:

$$\dot{Q}_c = \sum_{i=1}^{n_{fac}} \left(SGF_n * c_{f,win} \gamma_w A_{fac} (\dot{q}_{refl} + \dot{q}_{dif} + \dot{q}_{dir}) \right) \quad (3.10)$$

$$\dot{Q}_r = \sum_{i=1}^{n_{fac}} \left(SGF_n * (1 - c_{f,win}) \gamma_w A_{fac} (\dot{q}_{refl} + \dot{q}_{dif} + \dot{q}_{dir}) \right) \quad (3.11)$$

The solar radiation on the windows can be restricted by the use of solar blinds. The blinds can either be on the outside or on the inside of the window and the blinds have set values, given as input, for solar radiation when they will be turned on and off.

3.3.1. Climate files/years

The model needs weather data to calculate the heat loss to the environment, necessary humidification, solar radiation, et cetera. The data from the climate years used in the model are hourly data for air temperature, soil temperature, relative humidity, direct solar radiation and diffuse solar radiation. Climate years contain weather data for an average year including a realistic cold and warm days. Climate years exist for thousands of cities / locations on the planet. The LEA model has a default climate file TRYDeBilt (Test Reference Year De Bilt), other climate data or weather data containing the relevant parameters however can be supplied, for instance future weather scenarios which account for climate change or historic weather data to verify the model input.

3.4. Heat transfer to the environment

The heat transfer coefficients used in the model are fixed input values. The outside heat transfer coefficient has a default value of 25 W/m²/K and the inside heat transfer coefficient has a default value of 8 W/m²/K. This assumption for the outside heat transfer coefficient will not be very accurate at high wind velocities. The assumptions for outside heat transfer coefficient will be described in chapter 3.4.2. The inside heat transfer coefficient will be described in 3.5.2.

3.4.1. Convective heat transfer to the soil

The heat transfer to the soil beneath the building is modelled as a convective heat transfer to the floor with a conductive heat transfer resistance. The heat transfer is calculated from the area of the building bound to the soil A_{bot} , the overall heat transfer coefficient U_{bot} for heat transfer to the soil, the temperature of the air in the building and the temperature of the soil T_{soil} :

$$\dot{Q}_{soil} = (T_{in} - T_{soil})U_{bot}A_{bot} \quad (3.12)$$

The temperature of the soil is assumed uninfluenced by the heat transfer from the building and is given by the climate file. The overall heat transfer coefficient is calculated from the conductive heat transfer resistance $R_{c,bot}$ and the heat transfer coefficient at the inside of the walls $h_{c,in}$.

$$U_{bot} = \frac{1}{\frac{1}{h_{c,in}} + R_{c,bot}} \quad (3.13)$$

The LEA model uses the heat transfer resistance as input values; this heat transfer resistance R_c is defined as the summation of the length L_n divided by the conductivity k_n of the different layers within the bottom façade.

$$U_{bot} = R_c = \sum \frac{L_n}{k_n} \quad (3.14)$$

The Biot number of the heat transfer to the floor is, determined by the internal heat transfer coefficient and the heat transfer resistance which is a building property and roughly varies between 0.5 and 3 m²K/W. The Biot number will thus vary between 4 and 24.

$$Bi = \frac{h L}{k} = h_{in}R_c = 8R_c \quad (3.15)$$

3.4.2. Convective heat transfer to the air

The heat transfer to the environment is calculated per building façade for all facades except for the non-elevated floors. The heat transfer is a sum of the heat transfer via the walls and the windows.

$$Q_{shell} = (T_{in} - T_{out}) \sum_{i=1}^{n_{fac}} (U_{wall}A_{wall} + U_{win}A_{win}) \quad (3.16)$$

The total heat transfer coefficient for the windows U_{win} is given as an input for the model. The total heat transfer coefficient for the walls is calculated with the inside and outside convective heat transfer coefficient and the conductive thermal resistance supplied per façade.

$$U_{wall} = \frac{1}{\frac{1}{h_{c,in}} + R_{c,wall} + \frac{1}{h_{c,out}}} \quad (3.17)$$

In the original model the heat transfer is assumed constant at 25 W/m²/K. However for this research the heat transfer coefficient calculated from the wind speed is used. The convective heat transfer at the building facades consists of a forced and a natural part.

The correlations as derived by Jürges are used extensively in the building [8-10] simulation. Jürges derived heat transfer coefficients correlations for flat plates as stated in equation (3.18) for given wind speeds U_∞ in m/s.

$$\begin{aligned} h_{c,out} &= 4.0U_\infty + 5.6, & U_\infty < 5m/s \\ h_{c,out} &= 7.1U_\infty^{0.78}, & U_\infty \geq 5m/s \end{aligned} \quad (3.18)$$

An intermediate-level model for convective heat transfer to buildings is derived by Gandrille et al.[11] in a dimensionless form with a fixed Prandtl Number of 0.71. The intermediate-level model of the convective heat transfer to the externals of the building is split in four relations for forced convection, two relations for natural convection and a relation for mixed convection.

With:

$$Nu = \frac{h_c L}{k}, \quad Re = \frac{U_\infty L}{\nu}, \quad Ra = \frac{\beta g \Delta T L^3}{\nu \alpha} \quad (3.19)$$

With h_c the convective heat transfer coefficient, L the length of the façade, k the thermal conductivity of in this case air, U_∞ the velocity of the air uninfluenced by the building, ν the kinematic viscosity of in this case air, β the coefficient of thermal expansion, g the gravitational constant, ΔT the difference in temperature between the façade and the air and α the thermal diffusivity of in this case the air.

Boundary layer flow for the roof and the walls parallel to the wind direction:

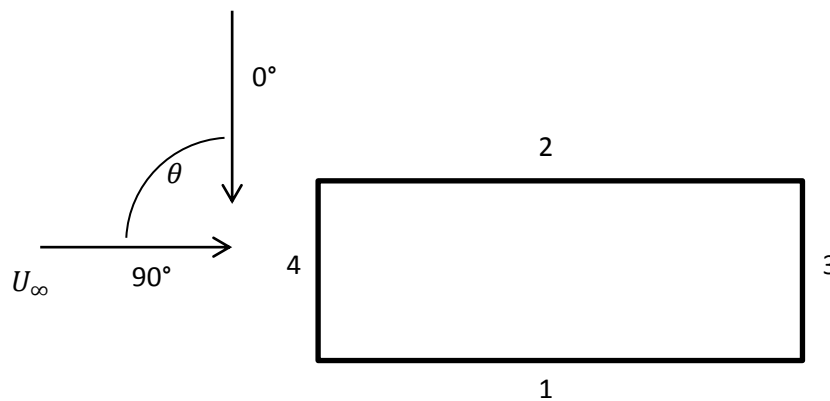


Figure 3.2 Orientation for the wind direction in relation to the building with façade 1 the 45 m wide leeward façade, façade 2 the windward 45m wide façade, façade 3 the leeward 12m wide façade and façade 4 the windward 12m wide façade.

$$Nu_p = \left[(0.59Re^{1/2})^6 + (0.032Re^{4/5} - 745)^6 \right]^{1/6} \quad (3.20)$$

Completely separated flow for the leeward walls of the building:

$$Nu_s = 0.20Re^{2/3} \quad (3.21)$$

Stagnation flow for the windward walls of the building:

$$Nu_{st} = 0.14Re^{0.69} \quad (3.22)$$

An interpolation is used for when the wind direction is neither parallel nor perpendicular to the building wall with the angle θ between the air flow direction and the orientation of the façade according to Figure 3.2:

$$Nu_f = \cos^2 \theta Nu_{s/st} + (1 - \cos^2 \theta) Nu_p \quad (3.23)$$

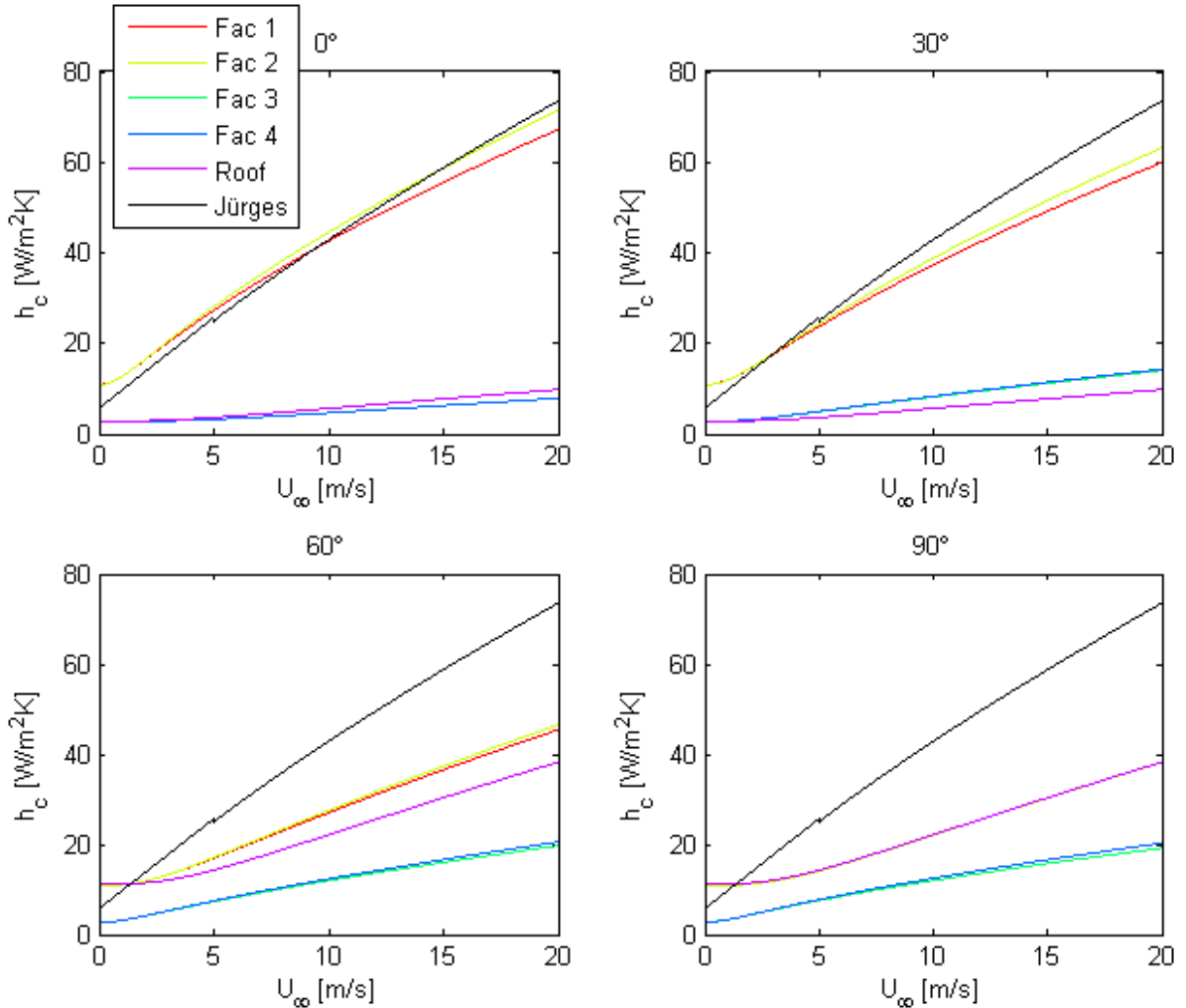


Figure 3.3 Convective heat transfer coefficient as a function of the wind velocity according to relations by Grandille et al. compared with the relations by Jürges. The convective heat transfer coefficients are calculated for building 62 as simulated in this study for different angles for the wind with a temperature difference between the air and the façades of 10 Kelvin. For 0° the wind is parallel with the smallest wall of 12 meter width and for 90° the smallest wall is perpendicular to the wind direction. Façade 1 is the 45 m wide leeward façade, façade 2 is the windward 45m wide façade, façade 3 is the leeward 12m wide façade and façade 4 is the windward 12m wide façade.

For buoyancy driven natural convection flow at vertical surfaces:

$$Nu_b = \left[(0.58Ra^{1/4})^6 + (0.11Ra^{1/3})^6 \right]^{1/6} \quad (3.24)$$

For buoyancy driven natural convection flow at horizontal surfaces:

$$Nu_b = \left[(0.54Ra^{1/4})^6 + (0.14Ra^{1/3})^6 \right]^{1/6} \quad (3.25)$$

When mixed convection is present a geometric mean for the natural and forced convection is used according to:

$$Nu_{bv} = [Nu_f^3 + Nu_b^3]^{1/3} \quad (3.26)$$

The relations as suggested by Gandrille et al. are compared with the relations suggested by Jürges for building 62 as simulated with the LEA model with dimensions in meters 12*46.8*45.45 (l*w*h) and a temperature difference between the air and walls of 10 kelvin. The convective heat transfer coefficient is plotted for the four vertical walls, the roof and the relation suggested by Jürges for the 12m wide wall parallel with the wind (0°) and for 30°, 60° and for the 12m wall perpendicular to the wind (90°) as illustrated in Figure 3.2.

For building 62 the convective heat transfer coefficients according to the relations by Gandrille et al. differ with the wind direction and the façade width. The convective heat transfer coefficient for the 45 meter wide façade is similar to the Jürges relation when either stagnation flow or separation flow occurs at 0° and when the stagnation or separation flow is the dominant flow. The convective heat transfer coefficients is significantly smaller than the relation suggested by Jürges for the 12m wide walls and the roof and for the 45m wide façade when boundary layer flow is the dominant flow present.

3.5. Floor heat balance

3.5.1. Heat transfer within the floor

After the calculation of the temperatures in the room for a time step, the resulting temperature of the floor and ceiling are calculated. The floor / ceiling system including the heat transfer is modelled symmetrically and one-dimensionally. The centre of the floor is modelled as adiabatic, so only the floor is modelled and its area is multiplied by two to account for the ceiling area. The floor is modelled with 2, 3 or 4 elements depending on the entered specific mass of the building. If the building is considered as a lightweight building ($\rho < 50 \text{ kg/m}^3$) the floor part is not modelled. The model calculates the heat transferred with the floor temperatures from the previous time step. The new temperature profile is calculated with the new heat transfer.

3.5.1.1. Biot number

The Biot number describes the rate of internal thermal conductive resistance of a solid to the rate of external thermal resistance by convection. The Biot number of the heat transfer to the floor is:

$$Bi = \frac{hL}{k} \quad (3.27)$$

With h being the heat transfer coefficient for heat transfer to the floor, L the relevant length scale (in this situation half the thickness of the floor) and k the thermal conductivity of the floor material, i.e. concrete. So the Biot number for heat transfer to the floor is:

$$Bi = \frac{h_{fl}L}{k_{conc}} = \frac{8 * 0.18/2}{1.13} = 0.64$$

Since the Biot number is close to one, a conduction analysis is done with the Fourier number and the Biot number.

3.5.1.2. Fourier number

The Fourier number describes the ratio of heat conduction to the rate of heat storage in a solid medium. The Fourier number of the heat transfer to the floor is:

$$Fo = \frac{\alpha t}{L^2} \quad (3.28)$$

With α being the thermal diffusivity, t the time and L the relevant length scale. The length of the floor is calculated from the building mass per square meter m . For an average building with a building mass of 250 kg/m^2 , the floor length will be 0.18 m and the applicable length is half the thickness in the floor when modelled as a symmetric concrete slab.

$$L_{fl} = \frac{m}{\rho_{conc}} \quad (3.29)$$

With the thermal diffusivity calculated from the specific heat $C_{p,conc}$ the thermal conductivity k_{conc} and the density of the concrete ρ_{conc} .

$$\alpha_{conc} = \frac{k_{conc}}{\rho_{conc}C_{p,conc}} = 8.1 * 10^{-7} \quad (3.30)$$

So the Fourier number could be expressed as a function of the characteristic time t_c which is about 10^4 seconds or 2.8 hours for the concrete floor:

$$Fo = \frac{t}{t_c} = \frac{t}{10^4} \quad (3.31)$$

For a single time step in the model of 120 seconds the Fourier number thus becomes $Fo \approx 0.01$.

For a symmetric unsteady conduction the dimensionless temperature $\theta = \frac{T-T_e}{T_0-T_e}$ could be written as a function of the dimensionless variables for time $Fo = \frac{\alpha t}{L^2}$ and space coordinate $\eta = \frac{x}{L}$. In which T_e is the temperature outside of the slab, T_0 the starting temperature in the slab and x the distance from the symmetric centre of the slab.

$$\theta(Fo, \eta) = e^{-\lambda^2 Fo} (A \cos(\lambda \eta) + B \sin(\lambda \eta)) \quad (3.32)$$

With the boundary conditions for a symmetric centre $\partial\theta/\partial\eta|_{\eta=0} = 0$, so $B = 0$ and the heat transfer to the concrete slab is:

$$-\frac{\partial \theta}{\partial \eta} \Big|_{\eta=1} = Bi \theta \Big|_{\eta=1}$$

Results in eigenvalues of according to:

$$\cot \lambda = \frac{\lambda}{Bi}$$

With constants A_n for the eigenvalues satisfying an initial condition with a uniform temperature T_0 :

$$\theta(0, \eta) = \sum_{n=1}^{\infty} A_n \cos(\lambda_n \eta) = 1$$

$$A_n = \frac{2 \sin \lambda_n}{\lambda_n + \sin \lambda_n \cos \lambda_n}$$

The temperature profile for heating of the slab with a constant outside temperature can be calculated via equation (3.33):

$$\theta(Fo, \eta) = \frac{T - T_e}{T_0 - T_e} = \sum_{n=1}^{\infty} e^{-\lambda_n^2 Fo} \frac{2 \sin \lambda_n}{\lambda_n + \sin \lambda_n \cos \lambda_n} \cos(\lambda_n \eta) \quad (3.33)$$

The temperature profile as described by equation (3.33) is plotted in Figure 3.4 for different Fourier numbers.

3.5.1.3. Floor heat balance in the LEA model

The heat accumulated in the top element of the floor is determined by the convection to the floor \dot{q}_c , the radiative load to the floor $\dot{q}_{r,load}$ and the heat transferred to the second part of the floor $\dot{q}_{fl,int}$:

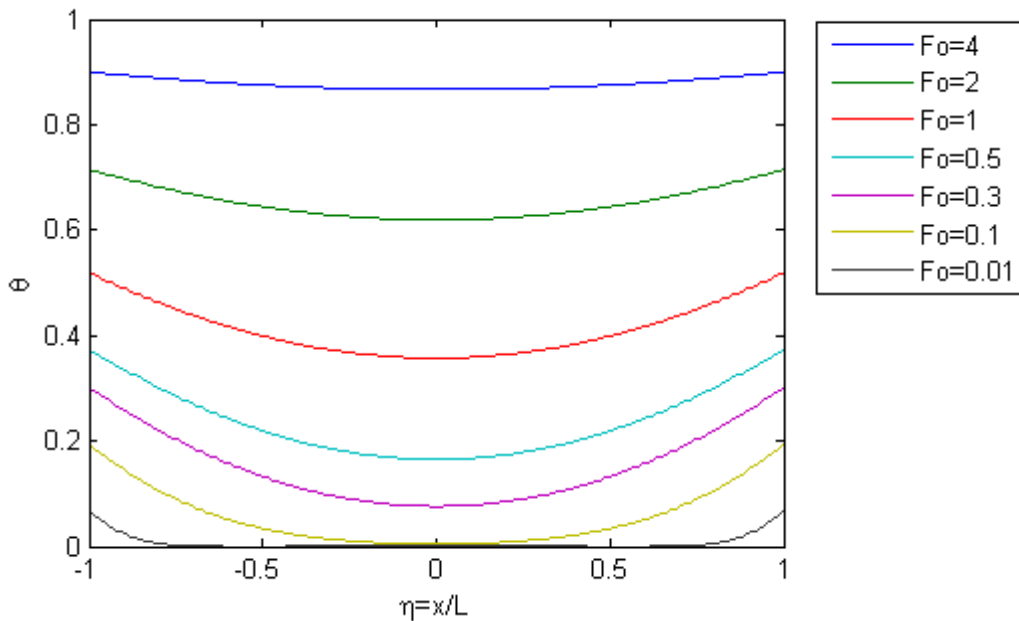


Figure 3.4 Dimensionless temperature profile $\theta = \frac{T - T_e}{T_0 - T_e}$ in for different dimensionless time values for a Biot = 0.64

$$\dot{q}_{acc} = \dot{q}_c + \dot{q}_{r,load} - \dot{q}_{fl,int} \quad (3.34)$$

$$\dot{q}_c = h_{fl}(T_{in} - T_{fl}) \quad (3.35)$$

With h_{fl} as described in 3.5.2, T_{in} the temperature of the air in the building, T_{fl} the temperature of the floor and \dot{q}_{rad} is the radiative load created by the presence of people, appliances and lighting as calculated in equation (3.7), all radiation is assumed to be absorbed by the floor/ceiling and not to the walls and windows. The conductive heat transferred from the first to the second element of the element of the floor is calculated with the conductivity of the concrete floor from the temperatures in the first and second element according to Fourier's law

$$\dot{q}_{fl,int} = -k_{conc} \frac{\partial T}{\partial x} \quad (3.36)$$

The heat transferred to the floor is accumulated in the concrete floor. The resulting temperature profile in the floor is calculated in the following equations.

Top part concrete floor:

$$\frac{\partial T}{\partial t} = \frac{\partial}{\partial x} \frac{\dot{q}_{fl}}{\rho_{conc} C_{p,conc}} \quad (3.37)$$

The intermediate part(s) of the concrete floor are calculated via the assumption of a linear profile in the concrete floor as follows:

$$\frac{\partial}{\partial x} \left(-k \frac{\partial T}{\partial x} \right) = C_{p,conc} \rho_{conc} \frac{\partial T}{\partial t} \quad (3.38)$$

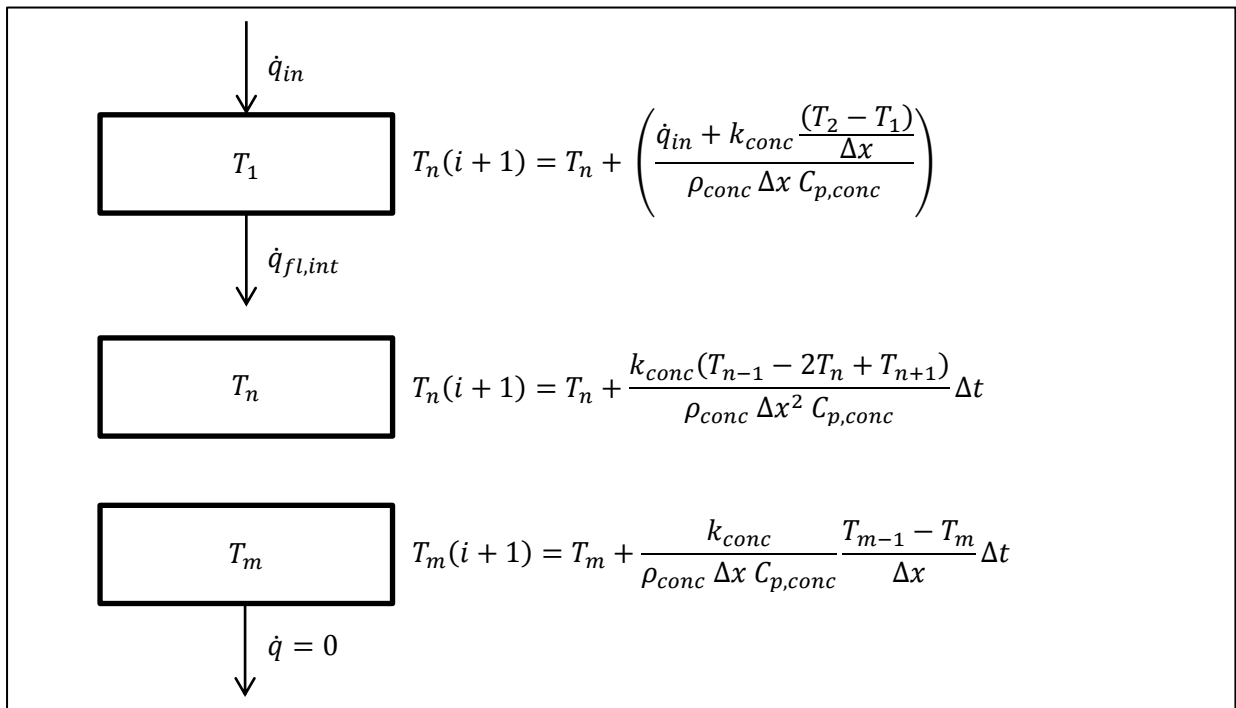


Figure 3.5 Schematic of the modelled heat transfer to and in the floor

The middle part of the concrete floor is modelled with one adiabatic side to create a symmetric temperature profile over the floor / ceiling system. All heat transferred to the middle part is thus accumulated here.

3.5.2. Heat transfer to the floors, walls and ceilings

The overall heat transfer coefficient h_{fl} used consists of a convective $h_{c,in}$ and a radiative part h_r .

$$h_{fl} = h_{c,in} + h_r \quad (3.39)$$

The radiative part is a linearization for the radiative heat transfer according to the relation in equation (3.40), with h_r the radiative heat transfer coefficient, the emittance ϵ and the Stefan-Boltzmann constant $\sigma = 5.67e - 8 \text{ W/m}^2\text{K}^4$.

$$q_r = \epsilon\sigma(T_{conc}^4 - T_a^4) \approx h_r(T_{conc} - T_a) \quad (3.40)$$

In which h_r is determined from the Taylor Series expansion to find the linear relation.

$$h_r = 4\epsilon\sigma T_{conc}^3 \quad (3.41)$$

For building applications an epsilon value of 0.9 [1] is generally used as the emissivity in the building. When $T_{conc} = 22$ and $T_{air} = 20$ are taken as a reference the radiation heat transfer coefficient is defined as: $h_r = 5.2 \text{ W/m}^2\text{K}$.

The convective part is determined by the convection type: natural, forced or mixed. In a regular building the main convection will be natural convection however locally mixed or forced convection can occur for instance near the ventilation jets and by movement of occupants of the building.

Much research has been done on the topic of the convective heat transfer coefficient of walls, floors and ceilings in buildings [12, 13]. The convective heat transfer coefficient within buildings depends on the interior of the building, whether the surface is a ceiling, a vertical wall or a floor, the temperature difference between the concrete and the air and whether the temperature of the air is higher or lower than the surface.

Although the convective heat transfer coefficient for natural convection differs as a result of these factors some relations between the Nusselt Number and the Rayleigh number are derived. Some of the relations in literature are derived for Grashof numbers, these are written here as a function of the Rayleigh number according to $Ra = Pr * Gr$. The relations between the Nusselt number and the Rayleigh number are split in three parts: heat transfer to floors or from ceilings, heat transfer to ceilings or from floors and heat transfer to and from vertical walls. The heat transfer from ceilings in an enclosure and the heat transfer to floors in an enclosure are described by the same relations as they cover the same phenomena, the same accounts for the heat transfer from floors in an enclosure and the heat transfer to ceilings in an enclosure.

3.5.2.1. Heat transfer to floors or from ceilings

For air at room temperature 22°C with constant Prandtl number and a Rayleigh number according to equation (3.42). With β the thermal coefficient of expansion, g the gravitational constant, ΔT the temperature difference between the floor and the air, L the length of the floor, ν the kinematic viscosity and α the thermal diffusivity.

$$Ra_{fl} = \frac{\beta g \Delta T L^3}{\nu \alpha} \quad (3.42)$$

With a standard room with a width of 3 to 6 meter and a temperature difference between the air and the floor surface of the room of 0.5 to 2K, the Rayleigh number will be in the range of:

$$10^9 > Ra > 5 * 10^{10}$$

Relations found for a Rayleigh number in this range have been listed in Table 3.1. The relations are plotted in Figure 3.5, the resulting convective heat transfer coefficients as a function of the length of the floor in the room are plotted in Figure 3.7 for a fixed temperature difference of 1 Kelvin. Figure 3.7 shows a small influence of the length of the room on the convective heat transfer coefficient in all Nusselt Rayleigh relations. The different studies suggest a range for the convective heat transfer coefficient of 1 – 4 W/m²K for a room of 3 meter wide and a temperature difference of 1 Kelvin. For an average room with a width of 3 – 4 meter an average heat transfer coefficient of 1.8 W/m²K can be used in a turbulent situation and for a laminar situation a value of 1 can be used. The relation suggested by Min et al.[14] exceeds the others by about a factor of 2, this relation is given for a situation where the floor is heated (with ΔT up to 60K) and all vertical walls and the ceiling are isothermal with a temperature equal to the air temperature in the room.

Figure 3.6 shows the relation between the temperature difference in the room between the floor and the air and the convective heat transfer coefficient. The convective heat transfer coefficient shows a clear dependence on the temperature gradient and can thus not be assumed constant for different temperature gradients, but could be described with a constant C times a power n of the temperature difference: $h = C \Delta T^n$.

Situation	Floor	Range	Source
Heated floor	$Nu = 0.33 Ra^{0.33}$	$10^9 \leq Ra \leq 10^{11}$	Min [14]
Turbulent	$Nu = 0.268 Ra^{0.31}$	$Ra > 2 * 10^7$	Min [14]
Turbulent	$Nu = 1.14 Ra^{0.24}$	$4 * 10^8 \leq Ra \leq 7 * 10^9$	Khalifa [15]
Laminar	$Nu = 0.476 Ra^{1/4}$	$7 * 10^7 < Ra < 7 * 10^9$	CIBSE [16]
Turbulent	$Nu = 0.118 Ra^{1/3}$	$7 * 10^7 < Ra < 7 * 10^9$	CIBSE [16]
Laminar	$Nu = 0.448 Ra^{1/4}$	$7 * 10^7 < Ra < 7 * 10^9$	ASHRAE [1]
Laminar and turbulent	$Nu = \left[\left(0.48 Ra^{1/4} \right)^6 + \left(0.113 Ra^{1/3} \right)^6 \right]^{1/6}$	$0 < Ra < \infty$	Alamdari [17]

Table 3.1 Relations between Rayleigh and Nusselt numbers for convective heat transfer at a floor in an enclosure

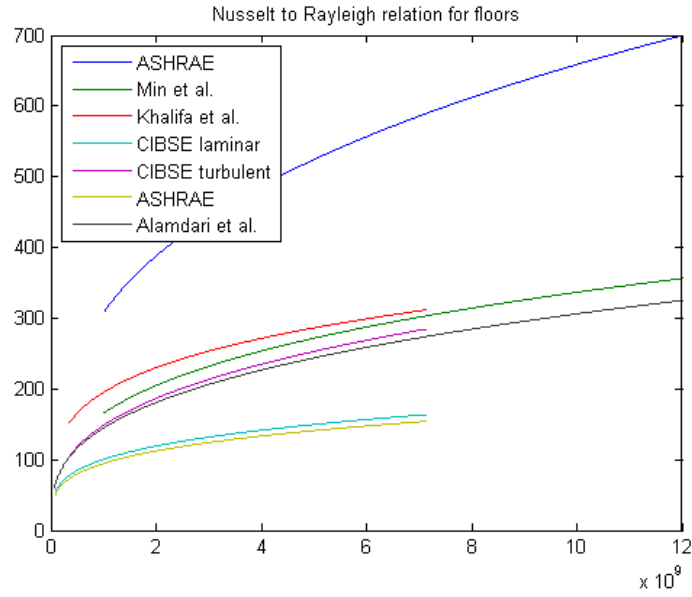


Figure 3.5 Rayleigh Nusselt relations from literature for floors as found in literature as listed in Table 3.1 for Rayleigh numbers in the range $10^9 < Ra < 10^{10}$

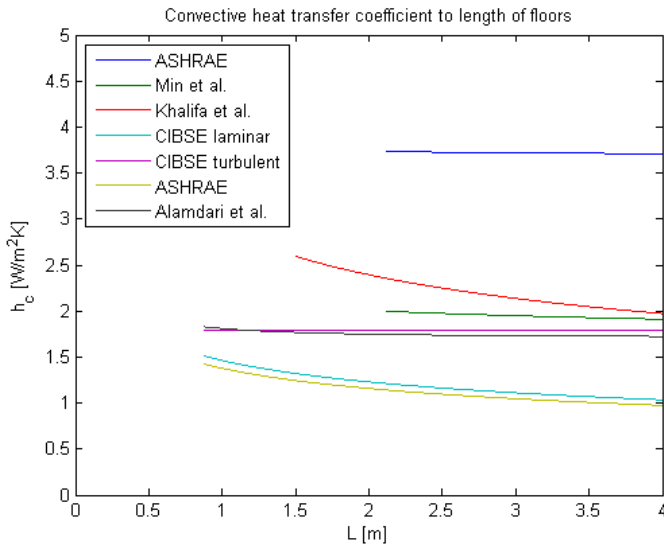


Figure 3.7 Convective heat transfer coefficient to length ratio from literature for floors with a temperature difference between the air and the floor of 1 Kelvin

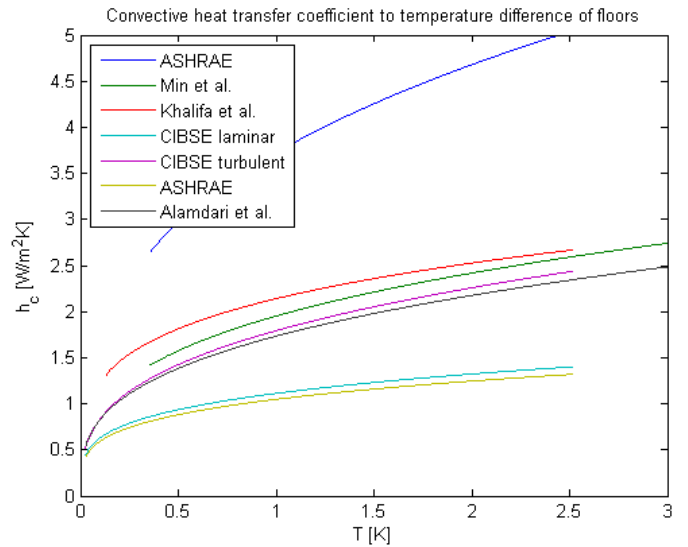


Figure 3.6 Convective heat transfer coefficient to temperature difference between the air in the room and the floor from literature as listed in Table 3.1 for floors with a length of 3 meter

3.5.2.2. Heat transfer to ceilings or from floors

With a standard room with a width of 3 to 6 meter and a temperature difference of 0.5 to 2K, the Rayleigh number will be in the range of:

$$10^9 > Ra > 5 * 10^{10}$$

Relations for natural convection to the ceiling of an enclosure are found in literature and listed in Table 3.2. The relations between the Rayleigh number and the Nusselt number are plotted in Figure 3.8. The relations between the convective heat transfer coefficient and the length of the ceiling and the temperature difference are plotted in Figure 3.9 and Figure 3.10.

The results for the convective heat transfer coefficient for heat transfer to the ceiling are similar to the results for the floor. The length of the ceiling has a much smaller impact on the heat transfer coefficient than the temperature difference between the ceiling and the air in the room. The convective heat transfer coefficients for a fixed temperature difference of 1 Kelvin can be approximated by $0.5 \text{ W/m}^2\text{K}$ and decreases with an increasing room length. The convective heat transfer coefficient for a fixed room height as a function of the temperature difference increases with an increasing temperature.

The relation suggested by Min et al.[14] exceeds the others by about a factor of 4, this relation is given for a situation where the ceiling is heated (with ΔT up to 60K) and all vertical walls and the floor are isothermal with a temperature equal to the air temperature in the room.

Situation	Ceiling	Range	Source
Heated ceiling, turbulent	$Nu = 0.71 Ra^{0.255}$	$10^9 \leq Ra \leq 10^{11}$	Min [14]
	$Nu = 0.060 Ra^{0.255}$	$10^9 \leq Ra \leq 10^{11}$	Min [14]
Laminar	$Nu = 0.217 Ra^{1/4}$	$0.7 * 10^8 < Ra < 0.7 * 10^{10}$	CIBSE [16]
Laminar	$Nu = 0.200 Ra^{1/4}$	$0.7 * 10^8 < Ra < 0.7 * 10^{10}$	ASHRAE [1]
Laminar	$Nu = 0.52 Ra^{1/5}$	$0.7 * 10^8 < Ra < 0.7 * 10^{10}$	Alamdari [17]

Table 3.2 Relations between Rayleigh and Nusselt numbers for convective heat transfer at a ceiling in an enclosure

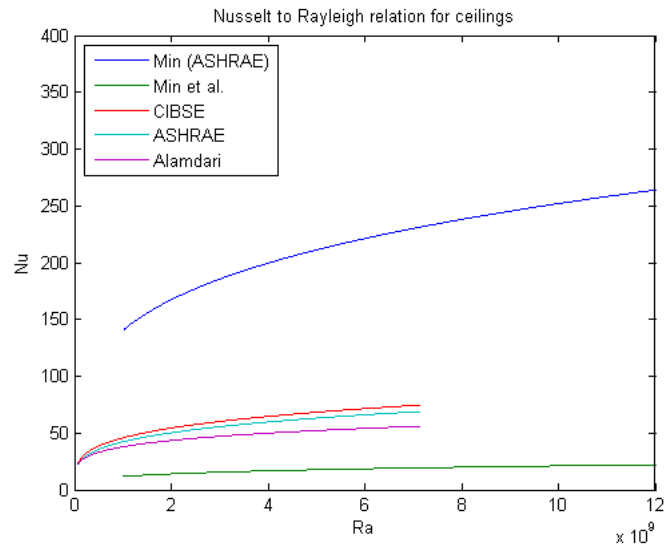


Figure 3.8 Nusselt to Rayleigh relations for vertical walls in an enclosure from literature as listed in Table 3.2

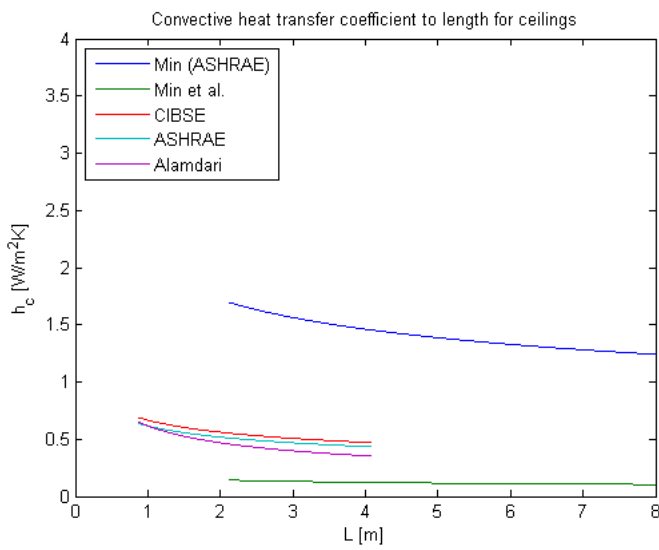


Figure 3.9 Convective heat transfer coefficient to length ratio from literature for vertical walls with a temperature difference between the air and the vertical wall of 1 Kelvin as listed in Table 3.2

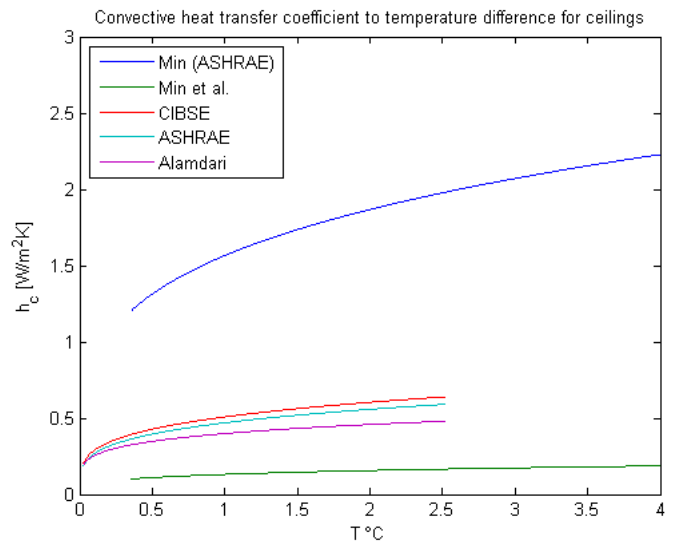


Figure 3.10 Convective heat transfer coefficient to temperature difference between the air in the room and the floor from literature as listed in Table 3.2 for a vertical wall with a height of 3 meter

3.5.2.3. Heat transfer to or from vertical walls

Typical Rayleigh numbers for vertical walls are determined by the temperature difference between the air and the wall ΔT (0.5-2K) and the height of the room (2.6-3m) and are in the range of:

$$9 * 10^8 > Ra > 6 * 10^9$$

Relations between Nusselt and Rayleigh number for vertical walls in an enclosure are listed in Table 3.3 and plotted in Figure 3.11 for the applicable range.

The convective heat transfer coefficient as function of the height of the room is plotted in Figure 3.12. The figure shows a large deviation in the convective heat transfer coefficients. The convective heat transfer coefficient as function of the temperature difference between the air in the room and wall are plotted in Figure 3.13. For a room of 3 meter height and 1 Kelvin temperature difference Khalifa and Marshall suggest a coefficient of $0.3 W/m^2K$, while Min et al. suggests a coefficient of $2 W/m^2K$.

Situation	Vertical wall	Range	Source
Heated floor	$Nu = 0.22 Ra^{0.32}$	$10^9 \leq Ra \leq 10^{11}$	Min [14]
$T_{wall} < T_{air}$	$Nu = 0.103 Ra^{1/3}$	Turbulent	Heidt [18]
$T_{wall} > T_{air}$	$Nu = 0.063 Ra^{1/3}$	Turbulent	Heidt [18]
Heated vertical wall	$Nu = 0.595 (Ra^*)^{1/5}$	Laminar $Ra^* < 6.3 * 10^9$	Fohanno [19]
Heated vertical wall	$Nu = \frac{(Ra^*)^{1/2}}{16.1(Ra^*)^{3/14} - 568.4}$	Turbulent $Ra^* > 6.3 * 10^9$	Fohanno [19]
Turbulent	$Nu = 0.176 Ra^{0.32}$	$Ra > 7 * 10^8$	Min [14]
	$Nu = 0.133 Ra^{0.285}$	$7 * 10^8 < Ra < 7 * 10^9$	Allard [20]
	$Nu = 1.46 Ra^{0.14}$	$3 * 10^7 < Ra < 7 * 10^9$	Khalifa [15]
Turbulent	$Nu = 0.104 Ra^{1/3}$	$7 * 10^7 < Ra < 7 * 10^{11}$	ASHRAE [1]
Turbulent	$Nu = \left[\left(0.51 Ra^{1/4} \right)^6 + \left(0.085 Ra^{1/3} \right)^6 \right]^{1/6}$	$7 * 10^7 < Ra < 7 * 10^9$	Alamdari [17]

Table 3.3 Relations between Rayleigh and Nusselt numbers for convective heat transfer at a vertical wall in an enclosure

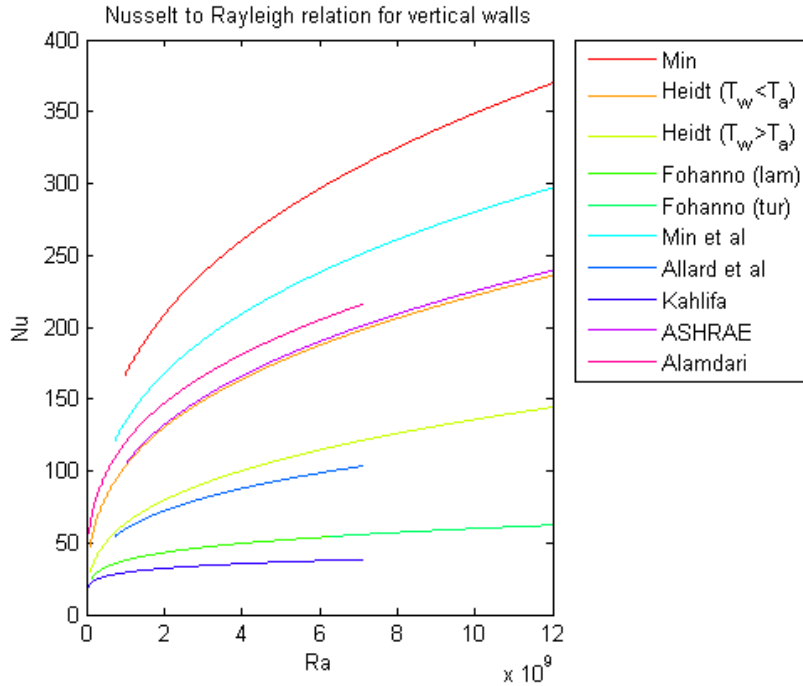


Figure 3.11 Nusselt to Rayleigh relations for vertical walls in an enclosure from literature as listed in Table 3.3.

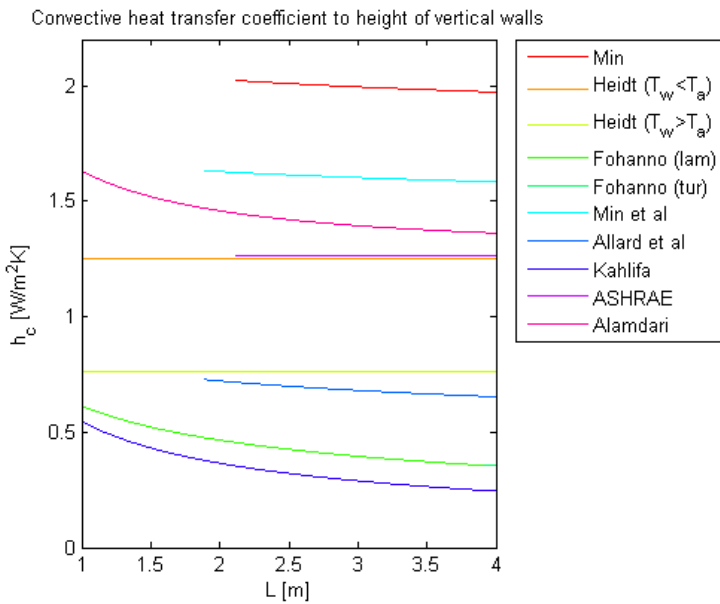


Figure 3.12 Convective heat transfer coefficient to length ratio from literature for vertical walls with a temperature difference between the air and the vertical wall of 1 Kelvin

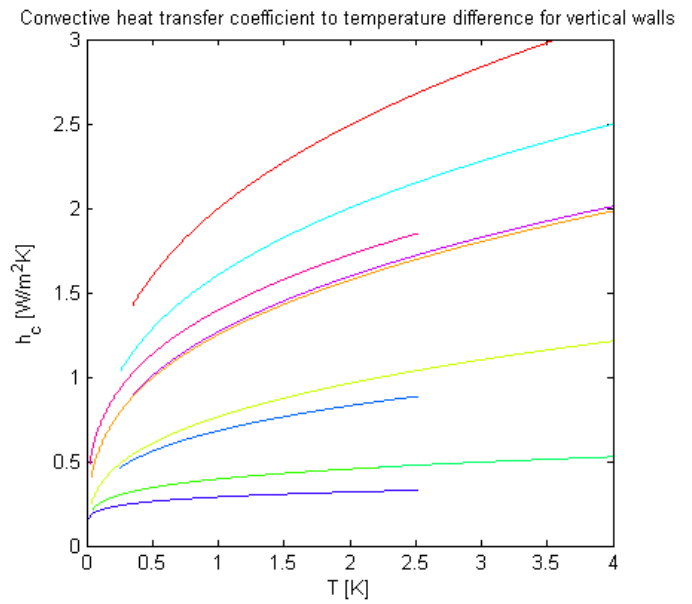


Figure 3.13 Convective heat transfer coefficient to temperature difference between the air in the room and the floor from literature as listed in Table 3.3 for a vertical wall with a height of 3 meter

3.5.2.4. Conclusion on internal heat transfer coefficients

Many studies have been done on the convective heat transfer coefficients in rooms. These studies proposed several relations between the Rayleigh and Nusselt numbers listed for floors (Table 3.1), ceilings (Table 3.2) and vertical walls (Table 3.3). The relations proposed show a large bandwidth of results within the Rayleigh range applicable for building simulation.

Typical values for the convective heat transfer coefficients for turbulent heat transfer in an empty enclosure at floors and ceilings are respectively 2 and 1.5 W/m²K for a turbulent situation. Typically the convective heat transfer coefficient for heat transfer at vertical walls is in the range 0.3 - 2 W/m²K, however a large range is found in literature.

The height and width of the room have a small effect on the convective transfer coefficient. The temperature difference however does have a substantial impact on the heat transfer coefficient.

The relations listed are all for enclosures without ventilation and obstacles and without windows or other local temperature differences influencing the air flow and convection in the described enclosure. In the real situation when the room is occupied the convective heat transfer coefficient to the floor, ceiling and non-obstructed vertical walls will be higher.

The effects of low rate ventilation, configuration of the radiators and windows in the room and presence of furniture have been studied [12, 21]. The studies show large variation in (local) convective heat transfer coefficients for different configurations.

3.5.2.4.1. Effect of internal heat transfer coefficient in the LEA model

The sensitivity of the model on the internal heat transfer coefficient is tested by inserting different values and comparing the total and peak heat demand. Two smaller and two larger values are tested and three power functions of the temperature difference are tested according to relations from literature. Writing the Nusselt to Rayleigh number relation for the convective heat transfer coefficient according to equation (3.43) gives the heat transfer coefficient as a function of the temperature difference. Three relations from literature are used, the relation given by CIBSE for turbulent heat transfer to the floor, the relation given by ASHRAE for heat transfer to floors for laminar situation and the relation given by ASHRAE in for heat transfer to the ceiling.

$$h = h_r + h_c = h_r + \frac{L}{k} * C \left(\frac{\beta g L^3 \Delta T}{\nu \alpha} \right)^n \quad (3.43)$$

Heat transfer coefficient [W/m ² K]		Total heat demand [MWh]	Peak heat demand [kW]	Nusselt-Rayleigh relation
<i>h</i> = 8 (standard value)		410	738	
<i>h</i> = 6		403 (-1.7%)	680 (-8.1%)	
<i>h</i> = 7		407 (-0.8%)	711 (-3.7%)	
<i>h</i> = 9		413 (+0.6%)	761 (+3.1%)	
<i>h</i> = 10		415 (+1.2%)	781 (+5.8%)	
<i>h</i> = 5.2 + 1.43 Δ<i>T</i>^{1/3}	CIBSE	407 (-0.6%)	717 (-2.9%)	<i>Nu</i> = 0.118 <i>Ra</i> ^{1/3}
<i>h</i> = 5.2 + 3.73 Δ<i>T</i>^{0.33}	Min	411 (+0.4%)	781 (+5.8%)	<i>Nu</i> = 0.33 <i>Ra</i> ^{0.33}
<i>h</i> = 5.2 + 0.41 Δ<i>T</i>^{0.25}	ASHRAE	404 (-1.5%)	672 (-9.1%)	<i>Nu</i> = 0.200 <i>Ra</i> ^{1/4}

Table 3.4 The effect of the peak and total heat demand for the LEA model for different internal heat transfer coefficients tested with building 62 as described in chapter 5. The maximum inside temperature is listed for the situation when no local cooling is used.

The listed results in Table 3.4 show a significant impact on the chosen relation for the convective heat transfer coefficient. A higher internal heat transfer coefficient increases the peak heat demand and the total heat demand, because heat is transferred to the concrete at a higher rate.

3.6. Ventilation

The heat entering or leaving the building via ventilation Q_v consists of a mechanical part $Q_{v,mech}$ and a natural part $Q_{v,nat}$:

$$Q_v = Q_{v,mech} + Q_{v,nat} \quad (3.44)$$

3.6.1. Heat transfer via mechanical ventilation

The air supplied to the rooms via mechanical ventilation is heated or cooled in the air handling unit to temperatures as defined by the heating curve (the supply temperature). The heating curve describes the air supply temperature as a linear function of the outside temperature, an example is shown in Figure 3.14. If no heat recovery is present the supply temperature is equal to the outside temperature. The ventilation rate is an operational parameter for the building and an input for the model. The ventilation rate is given as a volume per unit of time. The mechanical ventilation rate has values for opening hours and for non-opening hours of the building.

The amount of heat entering or leaving the building as a result of colder air entering via mechanical ventilation is calculated from the ventilation rate \dot{V}_{mech} , the density of air ρ_{air} , the specific heat of the air $C_{p,air}$ and the temperature difference between the supplied air T_{sup} and the temperature in the rooms T_{in} :

$$\dot{Q}_{v,mech} = \dot{V}_{mech} \rho_{air} C_{p,air} (T_{in} - T_{sup}) \quad (3.45)$$

3.6.2. Heat transfer via natural ventilation

Natural ventilated air is not heated in the air handling unit according to the heating curve. The temperature of the air entering the building is equal to the outside temperature. The natural ventilation rate \dot{V}_{nat} and the infiltration rate \dot{V}_{inf} are given as inputs for the model. The heat leaving the building via natural ventilation and infiltration is calculated from inside to outside temperature difference:

$$\dot{Q}_{v,nat} = (\dot{V}_{nat} + \dot{V}_{inf}) \rho_{air} C_{p,air} (T_{in} - T_{out}) \quad (3.46)$$

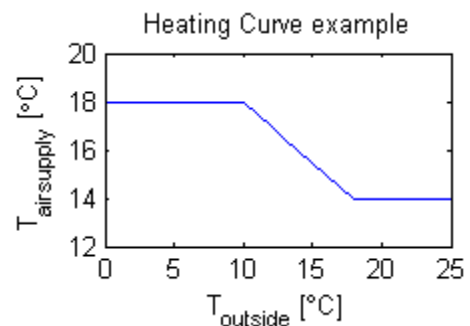


Figure 3.14 Example of heating curve used in building where outside temperature determines the temperature of the supplied ventilation air

3.6.3. Air handling unit

The air handling unit heats or cools the air before entering the building via mechanical ventilation. The amount of heat supplied to the air in the air handling unit is:

$$\dot{Q}_{AHU} = \dot{V}_{mech} \rho_{air} C_{p,air} (T_{sup} - T_{out}) \quad (3.47)$$

If prescribed in the model input the air handling unit can also humidify or dehumidify the air. The model calculates whether the air needs to be dehumidified or humidified (either via steam or water depending on model input) by checking the humidity against its maximum and minimum prescribed values.

The absolute humidity and the enthalpy for the air before the AHU and for the desired supply air are calculated. The absolute humidity is the basis for the calculation of the desired humidification and the enthalpy is the basis for the calculation of the heat transferred to the air. The thermodynamic properties are calculated via approximations of the Mollier diagram for air. An approximation is made for the maximum absolute humidity as a function of the temperature with a deviation smaller than 0.2g/kg for temperatures below 50°C.

The enthalpy of the wet air is calculated from the specific heat of the water $C_{p,w}$ and air $C_{p,a}$ and the heat of evaporation of water h_{we} which are taken as constants. The enthalpy is thus a function of the temperature T [°C] and the absolute humidity of the air x [g_{water}/kg_{air}] as calculated in equation (3.48). Unlike the room energy use, the energy use in the air handling unit is calculated once per hour.

$$h(T, x) = C_{p,a}T + (h_{we} + C_{p,w}T)x \quad (3.48)$$

3.6.3.1. Humidification and dehumidification

Humidification can be done either via the addition of water or steam depending on the air handling unit. Energy added when humidifying with water is neglected since no heating or cooling is done. The energy associated with the humidification of the air in the air handling unit with steam is calculated from the absolute humidity of the air before x_{curr} and after the air handling unit x_{AHU} , the heat of evaporation of water h_{we} and the mass flow of the air through the air handling unit \dot{m}_{air} :

$$\dot{E}_{humid} = h_{we}(x_{AHU} - x_{curr})\dot{m}_{air} \quad (3.49)$$

When only humidification and no heating or cooling is necessary, the desired humidity cannot always be reached since too much added moist will cool the air below the desired temperature. In this case the temperature bounds are more important.

Dehumidification is done via cooling to the desired absolute humidity, extracting the condensed water and then reheating to the desired temperature. If no reheat is present in the air handling unit no dehumidification can take place.

3.6.3.2. Heat recovery

When heat recovery equipment is present in the air handling unit, the model will calculate the amount of heat recovered based on the inside air, outside air and the demand temperature, the heat recovery efficiency and the control system of the heat recovery. When heat recovery is used

the heat supply for the air handling unit can be calculated similarly to the normal heat recovery with the heat recovery efficiency η_{hr} taken into account.

$$\dot{Q}_{AHU} = (1 - \eta_{hr})\dot{V}_{mech}\rho_{air}C_{p,air}(T_{supply} - T_{out}) \quad (3.50)$$

3.7. Review on the model

Some inaccuracies in the LEA model can be identified. The model is based on uniformity and an office use, so the input is an average over the facades and the building. The accumulation of heat in the building is simplified by accumulation in the ceiling and floor modelled as being symmetrical. The accumulation in the walls is not modelled separately.

Also the heat transfer coefficients are fixed single value averages for the inside and outside heat transfer to the walls in the original LEA model. In literature a wide range of relations for the heat transfer coefficient exists, making the heat transfer coefficient an uncertainty for the modelled heat demand. The outside convective heat transfer coefficient is changed to a wind speed dependent value for this study, while the actual outside convective heat transfer coefficient is a function of the local wind speed, size of the building, temperature difference between the building and the air, the angle between the wind direction and the façade direction, et cetera.

Also the usage profiles of the university buildings are not very constant for the university buildings both in time and in equal distribution within the buildings, especially at locations with many students.

3.8. Changes to the LEA model

To create a more flexible and more constant heat demand some adaptations are made to the model. A function is made to prescribe the heat input to the model. The heat input can be prescribed as a base load heat demand or as any other heat supply profile. The heat input adaptation is prescribed in chapter 3.8.1. Also a module for phase change materials is developed as described in chapter 4.

3.8.1. Continuous heating / base load heat

In normal operation the heat demand peaks in the morning when all buildings connected to the heating grid demand peak heat to increase the temperature from the night values to the day values. To lower the peak the building can be preheated during the night. As a result the peak heat demand will decrease and the total heat demand will increase. Secondly a base load heat demand can be interesting when also a base load supply is fixed to grid. For the TU Delft grid the planned geothermal well could supply such a base load of heat.

In normal operation of the LEA model the heat demand is calculated from the maximum and minimum internal temperature and the heat loss and gain from the environment, people, installations, et cetera. With the heat supply strategy function a heat supply profile can be given as an input.

The supplied heat demand profile will be a minimum heat demand for when the inside temperature is lower than the minimum daytime temperature. When the regular heat demand is larger than the supplied temperature profile extra heat will be added calculated. The base load heat strategy function will thus only be active during non-operating hours of the building.

3.8.2. Use of the heat input functionality

The heat supply functionality can be used for several purposes, for instance for a base load heat to match with the constant supply from a geothermal source.

The base load functionality can also be used as a feedback from the WANDA¹ model. The WANDA model is used for simulation of the TU Delft district heating grid in the IPIN project. The connection between the WANDA model and the LEA model uses the heat demand as calculated by the LEA model to calculate the maximum heat that can be supplied by the district heating system. The supplied heat could be lower than the demanded heat at quick ramp ups in heat demand or at a demand exceeding the maximum supply. The WANDA model gives feedback to the LEA model for the maximum heat supply to the building, which in turn can recalculate the heat demand with this desired heat demand. However since the modelled temperature in the building is limited by its set minimum value care should be taken when using this approach.

Another strategy would be to use successive heating for the different buildings at the campus. This successive heating can also be modelled by supplying a predetermined profile to the LEA model with an early night heat demand.

¹ WANDA is a hydraulic simulation model by Deltares, which is used in the INPIN project to simulate the TU Delft district heating grid

4. PCM module

To incorporate the use of phase change materials (PCMs) in the LEA model a new module is developed for phase change materials. The module can be loaded with properties for PCMs used in the built environment. The PCM uses the inside air temperature and the wall temperature as input variables to calculate the heat transfer to the indoor air and to the air above the suspended ceiling.

4.1. Phase change materials use

The phase change materials increase the thermal mass at its melting temperature range. Part of the internal heat production by people, appliances and lighting and the heat entering via solar radiation is stored in the phase change material modules and can be released when temperature in the building is lower than the temperature in the PCM. This is shown in Figure 4.1 where “A” represents the time in which the PCM could accumulate heat which is could then be transferred back to the air during “B”.

Phase change materials increase the thermal mass of the building at the phase change temperature range of the applied PCM. The PCM changes phase not at one specific temperature, but at a temperature range. The properties of the PCM are described with a melting and a solidification / coagulation temperature. PCMs can be made for any given temperature range for building applications according to PCM manufacturers. For PCM use in building applications the melting and solidification temperatures are dependent on the purpose of the PCM. In the this model the PCM is used to mitigate the indoor temperature, so the melting and solidification temperatures should be close to each other and within the indoor temperature range.

At any time the PCM will contain a combination of the liquid, solid and mushy phase. The mushy phase is the phase in between the liquid and the solid phase. The phases in the PCM can coexist in the PCM, thus in the PCM one, two or three phases can be present at the same time.

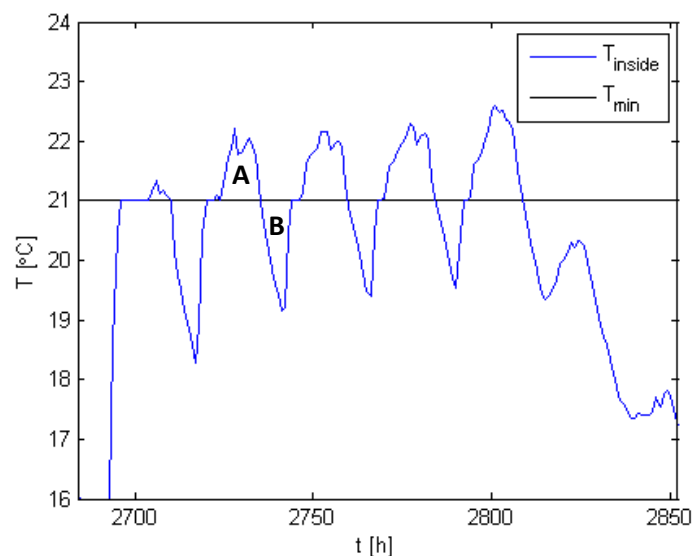


Figure 4.1 Potential for heat storage in phase change materials. When the temperature in the building exceeds the minimum temperature in the building for opening hours, heat can be stored to reduce heat demand for later.

4.2. PCM modelling approach / method

4.2.1. Modelling approach

PCMs can be modelled with different approaches differing in computational time and accuracy. The most accurate models need a large computational power and the models using less CPU are usually less accurate. The most accurate simulation of phase change materials is done via a computational fluid dynamics (CFD) model. With the CFD model an accurate 2D representation of the PCM and the flows of the liquid and mush zone and the convective and conductive heat transfer can be made. However this requires a large computational power when a full year is modelled. Enthalpy based models are also widely used within the simulation of phase change materials. Enthalpy based models are less accurate and need less CPU than CFD models.

In this project the phase change materials are modelled according to the modelling methodology from Mirzaei [22]. This methodology models the phase change materials as a one-dimensional circuit of resistive and capacitive modules for the different phases present in the PCM-module. The size of the RC-components changes over time as a result of the shift in the size of the phases present. The modelling approach gives results accurate enough without the need for an extensive CFD calculation and a large CPU cost.

Combinations of liquid, mush and solid phase and single phases in the PCM are possible and are modelled. The heat transfer to and within the PCM is modelled as unsteady one-dimensional heat transfer.

The existence per phase is modelled such that all material present in one phase is modelled with one resistive-capacitive-component. This differs from the more extensive modelling approaches like CFD models, which calculate presence of phases for all grid points. Within a configuration anywhere between one and three phase modelled components can be present.

Within the phases in the PCM a linear temperature profile is assumed and within the mushy zone a linear distribution of the liquid fraction and the density is assumed. The bound of the mushy zone will always be at the melting and the solidification temperature when the bound is with the fluid or the solid zone.

If the Biot number is close to one, the assumption of a linear temperature profile is valid. The Biot number is determined for the solid situation, for the mushy situation the Biot number is equal and for the liquid situation the governing heat transfer phenomenon is convective so the Biot number doesn't apply.

$$Bi_{PCM} = \frac{h_c L}{k_s} = \frac{10 * 0.05}{0.6} = 0.83 \approx 1$$

4.3. PCM model

4.3.1. Phenomena

In this chapter the relevant phenomena in the PCM and how these are modelled are briefly described. The phenomena modelled are:

1. Heat transfer to the phase change material
2. Conductive heat transfer through the solid
3. Conductive heat transfer through the mush
4. Convective heat transfer through the liquid
5. Heat accumulation in the solid
6. Heat accumulation in the liquid
7. Heat accumulation by phase shift from solid to mush
8. Heat accumulation by phase shift from mush to liquid
9. Heat accumulation in the mush

4.3.1.1. Heat transfer to the phase change material

Heat is transferred to the PCM from the room and from the ceiling. The heat transfer coefficients depend on the configuration of the PCMs which is described in chapter 4.5.

Heat transfer from the air to the PCM with the heat transfer coefficient h_{in} :

$$\dot{q}_{in} = \dot{q}_{in,air} = h_{in}(T_1 - T_{air}) \quad (4.1)$$

Heat transfer from the ceiling to the PCM:

$$-\dot{q}_{out} = \dot{q}_{in,ceil} = h_{ceil}(T_{14} - T_{ceil}) \quad (4.2)$$

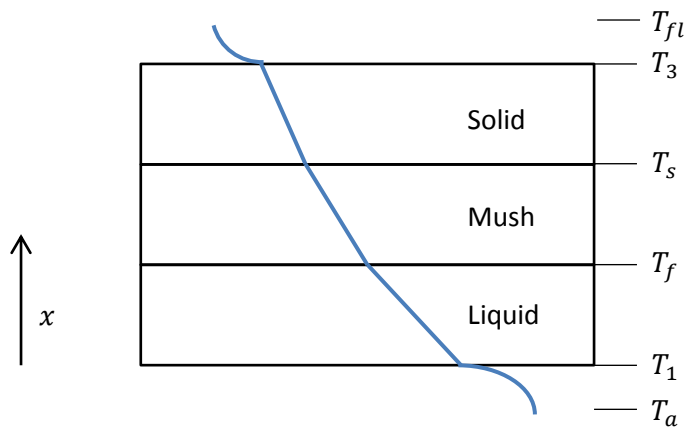


Figure 4.2 Schematic of temperature distribution in PCM

4.3.1.2. Heat transfer within the PCM

Heat transfer in the PCM is modelled between the heat storage components of the PCM. So heat transfer is modelled between the solid and the mush, through the mush and between the mush and the liquid part. The three heat transfer parts in the PCM are described with 3 phenomena:

conductive heat transfer through the solid, conductive heat transfer through the mush and convective heat transfer in the liquid.

The conductive heat transfer through the mush and the solid are calculated according to Fourier's law of heat conduction with the one-dimensional conductive heat transfer equations with the conductivity of the solid k_s and the mush k_m as described by equations (4.3) and (4.4).

$$\dot{q}_s = -k_s \frac{dT}{dx} \quad (4.3)$$

$$\dot{q}_m = -k_m \frac{dT}{dx} \quad (4.4)$$

To determine how the heat transfer through the liquid can be modelled the Rayleigh number is determined to check whether cellular convection will take place. The Rayleigh number is a dimensionless number which describes the rate of buoyancy driven flow for natural convection. If the Rayleigh number is smaller than 1708 no cellular convection will take place and the heat transfer can be considered as conductive heat transfer. The Rayleigh number Ra is calculated from the thermal expansion coefficient β , the difference in temperature at the two sides of the fluid in the PCM, the gravitational constant g , the length of the fluid in the PCM L_f , the kinematic viscosity ν and the thermal diffusivity α . β is calculated from the data sheet for the PCM used in the simulation, which states a 4% volume expansion around the phase change range with a ΔT of 20K. So $\beta \approx 0.002$

$$Ra = \frac{\beta \Delta T g L_f^3}{\nu \alpha} \quad (4.5)$$

With for the properties of the phase change material used in the simulation (see Table 4.1):

$$\nu = 1.111e - 4 \text{ m}^2/\text{s}, \quad \alpha = \frac{k}{\rho C_p} = \frac{0.8}{1430 * 2000} \text{ m}^2/\text{s}$$

So for an average case with $\Delta T = 1K$ and $L = 0.01m$, the Rayleigh number will become:

$$Ra_{avg} = 6.5e2$$

So for an average situation no cellular convection will be present in the PCM. The leading phenomenon for heat transfer through the liquid will thus be conduction.

For a more extreme situation where the PCM is completely is a liquid phase at a temperature difference of about 4K:

$$Ra \approx 3.2 * 10^5, \quad \Delta T = 4K, \quad L_f = 0.05m$$

For Rayleigh numbers between $1870 \leq Ra_L \leq 10^5$ the relation by Hollands [2] is used as written in (4.6). If one of the terms in the relation is negative it should be set to zero, so for $Ra < 5350$ the Nusselt number is equal to 1 and the heat transfer can be modelled as conductive heat transfer.

$$Nu_L = 1 + 1.44 \left[1 - \frac{1708}{Ra} \right] \left[\left(\frac{Ra}{5830} \right)^{\frac{1}{3}} - 1 \right] \quad (4.6)$$

For situations with a higher Rayleigh the relation for the Nusselt number by Globe and Dropkin is used [23], which uses the Rayleigh number Ra and the Prandtl number Pr :

$$Nu_L = 0.069Ra^{1/3}Pr^{0.074} \quad (4.7)$$

This relation can be used for a Rayleigh range of $3 * 10^5 \leq Ra_L \leq 7 * 10^9$

The Prandtl number is calculated from the specific heat capacity $C_{p,f}$, the dynamic viscosity μ_f and the thermal conductivity k_f .

$$Pr = \frac{C_{p,f}\mu_f}{k_f} \quad (4.8)$$

For Rayleigh numbers smaller than 5830 the Nusselt number is set to one equalling conductive heat transfer. For $3 * 10^5 \leq Ra_L \leq 10^5$ no relation was found in literature. For this model a linear interpolation is used between the relation of equation (4.6) and (4.7) for $10^5 < Ra_L < 3 * 10^5$. The heat transfer coefficient h_c can be expressed as a function of the Nusselt number, the thickness of the fluid layer L_f and the thermal conductivity of the fluid k_f :

$$h_c = Nu_L \frac{k_f}{L_f} \quad (4.9)$$

If Nusselt is smaller than one, heat transfer is via conduction primarily and the heat transfer coefficient is $h_c = k/L$.

4.3.1.3. Accumulation of heat in the PCM

The heat transferred to the PCM is accumulated in the PCM via five phenomena: temperature increase of the liquid, temperature increase of the solid, phase change from solid to mush, phase change from mush to liquid and temperature increase of the mush. Depending on the composition at the time step the different phenomena are modelled. Temperature increase of the mush is only present when the mush is not bound with the liquid and the solid phase.

The heat storage in the solid and liquid are modelled by the integral over the length of the fluid or solid part of the PCM L_f, L_s with an assumed constant specific heat capacity C_p and density ρ , as stated in (4.10) and (4.11). The temperature is assumed to be linear and the temperature at the bound with the mush phase is equal to the solidification temperature or the melting temperature for the solid and the liquid phase.

$$\dot{q} = C_{p,f}\rho_f \int_0^{L_f} \frac{dT}{dt} dx \quad (4.10)$$

$$\dot{q} = C_{p,s}\rho_s \int_0^{L_s} \frac{dT}{dt} dx \quad (4.11)$$

Storage of heat by phase shift from solid to mush takes place when the temperature in the solid exceeds the solidification temperature. Storage of heat is in this case proportional to the mass accumulation of mush from solid. As a result of the accumulation of mush, the linear temperature profile will shift. This results in an increase in liquid fraction for all x in the mush and thus the stored heat in the PCM module. This is represented by the change from 1 to 2 in Figure 4.3.

The heat storage can be calculated via equation (4.12) with the relations for the density and liquid fraction as indicated in equations (4.14), (4.15) and (4.16) and with λ for the latent heat, Δt for the used time step, l_s for the increase in length of the solid phase and L_m for the length of the mushy zone.

$$\dot{q}_{s \rightarrow m} = -\frac{\lambda}{\Delta t} \left[\int_0^{l_s} \rho_1 \beta_1 dx + \int_{l_s}^{L_m} (\rho_1 \beta_1 - \rho_2 \beta_2) dx \right] \quad (4.12)$$

The storage of heat by phase shift from mush to liquid is similar to the storage by the phase change from solid to mush and can be described by the transition from 2 to 3 in Figure 4.3 and by equation (4.13):

$$\dot{q}_{m \rightarrow f} = -\frac{\lambda}{\Delta t} A \left[\int_{l_s}^{L_m} (\rho_2 \beta_2 - \rho_3 \beta_3) dx + \int_{L_m}^{L_m+l_f} (\rho_f - \rho_3 \beta_3) dx \right] \quad (4.13)$$

With:

$$\rho_1 = \rho_s + \frac{\rho_f - \rho_s}{l_s + l_m} x, \quad \beta_1 = \frac{x}{l_s + l_m} \quad (4.14)$$

$$\rho_2 = \rho_s + \frac{\rho_f - \rho_s}{l_m} (x - l_s), \quad \beta_2 = \frac{x - l_s}{l_m} \quad (4.15)$$

$$\rho_3 = \rho_s + \frac{\rho_f - \rho_s}{l_m + l_f} (x - l_s), \quad \beta_3 = \frac{x - l_s}{l_m + l_f} \quad (4.16)$$

$$L_s(i) = L_s(i-1) + l_s \quad (4.17)$$

$$L_m(i) = L_m(i-1) - l_s + l_f \quad (4.18)$$

$$L_f(i) = L_f(i-1) - l_f \quad (4.19)$$

When the mush is not bound with the solid or liquid the temperature at the bound can increase or decrease. The accumulation of heat means an increase of the liquid fraction in the mush. The accumulation of heat in the mush is described in equation (4.20) with T_f the melting temperature

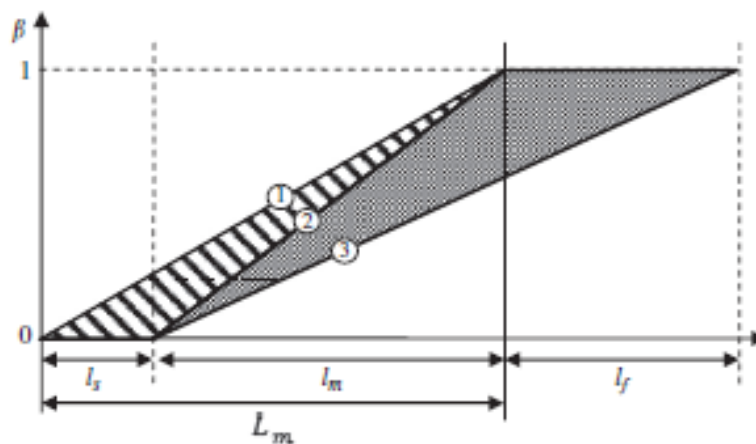


Figure 4.3 Phase shift in PCM as applied in model by heating, with beta the liquid fraction and L the length of the PCM. The PCM shifts from solid to mush 1 \rightarrow 2, and part of the mush is changed to liquid 2 \rightarrow 3.

and T_s the solidification temperature.

$$\dot{q} = \frac{\lambda}{T_f - T_s} \int_0^{L_m} \rho_m \frac{dT}{dt} dx \quad (4.20)$$

With:

$$\rho_m = \rho_s + \beta(\rho_f - \rho_s), \quad \beta = \frac{T - T_s}{T_f - T_s} \quad (4.21)$$

4.3.1.4. Time step

The LEA model is simulated with a time step of 120 seconds, though for the PCM a smaller time step is necessary, because of the small size of the PCM. The time step is fixed to one second in the PCM module, so for every time step in the LEA model 120 steps will be simulated by the PCM module.

4.3.1.5. Existence of phases

When the PCM is operated different configurations of phases are possible and transition to other phases is modelled. A phase is removed in the model when the length of the phase drops below the set minimum threshold length for a phase. This threshold depends on the time step used in the model and is set such that no numerical errors occur. The smaller the time step the smaller the threshold can be and the more accurate the model is.

Phases are added when the temperature in an existing phase exceeds the temperature bounds by more than the temperature threshold (T_{th}). For instance when the PCM consists of a mushy phase only and at one side $T > T_f + T_{th}$, the next time step will be calculated with a coexistence of mush and liquid.

The new situation will be calculated such that the accumulated heat in the PCM is kept constant according to equation (4.22) for the transition from the solid composition to the solid and mush composition. With T_1^s the temperature at position 1 for the solid phase

$$((T_1^s - T_s) + (T_3^s - T_s))C_{p,s}L_{PCM}\rho_s = \frac{T_1^m - T_s}{T_f - T_s}\lambda L_m\rho_m + (T_3^s - T_s)C_{p,s}L_s\rho_s \quad (4.22)$$

When a phase is added the length of the new phase will be calculated and when a phase is removed the new temperature is calculated.

4.4. Choice of PCM and PCM characteristics

General strong points of possible phase change materials are large latent heat and a high thermal conductivity to easily store a large amount of heat. The choice of the PCM for a particular goal is also based on the solidification and melting temperatures of the material. When a PCM is used within buildings the optimum phase change temperatures are between the maximum and minimum indoor temperatures.

As this research focuses on the passive application of PCM material, the material is used in a relatively thin layer making the thermal conductivity less important. The material used for simulation is based on n-paraffins and waxes and commercially available at the company Rubitherm Technologies GmbH with the name Rubitherm RT 21[24]. The thermal properties of the material are

listed in Table 4.1. The melting and congealing take place over a temperature range. For the model the temperatures are used where the most latent heat is stored / released, these values are given in the data sheet.

Property	Variable	Unit	Value
Melting temperature (area)	T_s	$^{\circ}C$	21 (18 – 23)
Congeaing temperature (area)	T_f	$^{\circ}C$	22 (22 – 19)
Heat storage capacity (15-30°C)	λ	kJ/kg	134
Density solid	ρ_s	kg/m^3	$8.8 * 10^2$
Density liquid	ρ_l	kg/m^3	$7.7 * 10^2$
Thermal conductivity	k	W/mK	0.2
Kinematic viscosity	ν	m^2/s	$2.571 * 10^{-5}$

Table 4.1 Thermodynamic properties of simulated phase change material Rubitherm RT21 [24]

The heat storage capacity is given for the temperature increase of 15 °C, while the phase change is modelled for a temperature difference of 1 °C. The latent heat between the melting temperature and the solidification temperature used is the total heat storage capacity minus the specific heat capacity ($C_p = 2000 J/kgK$) times 14. So the latent heat used is 106 kJ/kg .

The amount of phase change material to be put in a building is determined from the heat demand of the building. To obtain maximum usability of the phase change material the latent heat of the phase change material is set to 80% of the average heat load by appliances, people, lighting and solar radiation during the mid-season.

As described earlier up to about 60% of the ceiling surface could be used for phase change materials. So the thickness of the PCM is calculated from:

$$L_{PCM} = \frac{Q}{\rho_{PCM} A_{PCM} \lambda_{PCM}} \quad (4.23)$$

4.5. Configuration of PCM modules

The PCM modules can be configured in several ways in the building both in active and passive application. In this report only PCMs used on the room level are considered, so external buffer vessels are not taken into account. Different options exist for using phase change materials on a room level are:

- PCMs above suspended ceilings
- PCMs incorporated in gypsum panels
- PCMs in concrete walls and ceilings
- PCMs hanging on fins in rooms

4.5.1. PCMs on the suspended ceiling

For this project the PCMs are modelled situated at the suspended ceilings (or dropped ceiling) of the room. The suspended ceiling tiles are replaced with PCM tiles. These tiles are designed for maximum heat transfer from the rooms to the PCM modules. Heat is transferred from the air and from the walls to the PCM at a temperature difference between the PCM and the wall at one side and the PCM and the inside air temperature at the other side. The temperature of the wall and the air are used as input variables and the heat transferred to and from the inside air and the wall are the output variables.

Because of lighting, ventilation and acoustics in the room up till about 60% of the suspended ceiling surface can be used for PCMs.

The heat transfer coefficient for heat transfer from the room to the PCM h_{in} is equal to the heat transfer coefficient for heat transfer from the floor/ceiling to the air as described in in chapter 3.5.2. A heat transfer coefficient of $8 \text{ W/m}^2\text{K}$ is used.

The heat transfer coefficient for heat transfer from the upper side of the phase change material h_{ceil} to the air above the ceiling is preferred small to keep the stored heat in the PCM and more easily release the heat to the air when the temperature in the room drops. A heat transfer coefficient of $0.2 \text{ W/m}^2\text{K}$ is used to model the heat transfer from the PCM to the ceiling.



Figure 4.4 PCMs in suspended ceiling configuration

4.5.2. PCMs in hanging fins from ceiling

PCMs hanging on fins in rooms are also modelled. The PCMs hanging on fins can increase the area of heat transfer with the room since both sides of the PCM exchange heat with air and a large convective area can be used when long slaps of PCM material are hung at the ceiling. Also forced convection could be applied when fins are hanging on the ceiling forced convection can be used to increase heat transfer from the air. The area to volume ratio is increased which decreases the phase change time of the PCM. A schematic of PCMs with the fin configuration is shown in Figure 4.5. The PCM fin configuration requires a larger modification of the interior than the suspended ceiling configuration requires.

When PCM are hung in the room the PCMs the radiative area $A_{PCM,r}$ is equal to the area over which the PCMs are hung, while the convective area A_c is equal to the area of the PCM modules as indicated in Figure 4.5.

The convective heat transfer area will be a twice the product of the number of PCM fins per meter length n_{PCM} and the height of the PCM fin h_{PCM}

$$A_{PCM,c} = 2n_{PCM} * h_{PCM} \quad (4.24)$$

The average Nusselt number for laminar flow over a hot plate with a sharp leading edge can be calculated with the relation from Churchill and Chu [2]:

$$\overline{Nu}_h = 0.68 + 0.67(Ra\Psi)^{1/4}, \quad Ra \leq 10^9 \quad (4.25)$$

With the Prandtl number relation Ψ :

$$\Psi = \left[1 + \left(\frac{0.492}{Pr} \right)^{9/16} \right]^{-16/9} \quad (4.26)$$

For a configuration where $h_{PCM} = 0.2$, $n_{PCM} = 5$ and $\Delta T = 1.5K$, the average heat transfer coefficient is approximately $5.5 W/m^2K$, compared to a maximum of $3 W/m^2K$ for the suspended ceiling case. For the fin case the convective heat transfer area is 2 times the ceiling area needed to hang the fins.

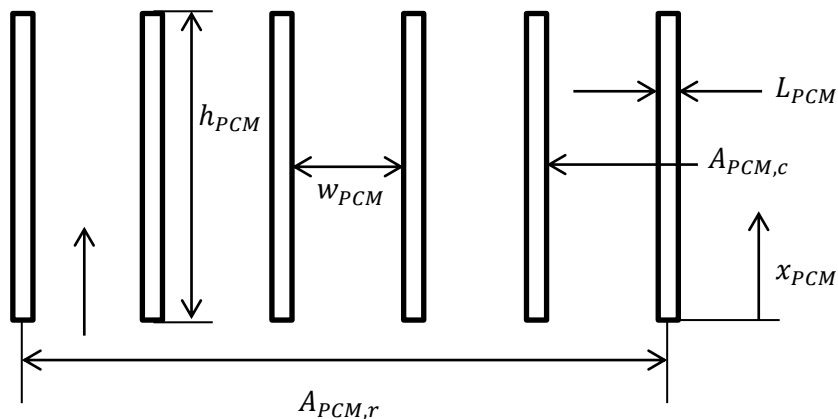


Figure 4.5 Schematic of PCM modules in fin configuration

Comparing the convective heat transfer for the fins in PCM configuration with the PCMs at a suspended ceiling configuration, the convective heat transfer will be 2.9 times as high.

The heat transfer in the case of the fins will be:

$$\dot{Q}_{PCM} = (h_c A_{PCM,c} + h_r A_{PCM,r}) \Delta T \quad (4.27)$$

So the ratio of heat transfer for a fin case compared to the ceiling case will be:

$$\frac{(A_{PCM,c} * h_c + A_{PCM,r} h_r)}{A_{PCM}(h_c + h_r)} \quad (4.28)$$

The local heat transfer coefficient will differ from the average heat transfer coefficient:

$$h(x_{PCM}) = h_c(x_{PCM}) + h_r(x_{PCM}) \quad (4.29)$$

The radiative heat transfer coefficient is a function of the shape factor for radiative heat transfer from the PCM fin to the room. Between the PCM fins no radiative heat transfer takes place since the PCM fins have a uniform temperature at the outside bound. The view factor is a function of the width between two PCM plates w_{PCM} and the vertical position x_{PCM} and is plotted in Figure 4.7b.

$$h_r(x_{PCM}) = F_s(x) \bar{h}_r = \frac{1}{\pi} \tan^{-1} \left(\frac{w}{x} \right) \bar{h}_r \quad (4.30)$$

The heat transfer coefficients for the 4 configurations are listed in Table 4.2.

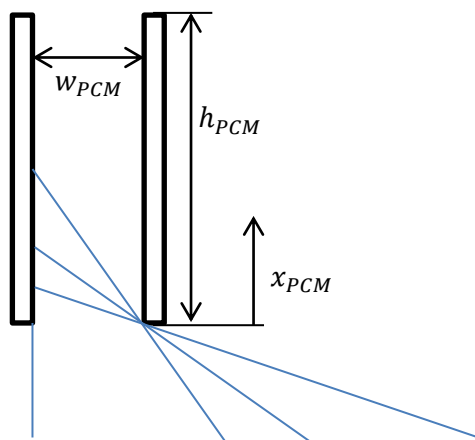


Figure 4.7a Schematic representation of shape factor

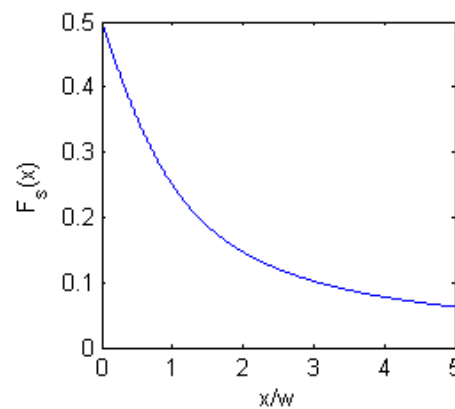


Figure 4.7b Shape factor for PCM fins as a function of the position on the fins x to the width between 2 fins

	Situation 1	Situation 2	Situation 3	Situation 4
h_{PCM} [m]	0.2	0.5	0.2	0.5
L_{PCM} [m]	0.02	0.02	0.02	0.02
w_{PCM} [m]	0.18	0.18	0.08	0.08
n_{PCM}	5	5	10	10
ΔT [K]	1.5	1.5	1.5	1.5
Ra	$1.3 \cdot 10^6$	$2 \cdot 10^7$	$1.3 \cdot 10^6$	$2 \cdot 10^7$
\overline{Nu}_h	18	35	18	35
\overline{h}_c [W/m^2K]	2.3	1.8	2.3	1.8
\overline{h} [W/m^2K]	4.9	2.8	3.6	2.3
$\overline{h} * A_c/A_{ceiling}$ [W/m^2K]	9.8	14.2	14.4	23.2
Ratio of heat transfer for finned PCM to suspended ceiling PCM	1.2	1.8	1.8	2.9

Table 4.2 Heat transfer coefficients for the PCM fins for 4 different combinations of height and distribution

5. Simulation of TU Delft buildings with the LEA model

Three buildings at the TU Delft campus are selected based on criteria stated in 5.1. The selected buildings are simulated in their normal case as a reference scenario. All buildings are simulated with the use phase change materials and with different heating strategies. The results are combined to identify an optimum configuration in which the peak demand is lowered and fluctuations are decreased to better adapt to the heat supply.

5.1. Buildings

The model as described in chapter 4 will be applied to three buildings at the TU Delft campus. Therefore three buildings on the TU Delft district heating grid are selected and modelled.

The selection of buildings at the TU Delft campus is done with several selection criteria. Buildings are selected which are suitable to be modelled in the LEA model and show some differences in the characteristics. The suitability of the LEA model for the buildings is described in chapter 3.

The selection criteria used are: office like buildings, uniformity and different levels of insulation and thermal inertia. The first two selection criteria are criteria for which the LEA model is designed and thus gives the best results. Buildings with different levels of insulation and thermal inertia were preferred however in the TU Delft campus all buildings are heavy buildings and have similar levels of thermal inertia. As a result a strategy can be developed on a grid level to lower the peak heat demand and the hourly fluctuations in the heat demand. Buildings are chosen which are more suited to the LEA model in terms of use profile and an office like application to present more reliable results. Buildings with a highly fluctuation use like the Aula or the sport centre or buildings with large non-office functions like industrial design and the university library are not selected.

The three selected buildings are OTB, TBM and the high-rise part of the aerospace faculty. The high-rise part is decoupled from the other parts by creating adiabatic walls at the intersections via the input of a very high heat transfer resistance.

The buildings will be briefly described and the heat profiles according to the Rotterdam weather of 2011 will be calculated and matched to the 2011 heat use data.

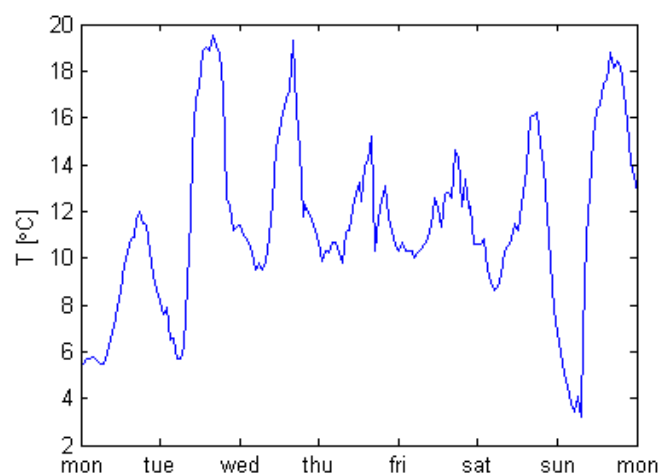


Figure 5.1 Outside temperature according to the TEMPREF base case for De Bilt in week 18. The temperature difference between day and night makes this week suited for diurnal storage with PCMs.

5.1.1. 62 Aerospace building

The high-rise part of the aerospace building is a 13 floor part of the building which hosts offices and project workspaces. The modelled part starts from the second floor and part of one side façade and part of the bottom façade are bound to other parts of the building and thus modelled as adiabatic.

The total heat demand of the aerospace faculty in 2011 was 2564 MWh. The part of the heat used for the high-rise part of the aerospace faculty is unknown. The input variables for the simulation of the AEh building with the LEA model are given in appendix 1.

The total heat demand calculated with the LEA model is 348 MWh and the peak heat demand is 0.69MW, the heat demand calculations will be related to this situation.

5.1.2. 31 TBM

The TBM building is the building for the Technology, Policy and Management faculty and hosts offices, lecture halls and student working places. The building is characterized by a large external area to volume ratio.

The input variables for the simulation of the TBM building with the LEA model are given in appendix 1. The total heat demand in 2011 was 763 MWh and the total heat demand calculated with the LEA model is 755 MWh with a peak heat demand of 1.02MW.

5.1.3. 30 OTB

The OTB building is a building with about 9300 m² gross floor area, which contains the service desk for the university and some offices, the OTB building has few education facilities. Building 30 has a high ventilation rate and low occupation compared to buildings 62 and 31, as a result the internal load is smaller and the temperature in the building is lower in summer periods compared to 62 and 31. The input variables for the simulation of the OTB building with the LEA model are described in appendix 1.

The total heat demand in 2011 was 494 MWh and the total heat demand calculated with the LEA model is 488 MWh with a peak heat demand of 0.80 MW.

5.2. Simulations and results

5.2.1. PCM simulation 62 AE

The application of PCMs on the suspended ceiling and on PCM fins is simulated for building 62 with the climate scenario TEMPREF base case for De Bilt, with different heating strategies. The total annual heat demand and the peak heat demand are calculated for PCM use and for the reference heat strategy.

The amount of phase change material is calculated from the mid-season heat demand according to equation (4.23). The internal heat load and the solar heat load combined are about 1.0 MWh per day in the mid-season (March to October), so the latent heat to be stored in the phase change materials is set to 80% of the load: 800kWh or 2.9GJ, which is equal to 0.2 % of the total heat demand of the building. The thickness of the PCM on the suspended ceiling used is thus:

$$L_{PCM} = \frac{Q}{\rho_{PCM} A_{PCM} \lambda_{PCM}} = \frac{2.9 * 10^9}{880 * 4.6 * 10^3 * 106 * 10^3} = 0.007m$$

The two simulated configurations have an equal amount of phase change material. The fin height used is 0.20 m and the thickness is equal to the thickness of the PCM on the suspended ceiling.

5.2.1.1. Standard heating strategy building 62

The peak heat demand will increase as a result of the applied PCMs, because sensible part of the phase change material has to be heated as well during peak heat demand. The effect on the total heat demand however is limited. As can be seen clearly in Figure 5.2 heat is stored in the phase change material during the day and released during the night. Only up to 35% of the heat storage capacity is used for the fin configuration while a full storage and release of heat would give the optimum efficiency of the phase change material. Not all stored heat is released during the night, so the PCM configurations as simulated are not showing optimum diurnal heat storage. As can be seen in Figure 5.2c, the PCM uses full heat storage capacity in the summer, so the phase change material operates as seasonal heat storage more than diurnal heat storage.

Looking at the peak heat demand and total heat demand as listed in Table 5.1 shows a small increase in the peak heat demand for a building with the use of PCM fins. This increased peak is caused by the sensible heat of the phase change material. When the building is cooled down to its minimum night value the PCM increases the thermal inertia of the building increasing the peak heat demand. The peak heat demand of the PCM on the suspended ceiling however is decreased by 12% compared with the base case. This is due to the fact that the PCM at the suspended ceiling acts as an insulation of the concrete resulting in a small heat transfer between the ceiling and the PCMs.

Heat demand for building 62	Peak [kW]	Total [MWh]	Total stored heat in PCM [MWh]
Standard heating no PCM (base case)	738	410	-
Standard heating 7 mm PCM suspended ceiling	647	406	73 (39)
Standard heating 7 mm PCM fins	740	409	71 (34)

Table 5.1 Peak and total heat demand for building 62 for one year simulated with TEMPREF base without PCM and with PCM in suspended ceiling configuration for the standard heating strategy. The amount of heat stored in the PCMs during one year and heat stored by means of phase change in parentheses.

The total heat demand also rises as a result of the application of phase change material; this is caused by the increased heat loss to the environment as a result of the increased average temperature in the building which increases the heat losses to the environment via the facades and via ventilation. The heat demand in the mid-season and summer (between hour 2000 and 7000) is reduced by 10% as a result of the PCM in both configurations, however only 10% of the heat demand is used in the mid-season, so the effect on the total heat demand is only a 1% decrease.

The total amount of heat transferred to the PCM at the suspended and the PCM fin are listed in Table 5.1. The total heat transferred to the PCM is not just the amount of phase change but also includes heat transfer in summer periods when the PCM temperature fluctuates in liquid state and outside opening hours in colder periods when the PCM temperature fluctuates in solid state.

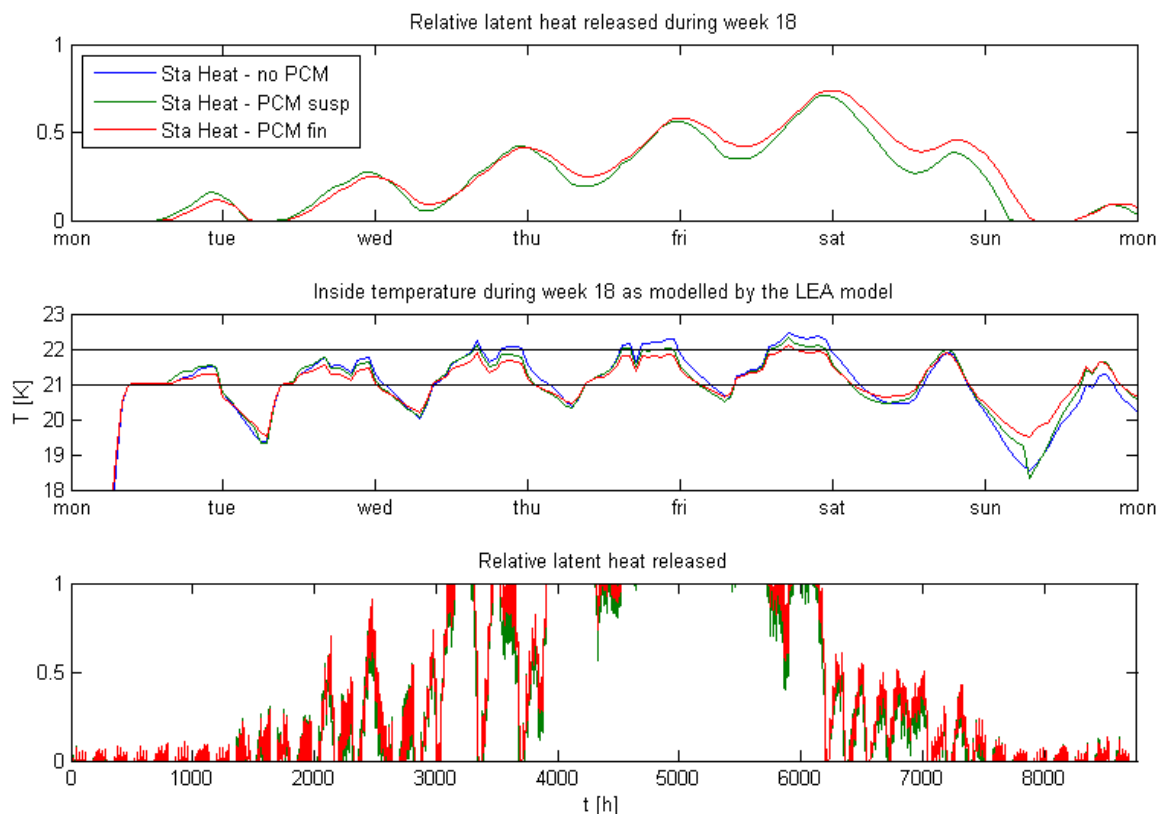


Figure 5.2 Results of simulation of building 62 without PCM, with 7 mm PCM on suspended ceiling and with 7 mm thick PCM fins with the TEMPREF base case climate scenario for a standard heating strategy. The first figure shows the heat stored to the total latent heat of the PCM in the PCM for a week in the season in which the PCM shows maximum use. The fin configuration shows a higher stored heat rate since the area to volume ratio is higher. The second figure shows the temperature in the building for the same week, the PCM has a mitigating effect on the temperature, with the effect at PCM fins higher than at the suspended ceiling case. The third figure show the rate of heat stored in the PCM throughout the simulated year starting from January first to December 31th.

5.2.1.2. 24/7 heating strategy building 62

The results for the simulation of the heat demand for building 62 with the 24/7 heating strategy are shown in Table 5.2 and Figure 5.3. Figure 5.3a shows the amount of heat stored for a week in the season when during daytime the heat gain from solar energy and internal production exceeds the heat loss to the environment (between hour 2000 to 7000). The amount of heat stored during one day is up to 30 % of the total heat storage capacity of the phase change material for the PCM fin configuration. The amount of heat released during the night is up to 20% of the PCM heat storage capacity as a result of the small temperature difference between the air temperature and the PCM temperature. When more heat is stored in the PCM the release of heat is larger due to the increased temperature gradient. For the suspended ceiling case the heat stored in one day is up to 27% and the heat released during the night is 18% of the total heat storage capacity.

Heat demand for building 62	Peak [kW]	Total [MWh]	Total stored heat in PCM [MWh]
24/7 heating no PCM	426	487	-
24/7 heating 7 mm PCM suspended ceiling	425	484	55 (42)
24/7 heating 7 mm PCM fins	422	478	53 (38)

Table 5.2 Peak and total heat demand for building 62 simulated with TEMPREF base without PCM and with PCM in suspended ceiling configuration for the 24/7 heating strategy. . The amount of heat stored in the PCMs during one year and heat stored by means of phase change in parentheses.

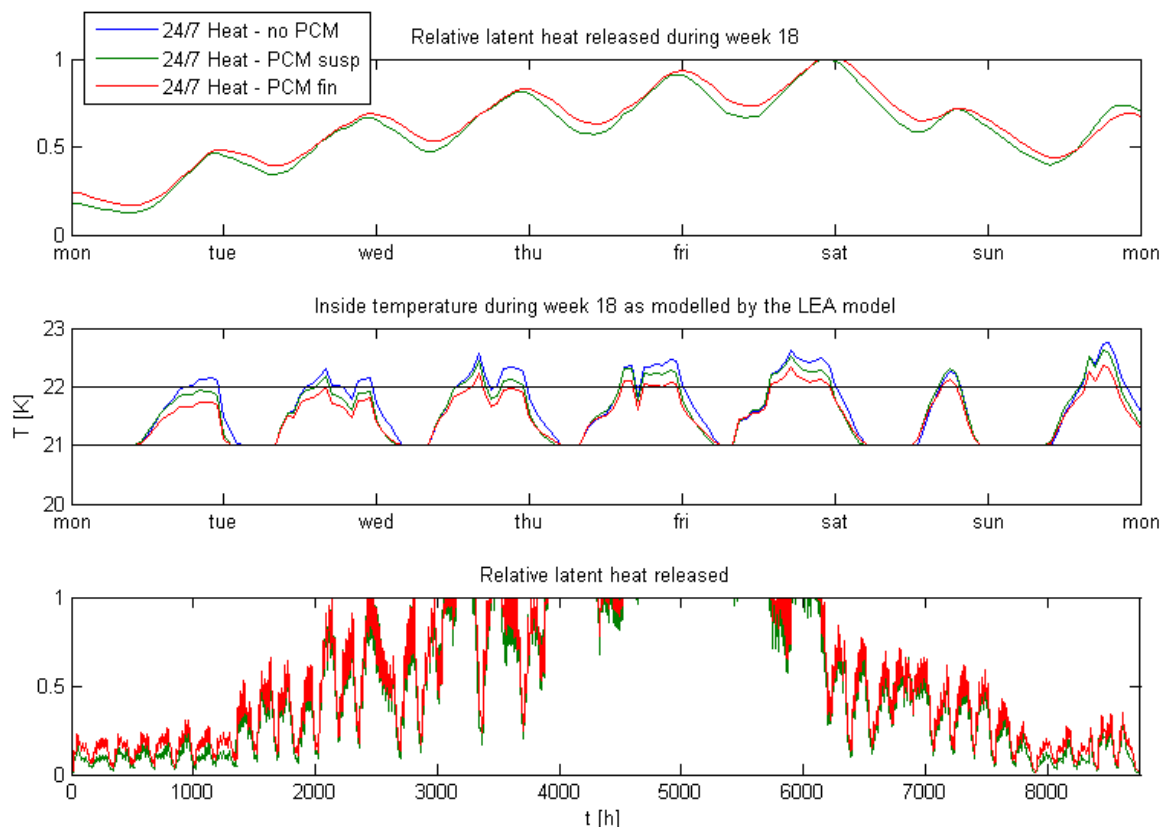


Figure 5.3 Results of simulation of building 62 without PCM, with 7 mm PCM on suspended ceiling and with 7 mm thick PCM fins with the TEMPREF base case climate scenario for a 24/7 heating strategy. The first figure shows the heat stored to the total latent heat of the PCM in the PCM for a week in the season in which the PCM shows maximum use. The fin configuration shows a higher stored heat rate since the area to volume ratio is higher. The second figure shows the temperature in the building for the same week, the PCM has a mitigating effect on the temperature, with the effect at PCM fins higher than at the suspended ceiling case. The third figure show the rate of heat stored in the PCM throughout the simulated year starting from January first to December 31th.

When the 24/7 heating strategy is applied in the simulation of building 62 the impact of PCMs on the total and peak heat demand is small as indicated in Table 5.2. The PCMs in the fin configuration show a decrease in the peak heat demand of 1% and a total heat demand reduction of 2%, while the PCMs in the suspended ceiling configuration show decreases of less than 1%.

The heat demand in the mid-season and summer (between hour 2000 and 7000) is reduced by 4% as a result of the PCM in the suspended ceiling configuration and by 10% in the fin configuration, however only 10% of the heat demand is used in the mid-season, so the effect on the total heat demand is only a 1% decrease.

5.2.2. PCM simulation 31 TBM

The application of PCMs on the suspended ceiling and on PCM fins is simulated for building 31 with the climate scenario TEMPREF base case for De Bilt, with different heating strategies. The total annual heat demand and the peak heat demand are calculated for PCM use and for the reference heat strategy.

The amount of phase change material is calculated from the mid-season heat demand according to equation (4.23). The internal heat load and the solar heat load combined are about 1.0 MWh per day in the mid-season, so the latent heat to be stored in the phase change materials is set to 80% of the load: 1200kWh or 4.32GJ, which is equal to 0.1 % of the total heat demand of the building. The thickness of the PCM on the suspended ceiling used is thus:

$$L_{PCM} = \frac{Q}{\rho_{PCM} A_{PCM} \lambda_{PCM}} = \frac{4.32 * 10^9}{880 * 6.0 * 10^3 * 106 * 10^3} = 0.008m$$

The two simulated configurations have an equal amount of phase change material. The fin height used is 0.20 m and the thickness is equal to the thickness of the PCM on the suspended ceiling.

5.2.2.1. Standard heating strategy building 31

The results for the simulation of building 31 for the standard heating strategy are shown in Figure 5.4 and Table 5.3. The PCM shows only up to 20% accumulation of heat in week 18. The higher

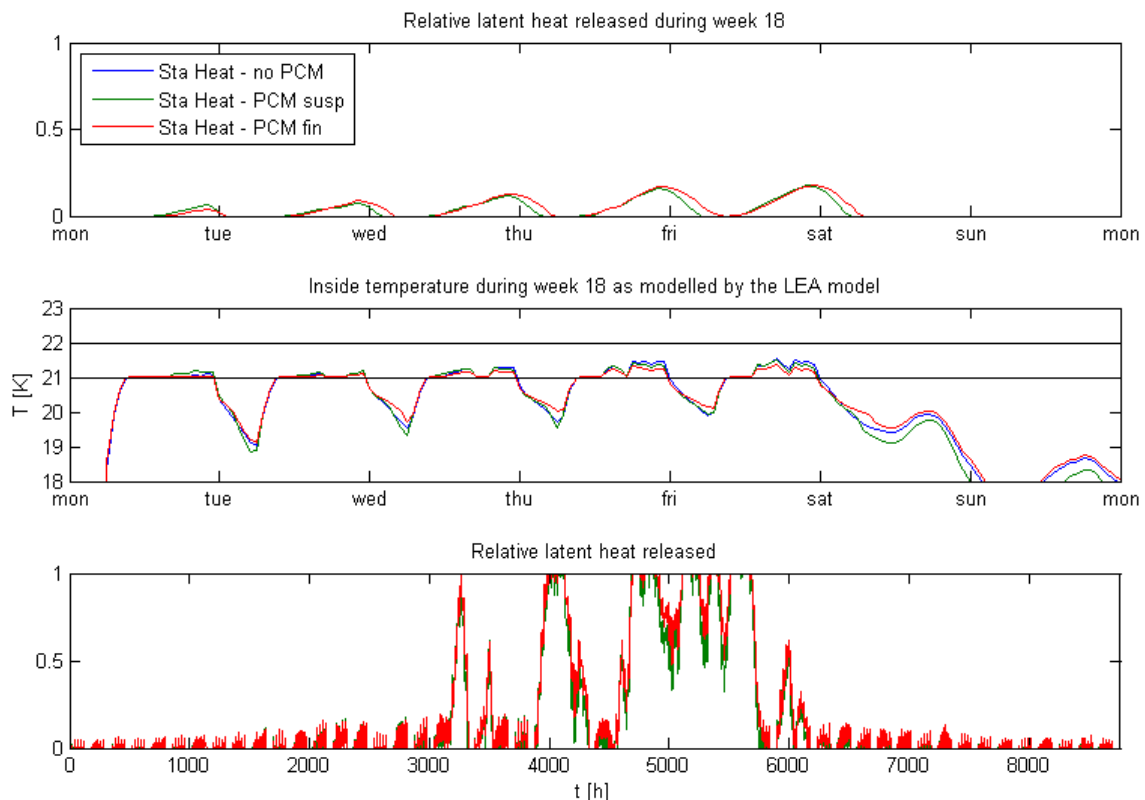


Figure 5.4 Results of simulation of building 62 without PCM, with 8 mm PCM on suspended ceiling and with 8 mm thick PCM fins with the TEMPREF base case climate scenario for a standard heating strategy. The first figure shows the heat stored to the total latent heat of the PCM in the PCM for a week in the season in which the PCM shows maximum use. The fin configuration shows a higher stored heat rate since the area to volume ratio is higher. The second figure shows the temperature in the building for the same week, the PCM has a mitigating effect on the temperature, with the effect at PCM fins higher than at the suspended ceiling case. The third figure show the rate of heat stored in the PCM throughout the simulated year starting from January first to December 31th.

ventilation rate in building 31 compared to building 62 creates a smaller increase of the temperature in the building in the mid-season. The PCM in building 31 therefore has a smaller potential compared to building 62. The temperature increase during week 18 doesn't exceed the melting temperature of the PCM, which limits the thermal storage in the PCM. The storage of heat in the phase change material only takes place at in warm summer weeks and not during the mid-season as intended.

The peak heat demand as a result of the application of PCM is reduced by 10% for the suspended ceiling configuration. This reduction of the peak is caused by the insulation effect of the PCM in front of the ceiling. The peak heat demand for the application of the PCM fins is increased by 1% as a result of the added thermal inertia of the building.

The total heat demand of the building is only slightly affected by the application of PCM. For the suspended ceiling PCM the total heat demand is reduced by 1%.

Heat demand for building 31	Peak [kW]	Total [MWh]	Total stored heat in PCM [MWh]
Standard heating no PCM	1090	850	-
Standard heating 8 mm PCM suspended ceiling	987	841	78 (37)
Standard heating 8 mm PCM fins	1100	852	80 (38)

Table 5.3 Peak and total heat demand for building 31 for one year simulated with TEMPREF base without PCM and with PCM in suspended ceiling configuration for the standard heating strategy. The amount of heat stored in the PCMs during one year and heat stored by means of phase change in parentheses.

5.2.2.2. 24/7 heating strategy building 31

When the 24/7 heating strategy is applied for building 31, the effect of the phase change material both on the suspended ceiling and in the fin configuration is limited. Both the peak and the total heat demand are decreased by maximum of 1% when the PCMs are applied. The heat demand decrease as a result of the storage in the PCM is compensated by the extra heat lost to the environment as a result of the higher internal temperature in the building.

Figure 5.5a shows the heat stored in the PCM in week 18, during this week only up to 15% of the total capacity of the PCM is used during one day. During the night up to 10% of the stored heat is transferred to the room. The temperature increase of the air in the room limits the amount of heat transferred to the phase change material.

Heat demand for building 31	Peak [kW]	Total [MWh]	Total stored heat in PCM [MWh]
24/7 heating no PCM	770	984	-
24/7 heating 7 mm PCM suspended ceiling	769	980	51 (47)
24/7 heating 7 mm PCM fins	766	974	51 (47)

Table 5.4 Peak and total heat demand for building 31 simulated with TEMPREF base without PCM and with PCM in suspended ceiling configuration for the 24/7 heating strategy. . The amount of heat stored in the PCMs during one year and heat stored by means of phase change in parentheses.

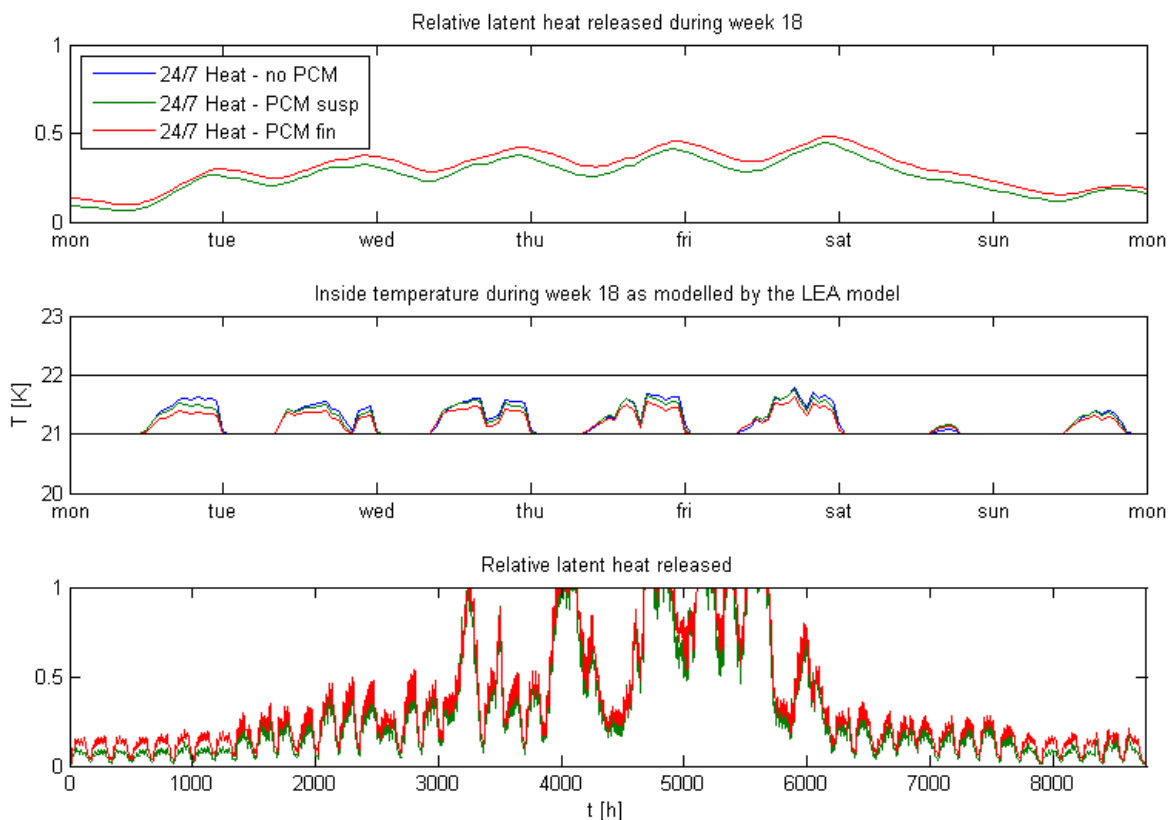


Figure 5.5 Results of simulation of building 31 without PCM, with 8 mm PCM on suspended ceiling and with 8 mm thick PCM fins with the TEMPREF base case climate scenario for a 24/7 heating strategy. The first figure shows the heat stored to the total latent heat of the PCM in the PCM for a week in the season in which the PCM shows maximum use. The fin configuration shows a higher stored heat rate since the area to volume ratio is higher. The second figure shows the temperature in the building for the same week, the PCM has a mitigating effect on the temperature, with the effect at PCM fins higher than at the suspended ceiling case. The third figure show the rate of heat stored in the PCM throughout the simulated year starting from January first to December 31th.

5.2.3. PCM simulation 30 OTB

The application of PCMs on the suspended ceiling and on PCM fins is simulated for building 62 with the climate scenario TEMPREF base case for De Bilt, with different heating strategies. The total annual heat demand and the peak heat demand are calculated for PCM use and for the reference heat strategy.

The amount of phase change material is calculated from the mid-season heat demand according to equation (4.23). The internal heat load and the solar heat load combined are about 1.7 MWh per day in the mid-season, so the latent heat to be stored in the phase change materials is set to 80% in this case 1.4 MWh or 5 GJ, which is equal to 0.1% of the total heat demand of the building. The thickness of the PCM on the suspended ceiling used is thus:

$$L_{PCM} = \frac{Q}{\rho_{PCM} A_{PCM} \lambda_{PCM}} = \frac{5 * 10^9}{880 * 7.8 * 10^3 * 106 * 10^3} = 0.007m$$

The two simulated configurations have an equal amount of phase change material. The fin height used is 0.20 m and the thickness is equal to the thickness of the PCM on the suspended ceiling.

5.2.3.1. Standard heating strategy building 30

The results for the simulation of building 30 with the phase change materials with the standard

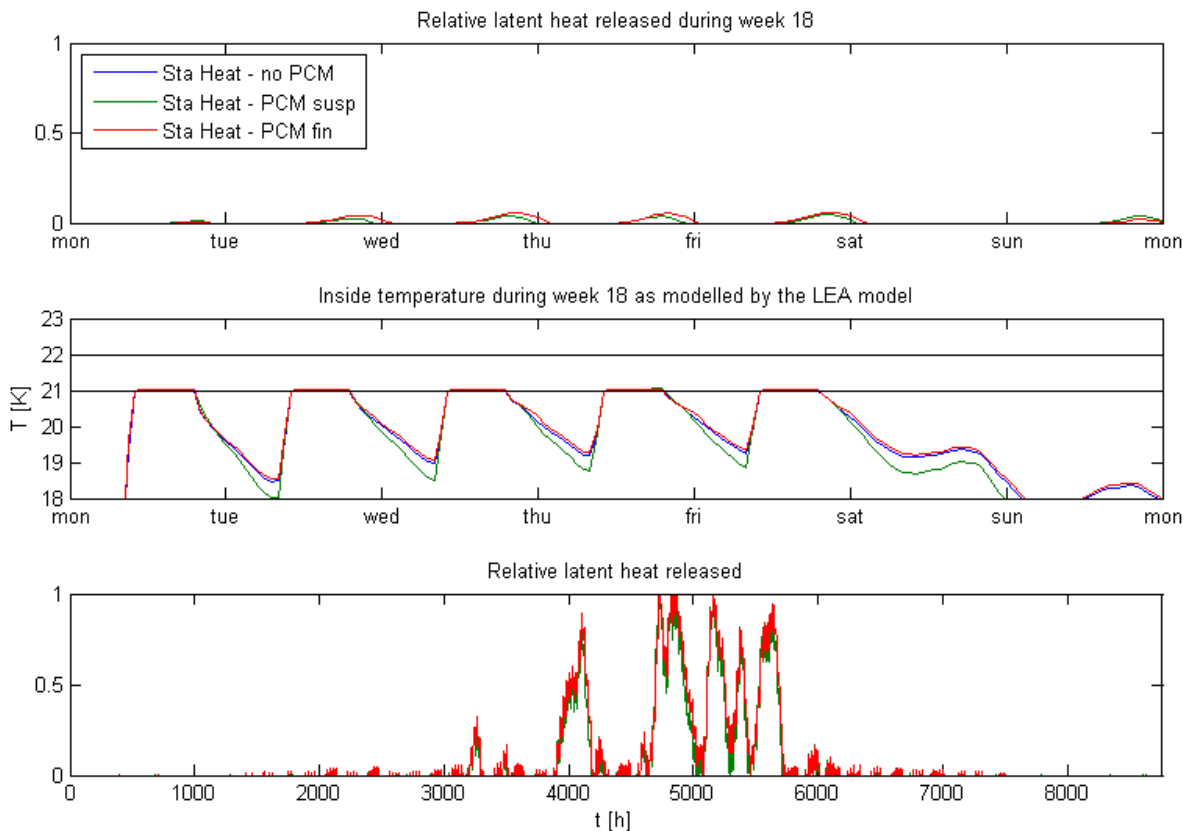


Figure 5.6 Results of simulation of building 30 without PCM, with 7 mm PCM on suspended ceiling and with 7 mm thick PCM fins with the TEMPREF base case climate scenario for a standard heating strategy. The first figure shows the heat stored to the total latent heat of the PCM in the PCM for a week in the season in which the PCM shows maximum use. The fin configuration shows a higher stored heat rate since the area to volume ratio is higher. The second figure shows the temperature in the building for the same week, the PCM has a mitigating effect on the temperature, with the effect at PCM fins higher than at the suspended ceiling case. The third figure show the rate of heat stored in the PCM throughout the simulated year starting from January first to December 31th.

heating strategy are shown in Table 5.5 and Figure 5.6. The PCMs on the suspended ceiling and the PCM fins both have a very small effect on the total heat demand. The average temperature in the building during opening hours is close to the minimum temperature and so little heat can be stored. The potential for PCMs in a building with small temperature variation is very low.

The peak heat demand will be lower when the PCM at the suspended ceiling is use due to the thermal insulation effect of the PCMs. The total heat demand for the suspended ceiling PCM is lowered by 2-3%. This small decrease doesn't compensate for the investment necessary for the phase change material.

Heat demand for building 30	Peak [kW]	Total [MWh]	Total stored heat in PCM [MWh]
Standard heating no PCM	847	515	-
Standard heating 7 mm PCM suspended ceiling	791	503	60 (16)
Standard heating 7 mm PCM fins	850	519	65 (16)

Table 5.5 Peak and total heat demand for building 30 for one year simulated with TEMPREF base without PCM and with PCM in suspended ceiling configuration for the standard heating strategy. The amount of heat stored in the PCMs during one year and heat stored by means of phase change in parentheses.

5.2.3.2. 24/7 heating strategy building 30

The results for the simulation of building 30 with the phase change materials with the standard heating strategy are shown in Table 5.6 and Figure 5.7. The effect of the application of PCMs at building 30 with a 24/7 heating strategy is very small. The peak and total heat demand are reduced by less than 1% for both configurations. The potential for PCMs in building 30 is thus very small.

Due to the high ventilation rate and the resulting low temperature in the building the heat transfer to the phase change materials is very small. As Figure 5.7c indicates the occurrences that the phase change material fully melts are very limited.

Heat demand for building 30	Peak [kW]	Total [MWh]	Total stored heat in PCM [MWh]
24/7 heating no PCM	491	633	-
24/7 heating 7 mm PCM suspended ceiling	490	631	29 (28)
24/7 heating 7 mm PCM fins	488	628	31 (30)

Table 5.6 Peak and total heat demand for building 30 for one year simulated with TEMPREF base without PCM and with PCM in suspended ceiling configuration for the 24/7 heating strategy. The amount of heat stored in the PCMs during one year and heat stored by means of phase change in parentheses.

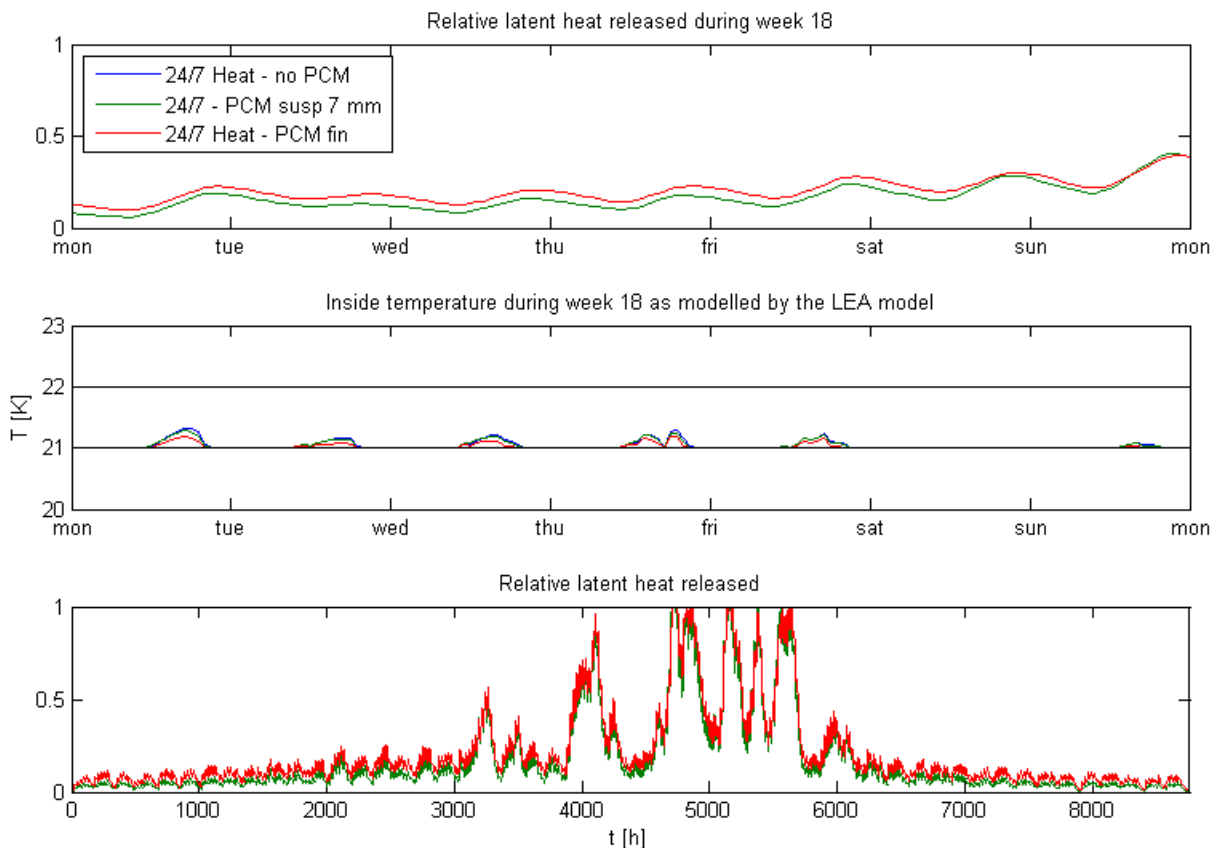


Figure 5.7 Results of simulation of building 30 without PCM, with 7 mm PCM on suspended ceiling and with 7 mm thick PCM fins with the TEMPREF base case climate scenario for a 24/7 heating strategy. The first figure shows the heat stored to the total latent heat of the PCM in the PCM for a week in the season in which the PCM shows maximum use. The fin configuration shows a higher stored heat rate since the area to volume ratio is higher. The second figure shows the temperature in the building for the same week, the PCM has a mitigating effect on the temperature, with the effect at PCM fins higher than at the suspended ceiling case. The third figure show the rate of heat stored in the PCM throughout the simulated year starting from January first to December 31th.

5.2.4. Conclusion for simulations of buildings with PCM

As a result of the application of phase change materials the heat demand in the mid-season is reduced by approximately 10%, however the annual heat demand is reduced only by 1%. Only a small decrease in total heat demand is achieved for both the standard heating and the 24/7 heating strategy. The reduction of the peak and total heat demand as a result of the application of PCM fins is listed in Table 5.7 for the 24/7 heating strategy.

When the minimum temperature in the building is not lowered outside of the opening hours of the building with the 24/7 heating strategy and the PCM fin configuration is applied the peak heat demand is reduced by 1 % and the total heat demand is reduced by 3 %. However the small change in heat demand doesn't justify the investment of the phase change materials.

Heat demand for 24/7 heating for	No PCM Peak [kW]	PCM fins Peak [kW]	No PCM Total [MWh]	PCM fins Total [MWh]
Building 62	426	422 (1%)	487	478 (2%)
Building 31	770	766 (<1%)	984	974 (1%)
Building 30	491	488 (<1%)	633	628 (<1%)

Table 5.7 Total and peak heat demand reduction for the three simulated buildings with the application of PCM fins when the 24/7 heating strategy is applied

Since the temperature in the summer doesn't drop below the melting temperature of the PCM, it remains liquid and no phase change takes place. The PCM only changes phase partially during spring and autumn. The main effects of the PCM in this configuration are the mitigated temperature in the first warm period after the winter, the lower peak temperature and the reduction of the heat demand in the start of the autumn because of the stored heat in the building.

The two main reasons the PCMs had only a minor impact on the heat demand of the building are the slow heat transfer to the PCMs and the fact that the temperature in the building does not drop below the melting temperature of the PCM. The first could be improved by achieving a higher heat transfer coefficient and the second part could be improved by using an intelligent heating strategy which optimizes the temperature and heat demand during the night.

As described in chapter 4.5.2 the application of PCM fins increased the product of the overall heat transfer coefficient and the area of heat exchange by a factor of 1.2 to 2.9. To further increase the convective heat transfer coefficient forced convection can be applied by using fans (during the night) to create extra circulation of air in the room. To which extend the heat transfer coefficient should be increased to achieve sufficient heat transfer in building 62 is described in chapter 5.3.

The effect of the different heating strategy is much larger than the effect of the application of the phase change materials as can be seen in Table 5.8. The 24/7 heating strategy results in a decrease of the peak heat demand of 40% and an increase in the total heat demand of 20% compared to the standard heating strategy.

Heat demand for	Standard Peak [kW]	24/7 Peak [kW]	Standard Total [MWh]	24/7 Total [MWh]
Building 62	738	426 (-42%)	410	487 (+19%)
Building 31	1090	770 (-29%)	850	984 (+16%)
Building 30	847	491 (-42%)	515	633 (+23%)

Table 5.8 Comparison of total and peak heat demand for the simulated buildings without the application of PCM.

Comparing the standard and the 24/7 heating strategy without the application of PCM for the three buildings shows the large potential for the application of an intelligent heating grid with an adaptive heat demand. At the cost of an increase of the total heat demand the peak heat demand could be lowered by up to 40% of its original value by just applying a simple 24/7 heating strategy. A heating strategy could be developed which optimizes the peak and total heat demand.

5.3. Increasing the convective heat transfer coefficient

For the PCM to work ok the PCM should melt and solidify every day. So conditions should be created in which the PCM is able to melt in 12 hours and to solidify in twelve hours. The heat transferred in twelve hours to the PCM should thus be equal to the latent heat of the PCM.

So the desired average heat transfer coefficient \bar{h} will be determined with an average temperature difference ΔT of 1K which would be the case if 20°C air would be used and the latent heat λ and the mass of the PCM per unit of area m/A .

$$Q = \bar{h} \Delta T t = \lambda \frac{m}{A} \quad (5.1)$$

$$\bar{h} = \frac{\lambda m}{t A \Delta T} \quad (5.2)$$

The configuration for building 62 will be calculated for the suspended ceiling and the fin configuration.

5.3.1. Heat transfer for forced flow over suspended ceiling

For the suspended ceiling configuration 6.16 kg of PCM material is used so the necessary average heat transfer coefficient is:

$$\bar{h} = \frac{1.06 * 10^5 * 6.16}{12 * 60 * 60 * 1} = 15.1 \text{ W/m}^2\text{K}$$

So the convective heat transfer coefficient should be the heat transfer coefficient minus the radiative part of the heat transfer:

$$\bar{h}_c = \bar{h} - \bar{h}_r = 15.1 - 5.2 = 9.9 \text{ W/m}^2\text{K}$$

To create forced convection at the suspended ceiling air should be blown along the suspended ceiling. The relation between the necessary air velocity and the heat transfer depends on whether the flow will be laminar or turbulent. The relations for laminar flow are described in 5.3.1.1 and the relations for turbulent flow are described in 5.3.1.2.

5.3.1.1. Laminar flow

For forced laminar flow over a flat plate for with $Pr > 0.5$ the relation for the Nusselt number is [2]:

$$Nu_x = \frac{\bar{h}_{cx} L}{k} = 0.332 Re_x^{1/2} Pr^{1/3} \quad (5.3)$$

With the length of the ceiling in the flow direction L and the thermal conductivity of air k . The Reynolds number is a function of the entering velocity of the air U_e and the kinematic viscosity of air ν . The Prandtl number is the ratio of the thermal diffusivity and the kinematic viscosity and can be calculated with the specific heat C_p , the kinematic viscosity, the density and the thermal conductivity of the air.

$$Re_L = \frac{U_e L}{\nu} \quad (5.4)$$

$$Pr = \frac{\alpha}{\nu} = \frac{C_p \nu \rho}{k} \quad (5.5)$$

To obtain the average convective heat transfer coefficient (5.6) should be evaluated to obtain a relation as in (5.7).

$$\bar{h}_c = \frac{1}{L} \int_0^L h_{cx} dx = \frac{1}{L} \int_0^L \left(\frac{k}{x}\right) 0.332 \left(\frac{U_e x}{\nu}\right)^{1/2} Pr^{1/3} dx \quad (5.6)$$

$$\bar{h}_c = 0.664 \frac{k}{L} \left(\frac{U_e L}{\nu}\right)^{1/2} Pr^{1/3} \quad (5.7)$$

So if an $\bar{h}_c = 67 \text{ W/m}^2\text{K}$ is to be obtained, the speed of the air along the horizontal ceiling the speed of the flow could be written as a function of the length of the ceiling L .

$$U_e = 2.27 \left(\frac{\bar{h}_c}{k}\right)^2 \frac{\nu}{Pr^{2/3}} L, \quad 10^3 < Re \leq 5 * 10^5 \quad (5.8)$$

If a room is evaluated with a length of the ceiling of 3 meter and using the properties of air at 20°C, the resulting necessary velocity of the air flow along the ceiling of $U_e = 25.5 \text{ m/s}$.

5.3.1.2. Turbulent flow

For this velocity and a ceiling length of 3 meter the flow will not be laminar but turbulent with a Reynolds number $2 * 10^6$. So the turbulent situation is examined. For the turbulent situation we need to consider the laminar part before the transition and the turbulent part of the flow.

$$\bar{h}_c = \frac{1}{L} \left[\int_0^{x_{tr}} h_c(\text{laminar}) dx + \int_{x_{tr}}^L h_c(\text{turbulent}) dx \right] \quad (5.9)$$

With the transition point x_{tr} of the flow calculated from the transition Reynolds Number:

$$Re_{tr} = \frac{x_{tr} U_e}{\nu} = 5 * 10^5$$

The local Nusselt number for a turbulent boundary layer can be written as:

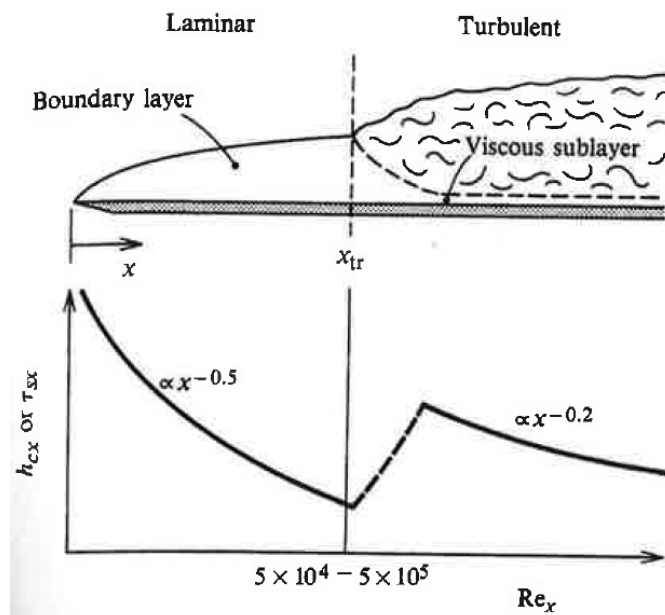


Figure 5.8 Transition from laminar to turbulent for forced convection over flat plate with the in the lower figure the local convective heat transfer coefficient as a function of the Reynolds number [2]

$$Nu_x = 0.029Re_x^{0.8}Pr^{0.43}, \quad 5 * 10^5 < Re < 10^7 \quad (5.10)$$

Combining equations (5.7), (5.9) and (5.10) give a relation for the average heat transfer coefficient for the laminar and turbulent regime is:

$$\bar{h}_c = \frac{1}{L} \left[\int_0^{x_{tr}} \left(\frac{k}{x} \right) 0.332Re^{1/2}Pr^{1/3} dx + \int_{x_{tr}}^L \left(\frac{k}{x} \right) 0.029Re_x^{0.8}Pr^{0.43} dx \right] \quad (5.11)$$

Solving the integral for the turbulent part

$$\bar{h}_{c_{tur}} = 0.036k[Re_L^{0.8} - Re_{tr}^{0.8}]Pr^{0.43} \quad (5.12)$$

Combined with the laminar part this gives:

$$\bar{h}_c = \frac{k}{L} \left[0.664Re_{tr}^{1/2}Pr^{1/3} + 0.036[Re_L^{0.8} - Re_{tr}^{0.8}]Pr^{0.43} \right] \quad (5.13)$$

So with $Re_{tr} = 5 * 10^5$ being a constant, only Re_L is a function of the velocity of the entering air U_e , so the equation can be rewritten for U_e as a function of L and \bar{h}_c .

$$U_e = \frac{\nu}{L} \left[Re_{tr}^{0.8} - \frac{0.664Re_{tr}^{1/2}Pr^{1/3} - \frac{\bar{h}_c L}{k}}{0.036Pr^{0.43}} \right]^{1.25} \quad (5.14)$$

This gives for the situation with $L = 3m$ and $\bar{h}_c = 9.9W/m^2K$ a velocity $U_e = 4.5 m/s$

A velocity of the air 2.6 m/s will result in a sufficient average heat transfer coefficient so melt all phase change material within 12 hours with a temperature difference between the air and the PCM of 1K. As a result of this velocity the average convective heat transfer coefficient will be high enough to melt all the PCM, but the local heat transfer coefficient will not be sufficient over the length of the total length of the ceiling (as indicated in Figure 5.8). With the velocity of 4.5 m/s the PCM will not melt completely where the heat transfer coefficient is lower than the average heat transfer coefficient.

5.3.2. Heat transfer for forced flow over PCM fins

To create forced convection for the PCM fin configuration a fan could be used to create forced flow along the PCM fins. If forced convection would be used for PCMs in the fin configuration in which all PCM melts and solidifies every day the heat transfer coefficient should be:

$$\bar{h} = \frac{\lambda m}{tA \Delta T} \quad (5.15)$$

For turbulent flow in ducts the relations for circular tubes can be used when the hydraulic diameter D_h is used as the diameter of the tube with the cross-sectional area A_c and the wetted perimeter.

$$D_h = 4 \frac{A_c}{P} \quad (5.16)$$

The fins are assumed to be hung over the full width of the ceiling so the width of the channel is equal to the length of the room and is assumed to be 3 m.

For fluids with a Prandtl number of order unity relations in the figure (figure 4.20 Mills) can be used to determine the rate of the average Nusselt number to the Nusselt number for fully developed flow for different entrance configurations. When a length of PCM plates would be chosen of 50 cm and a distance of 8 cm, the hydraulic diameter is $D_h \approx 0.156$ m .

For the fin configuration the flow in the channel will not be fully developed yet as a fully developed flow is achieved at 15-40 diameters of the entrance length. The effect of open end configuration on the average heat transfer coefficient depends on the duct length in hydraulic diameters. So for an open end configuration the length of the duct over the hydraulic diameter gives a ratio of $\frac{50}{15.6} \approx 3.2$, which results for a 90 ° open end in a ratio of

$$\frac{\bar{Nu}}{Nu_\infty} \approx 2.1 \quad (5.17)$$

For a smooth tube the relation for the Nusselt number is given by:

$$Nu_\infty = 0.023 Re_{D_h}^{0.8} Pr^{0.4}, \quad Re_{D_h} > 10^4 \quad (5.18)$$

So to write a function velocity of the flow along the PCM fins of the demanded heat transfer coefficient:

$$\bar{h}_c = 2.1 \left(\frac{k}{D_h} \right) \left(0.023 \left(\frac{U D_h}{\nu} \right)^{0.8} Pr^{0.4} \right) \quad (5.19)$$

Expressing the velocity necessary for sufficient heat transfer as a function of the necessary convective heat transfer coefficient and the hydraulic diameter gives:

$$U = \frac{\nu}{D_h} \left[\left(\frac{Nu_\infty}{\bar{Nu}} \right) \frac{43.5}{Pr^{0.4}} \left(\frac{\bar{h}_c D_h}{k} \right) \right]^{1.25} \quad (5.20)$$

So for the situation as listed in given in Table 4.2, the necessary heat transfer coefficient and necessary velocity can be calculated with equation (5.15) - (5.20). These are given in Table 5.9 for the situation with an average temperature difference of 1K and a heat transfer coefficient of:

$$\bar{h} = \frac{\lambda}{t} \frac{m}{\Delta T 2A_c} = \frac{1.06 * 10^5}{12 * 60 * 60 * 1} * \frac{17.6}{2} = 7.6 \text{ W/m}^2\text{K}$$

For the situation with a fin height of 20 cm or a distance between the fins of 18 centimetres the ratio between the length of the channel and the hydraulic diameter is not large enough to approach it as a duct, so the same approach is used as for the suspended ceiling case. For the fins the necessary velocities are in the laminar region.

The necessary velocities are listed in Table 5.9, as with the suspended ceiling configuration the necessary velocities will result in an uncomfortable situation in the rooms with PCM. The necessary velocities to obtain full phase change of the phase change material are between 1.3 and 5.8 m/s for the different configurations. These velocities will result in uncomfortable conditions in the rooms with phase change material fins. The comfort in the room is perceived equally by all people. Fanger and Christensen[25] established a relation for percentage of people dissatisfied by the air velocity in their neck region. The dissatisfaction is dependent on the temperature of the air. For a mean air velocity of 0.2 m/s between 10% and 30% of the people will be dissatisfied as indicated in Figure 5.9.

	Situation 1	Situation 2	Situation 3	Situation 4
h_{PCM} [m]	0.2	0.5	0.2	0.5
L_{PCM} [m]	0.02	0.02	0.02	0.02
w_{PCM} [m]	0.18	0.18	0.08	0.08
L / D_h	0.5	1.5	1.3	3.2
\bar{h}_c [W/m ² K] natural convection	2.3	1.8	2.3	1.8
\bar{h}_c [W/m ² K] forced convection	11.8	13.4	13.1	13.9
U_e [m/s]	1.8	5.8	2.2	1.3

Table 5.9 Velocities for forced convection necessary for sufficient heat transfer in PCM fin configuration

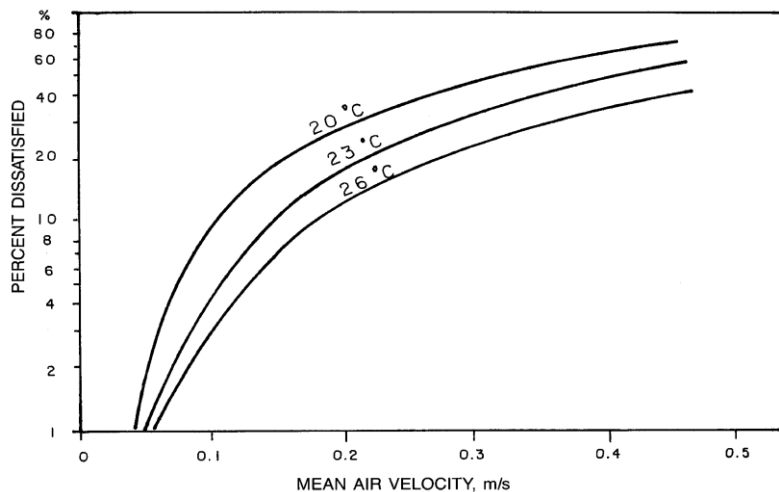


Figure 5.9 Percentage of people dissatisfied as function of mean air velocity[1]

5.4. Thin PCM

As can be seen in chapter 5.3 increasing the heat transfer coefficient results in uncomfortable air velocities in a room. Now let's look at the maximum amount of phase change material that could be used in a way that the PCM could melt every night under the right circumstances.

$$\dot{Q} = Ah \Delta T = \frac{\lambda m}{t} \quad (5.21)$$

5.4.1. Thin PCM in suspended ceiling configuration

This results in a mass of phase change material per square meter for the properties of the PCM of:

$$\frac{m}{A} = \frac{h \Delta T}{\lambda} t = \frac{8 * 1}{1.06 * 10^5} * (60 * 60 * 12) = 3.3 \text{ kg/m}^2$$

This corresponds to thickness of the PCM of 3.7 mm. A simulation is done to compare the peak and total heat demand of for the 7 mm PCM and the 3.7mm PCM at the dropped ceiling. The results of the simulation show similar results. The 3.7mm PCM stores slightly less heat than the thicker PCM, but no significant heat demand reduction is achieved by applying the thin PCMs.

5.4.2. Thin PCM in fin configuration

And for a finned PCM configuration with $h=0.20\text{m}$, the heat transfer coefficient $h = 4.9 \text{ W/m}^2\text{K}$:

$$\frac{m}{A} = \frac{h \Delta T}{\lambda} t = \frac{2 * 4.9 * 1}{1.06 * 10^5} * (60 * 60 * 12) = 4.0 \text{ kg/m}^2$$

This corresponds to thickness of the PCM of 4.5 mm. The thin fin of 5mm PCM is simulated and compared to the 7 mm PCM fin. As expected the thinner fin reduces the total heat demand of the building less than the 7 mm fin and the peak heat demand is not significantly changed due to the thinner fin.

6. Conclusions

Phase change materials as a means of diurnal thermal energy storage in a building during spring and autumn have a very small potential for the buildings at the TU Delft campus studied. The heat transfer to the phase change material is insufficient to provide significant thermal energy storage in the phase change material to overcome the extra heat lost to the environment via the facades and ventilation as a result of the higher average internal temperature.

About 90% of the heat is used in the cold winter period during which heat storage in the phase change materials is very small, since the heat transfer to the environment is larger than the heat gained from solar radiation and internal production from people, appliances and lighting. The remaining 10% of the heat is in spring and fall. The spring and fall heat demand is reduced by up to 10% as a result of the application of phase change materials, resulting in a total heat demand reduction of 1%. This total 1% reduction of the heat demand does not justify the high cost of the application of phase change materials.

The potential for the diurnal heat storage in PCM is limited by two main factors:

- A low heat transfer coefficient for heat transfer to the PCM
- The small temperature difference between day and night inside the building (enhanced by a high temperature outside the building)

Many different studies have been done to obtain correlations for heat transfer coefficients to floors and ceilings in buildings. These studies posed a large range in the results for a simple room. For more complex rooms occupied by people, furniture and ventilation equipment the heat transfer coefficients are even more uncertain. The heat transfer coefficient for heat transfer between the room air and the phase change material used in the model is thus inaccurate for the simulated buildings and can vary by more than 30% depending on the configuration used.

To increase the potential for PCMs in a building either the heat transfer coefficient, the area of the PCM or the temperature difference between the PCM and the room air need to be increased. The possibilities for an increase of the heat transfer coefficient via forced convection are limited by comfort for the occupants of the rooms. For building 62 the effect of using forced convection to increase the heat transfer coefficient is calculated. An air velocity of 2.6 m/s is required to obtain sufficient heat transfer on average along the ceiling to melt or solidify the PCM at the suspended ceiling in 12 hours with a temperature difference of 1 Kelvin. This will result in uncomfortable conditions for a building with an office or study application.

The temperature difference between the PCM and the air in the building will hardly ever be larger than 1 Kelvin in the TU Delft campus buildings, due to the large thermal mass of the building and the limited temperature fluctuations outside of the building in the Dutch climate. Buildings with a low thermal mass in a climate with larger temperature variations would increase the potential for PCM use.

Furthermore an intelligent climate control system would be necessary to maximize the heat demand reduction by the phase change material and the manual control needs to be bypassed. The use of phase change materials should be a key element in the design of such a control system to obtain maximum heat demand reduction.

In order for PCMs to work on a diurnal basis the heating control system has to be configured such that the night temperature is not much smaller than temperature during opening hours. The lowered night temperature increases the peak heat demand due to the increased sensible part of the thermal mass of the PCM, which also has to be heated when the building is heated.

7. Discussion and recommendations

7.1. The TU Delft district heating grid

The buildings at the TU Delft campus have a large thermal inertia and adding extra thermal inertia in the form of phase change materials has limited effect. If a lightweight building would have been used the effects would have been larger, but most likely still not cost-effective in the Dutch climate. In the Dutch climate the PCMs will not be effective as heat storage medium, because the number of days when both heat demand is present and when heat can be stored into the PCM is small. This is mainly due to the small temperature fluctuations of the outside temperature.

The difference in total heat demand and peak heat demand between the different heating strategies shows the potential for an intelligent thermal grid at the TU Delft campus. The large thermal inertia of the buildings creates the potential for a smart thermal grid, since heat can be stored in the building. Building simulation software should be used which uses the heat supply as an input and calculates the temperature. The LEA model turned out to be unsuited for such an approach since it uses the strict temperature bounds as an input instead of the heat supply.

An intelligent control system focussing on the heat supply could reduce the costs for the heat delivery at the TU Delft campus via optimization of the supply side. Since the building itself works as a large thermal buffer heat could be supplied to the building increasing its temperature beyond the minimum limit to shave peaks in the heat supply. The comfort temperatures for people are not as strict as suggested in the model. Also the control system of the ATES systems could be coupled to the grid control system to match the heat supply and demand on the grid. The ATES system could be used actively for peak shaving and optimization of the use of the preferred heat sources.

7.2. Future research

The heat balance in different rooms in the building will be different since the local heat production, the heat transfer with the environment and heat transfer to the building walls, floors and ceilings are not equal throughout the building. The uniformity assumed in the LEA model doesn't justify the local differences in and between the rooms. If simulations are done where the heat transfer in a building is a very important aspect, like simulation of phase change materials, modelling on a room level should be performed.

While society focuses on increasing the thermal insulation of buildings, the heat lost via the facades decreases and the part of heat demand caused by ventilation losses is increased. To further decrease heat demand a focus should be made on lowering the ventilation losses. Ventilation losses could be decreased by optimization of ventilation, increasing the heat recovery via mechanical ventilation and by research in the field of cleaning the air instead of replacement ventilation.

8. References

1. ASHRAE, *ASHRAE Fundamental Handbook* 1985.
2. Mills, A.F., *Basic Heat & Mass Transfer*. Second edition ed 1999.
3. *Energieonderzoek Centrum Nederland*.
4. Na Zhu, S.M., Shengwei Wang, *Dynamic characteristics and energy performance of buildings using phase change materials: A review*. *Energy Conversion and Management*, 2009. **50**: p. 3169-3181.
5. E. Osterman, V.V.T., V. Butala, N.A. Rahim, U. Stritih, *Review of PCM based cooling technologies for buildings*. *Energy and Buildings*, 2012. **49**: p. 37-49.
6. Dariusz Heim, J.A.C., *Numerical modelling and thermal simulation of PCM-gypsum composites with ESP-r*. *Energy and Buildings*, 2004. **36**: p. 795-805.
7. *IF Technology*. Available from: <http://www.iftechnology.nl>.
8. Smith, J.O., *Determination of the convective heat transfer coefficients from the surfaces of buildings within urban street canyons.*, 2010.
9. Jürges, W., *Der waermeuebergang an einer ebenen Wand*. *Gesundheits Ingenieur*, 1924. **19**: p. 5-52.
10. Thijs Defraeye, B.B., Jan Carmeliet, *Convective heat transfer coefficients for exterior building surfaces: Existing correlations and CFD modelling*. *Energy Conversion and Management*, 2010. **52**: p. 512-522.
11. T. Gandrille, G.P.H., C. Melo, *An Intermediate-level Model of External Convection for Building Energy Simulation*. *Energy and Buildings*, 1988. **12**: p. 53-66.
12. L. Peeters, I.B.-M., A Novoselac, *Internal convective heat transfer modeling: Critical review and discussion of experimentally derived correlations*. *Energy and Buildings*, 2011. **43**: p. 2227-2239.
13. Khalifa, A.J., *Natural convective heat transfer coefficient - a review II. Surfaces in two- and three-dimensional enclosures*. *Energy Conversion and Management*, 2001(42): p. 505-517.
14. TC Min, L.S., GV Parmelee, JD Vouris, *Natural convection and radiation in a panel-heated room*. *ASHRAE Trans.*, 1956. **62**: p. 337-358.
15. A.J. Khalifa, R.H.M., *Validation of heat transfer coefficients on interior building surfaces using a real-sized indoor test cell*. *International Journal of Heat and Mass Transfer*, 1990.
16. CIBSE, *CIBSE Guide*. Vol. A, B and C. 1986.
17. F. Alamdari, G.P.H., *Improved data correlations for buoyancy-driven convection in rooms*. *Building Services res.*, 1983. **4**: p. 49-58.
18. F.D. Heidt, H.J.S., *Steady state heat balance and surface temperature of solar radiated indoor walls*. Department of Physics, University of Siegen, FRG, , 1986.
19. Stéphane Fohanno, G.P., *Modelling of natural convective heat transfer at an internal surface*. *Energy and Buildings*, 2005. **38**: p. 548-553.
20. F. Allard, J.B., C. Inard, J.M. Pallier, *Thermal experiments of full-scale dwelling cells in artificial climatic conditions*. *Energy and Buildings*, 1987. **10**: p. 49-58.
21. Wallentén, P., *Convective heat transfer coefficients in a full-scale room with and without furniture*. *Building and Environment*, 2001. **36**: p. 743-751.
22. Parham A. Mirzaei, F.H., *Modeling of phase change materials for application in whole building simulation*. *Renewable and Sustainable Energy Reviews*, 2012. **16**: p. 5355-5362.
23. Incropera FP, D.D., Berman TL, Lavine AS, *Fundamentals of Heat and Mass Transfer (sixth edition)* 2006: Wiley.
24. *RUBITHERM® RT 21 (Phase Change Material based on n-Paraffins and Waxes)*.
25. P.O. Fanger, N.K.C., *Perception of draught in ventilated spaces*. *Ergonomics*, 1986. **29**(3): p. 215-235.

9. Appendix

9.1. Building data

9.1.1. Notes on building modelling

Properties of the TU Delft building for the model are used from building drawings and the study for measures needed for a transition to a low temperature heating system by (R. Kemperman and A.J. Nagtegaal, Deerns). However not all information was available or accurate. The building characteristics are fit to the heat demand of 2011 with the weather data of the Royal Netherlands Meteorological Institute (KNMI) in Rotterdam.

9.1.2. 30 OTB

The input for the LEA model is split in two parts: the geometry with data per façade and the general data.

9.1.2.1. Façade data

Façade	R_c	F_w	Glass U	SGF	LGF	C_f	Blinds
	m^2K/W	-	W/m^2K				
1 (floor)	3	-	-	-	-	-	-
2	2.5	0.555	1.6	0.4	0.6	0.024	Outside
3	2.5	0.034	1.6	0.4	0.6	0.024	None
4	2.5	0.463	1.6	0.4	0.6	0.024	Outside
5	2.5	0.361	1.6	0.4	0.6	0.024	None
6	2.5	0.553	1.6	0.4	0.6	0.024	Outside
7	2.5	0.034	1.6	0.4	0.6	0.024	None
8	2.5	0.456	1.6	0.4	0.6	0.024	Outside
9	2.5	0.080	1.6	0.4	0.6	0.024	None
10 (roof)	3	0.29	1.4	0.4	0.6	0.024	None
11 (roof)	3	0	-	-	-	-	-
12 (roof)	3	0	-	-	-	-	-

R_c = Conductive thermal resistance

F_w = window fraction

U = Overall heat transfer coefficient

SGF = Solar Gain Factor (in Dutch: ZTA)

LGF = Light Gain Factor (in Dutch: LTA)

C_f = Convection factor

9.1.2.2. General building data

Input variable	Value	Unit	Source/origin
Gross floor area	9326	m ²	Calculated from geometry
Net to gross area ratio	0.833	-	Standard
Gross height	4.5	m	Calculated from geometry
Net to gross height ratio	0.8	-	Standard
Building mass	250	kg/m ²	Standard
Opening hour	8		TU Delft website
Closing hour	18		TU Delft website
Number of days a week	5		TU Delft website
Persons in building	270		Energy monitor
Heat production appliances	6	W/m ² gr	Low occupation
Heat production lighting	6	W/m ² gr	Low occupation
Internal temperature min open	21	°C	Standard
Internal temperature max open	24	°C	Standard
Internal temperature min closed	16	°C	Standard
Internal temperature max closed	99	°C	No bound
Relative humidity min open	0	%	No bound
Relative humidity max open	100	%	No bound
Relative humidity min closed	0	%	No bound
Relative humidity max closed	100	%	No bound
Mechanical ventilation open	60000	m ³ /h	LT Study
Mechanical ventilation closed	0	m ³ /h	LT Study
Natural ventilation open	0	m ³ /h	LT Study
Natural ventilation closed	0	m ³ /h	LT Study
Infiltration	0.023	h ⁻¹	LT Study
Heating curve low outside	10	°C	Standard
Heating curve low inside	19	°C	Standard
Heating curve high outside	18	°C	Standard
Heating curve high inside	14	°C	Standard
AHU heat recovery present	Yes	Yes/No	LT Study
AHU heating present	Yes	Yes/No	LT Study
AHU cooling present	Yes	Yes/No	LT Study
AHU post heating present	No	Yes/No	LT Study
AHU mechanical ventilation present	Yes	Yes/No	LT Study
AHU humidification present	No	Yes/No	LT Study
AHU heat recovery efficiency	0.375	-	LT Study
Solar blinds Solar Gain Factor	0.19	-	Standard
Solar blinds Light Gain Factor	0.43	-	Standard
Solar blinds convection factor	0.05	-	Standard
Solar blinds switch on value	150	W/m ²	Standard
Solar blinds switch off value	125	W/m ²	Standard

9.1.3. 31 TBM

The input for the LEA model is split in two parts: the geometry with data per façade and the general data.

9.1.3.1. Façade data

Façade	R_c m ² K/W	F_w -	Glass U W/m ² K	SGF	LGF	C_f	Blinds
1 (floor)	1.5	-	-	-	-	-	-
2	2.5	0.050	1.6	0.4	0.6	0.024	Outside
3	2.5	0.250	1.6	0.4	0.6	0.024	Outside
4	2.5	0.250	1.6	0.4	0.6	0.024	Outside
5	2.5	0.250	1.6	0.4	0.6	0.024	Inside
6	2.5	0.200	1.6	0.4	0.6	0.024	Inside
7	2.5	0.000	1.6	0.4	0.6	0.024	Inside
8	2.5	0.250	1.6	0.4	0.6	0.024	Inside
9	2.5	0.000	1.6	0.4	0.6	0.024	Inside
10	2.5	0.250	1.6	0.4	0.6	0.024	Inside
11 (Roof)	2.5	-	-	-	-	-	-
12	2.5	0.800	1.6	0.4	0.6	0.024	Inside
13	2.5	0.800	1.6	0.4	0.6	0.024	Inside
14	2.5	0.500	1.6	0.4	0.6	0.024	Inside
15	2.5	0.250	1.6	0.4	0.6	0.024	Inside
16	2.5	0.250	1.6	0.4	0.6	0.024	Inside
17	2.5	0.000	1.6	0.4	0.6	0.024	Inside
18	2.5	0.250	1.6	0.4	0.6	0.024	Inside
19 (Roof)	4	-	-	-	-	-	-
20 (Roof)	3	-	-	-	-	-	-
21	2.5	0.250	1.6	0.4	0.6	0.024	Inside
22 (Roof)	2.5	-	-	-	-	-	-
23	2.5	0.000	1.6	0.4	0.6	0.024	Inside
24	2.5	0.000	1.6	0.4	0.6	0.024	Inside
25 (Roof)	2.5	-	-	-	-	-	-
26	2.5	0.250	1.6	0.4	0.6	0.024	Inside
27	2.5	0.250	1.6	0.4	0.6	0.024	Inside
28	2.5	0.950	1.6	0.4	0.6	0.024	Inside
29	2.5	0.250	1.6	0.4	0.6	0.024	Inside
30	2.5	0.250	1.6	0.4	0.6	0.024	Inside
31 (floor)	2.5	-	-	-	-	-	-
32 (floor)	4	-	-	-	-	-	-

R_c = Conductive thermal resistance

F_w = window fraction

U = Overall heat transfer coefficient

SGF = Solar Gain Factor (in Dutch: ZTA)

LGF = Light Gain Factor (in Dutch: LTA)

C_f = Convection factor

9.1.3.2. General building data

Input variable	Value	Unit	Source/origin
Gross floor area	12000	m ²	Calculated from geometry
Net to gross area ratio	0.8	-	Standard
Gross height	3.5	m	Calculated from geometry
Net to gross height ratio	0.8	-	Standard
Building mass	250	kg/m ²	Standard
Opening hour	7		TU Delft website
Closing hour	20		TU Delft website
Number of days a week	5		TU Delft website
Persons in building	350		Energy monitor
Heat production appliances	10	W/m ² gr	Standard
Heat production lighting	10	W/m ² gr	Standard
Internal temperature min open	21	°C	Standard
Internal temperature max open	24	°C	Standard
Internal temperature min closed	16	°C	Standard
Internal temperature max closed	99	°C	No bound
Relative humidity min open	0	%	No bound
Relative humidity max open	100	%	No bound
Relative humidity min closed	0	%	No bound
Relative humidity max closed	100	%	No bound
Mechanical ventilation open	3	h ⁻¹	LT Study
Mechanical ventilation closed	0	h ⁻¹	LT Study
Natural ventilation open	0	h ⁻¹	LT Study
Natural ventilation closed	0	h ⁻¹	LT Study
Infiltration	0.5	h ⁻¹	Standard
Heating curve low outside	10	°C	Standard
Heating curve low inside	19	°C	Standard
Heating curve high outside	18	°C	Standard
Heating curve high inside	14	°C	Standard
AHU heat recovery present	Yes	Yes/No	LT Study
AHU heating present	Yes	Yes/No	LT Study
AHU cooling present	Yes	Yes/No	LT Study
AHU post heating present	No	Yes/No	LT Study
AHU mechanical ventilation present	Yes	Yes/No	LT Study
AHU humidification present	No	Yes/No	LT Study
AHU heat recovery efficiency	0.3	-	LT Study
Solar blinds Solar Gain Factor	0.19	-	Standard
Solar blinds Light Gain Factor	0.43	-	Standard
Solar blinds convection factor	0.05	-	Standard
Solar blinds switch on value	150	W/m ²	Standard
Solar blinds switch off value	125	W/m ²	Standard

9.1.4. 62 Aerospace Engineering

The input for the LEA model is split in two parts: the geometry with data per façade and the general data.

9.1.4.1. Façade data

Façade	R_c m ² K/W	F_w	Glass U W/m ² K	SGF	LGF	C_f	Blinds
1 (floor)	3	-	-	-	-	-	-
2 (floor)	2.5	0	-	0.4	0.6	0.024	-
3	2.5	0.034	1.8	0.4	0.6	0.024	Inside
4	2.5	0.463	1.8	0.4	0.6	0.024	Inside
5	2.5	0.361	1.8	0.4	0.6	0.024	Inside
6	2.5	0.553	1.8	0.4	0.6	0.024	Inside
7 (roof)	3	0	-	-	-	-	-

R_c = Conductive thermal resistance

F_w = window fraction

U = Overall heat transfer coefficient

SGF = Solar Gain Factor (in Dutch: ZTA)

LGF = Light Gain Factor (in Dutch: LTA)

C_f = Convection factor

9.1.4.2. General building data

Input variable	Value	Unit	Source/origin
Gross floor area	9240	m ²	Calculated from geometry
Net to gross area ratio	0.8	-	Standard
Gross height	3.25	m	Calculated from geometry
Net to gross height ratio	0.8	-	Standard
Building mass	250	kg/m ²	Standard
Opening hour	7		TU Delft website
Closing hour	22		TU Delft website
Number of days a week	5		TU Delft website
Persons in building	300		Energy monitor
Heat production appliances	10	W/m ² gr	Standard
Heat production lighting	10	W/m ² gr	Standard
Internal temperature min open	21	°C	Standard
Internal temperature max open	24	°C	Standard
Internal temperature min closed	16	°C	Standard
Internal temperature max closed	28	°C	Standard
Relative humidity min open	0	%	No bound
Relative humidity max open	100	%	No bound
Relative humidity min closed	0	%	No bound
Relative humidity max closed	100	%	No bound
Mechanical ventilation open	3	h ⁻¹	LT Study
Mechanical ventilation closed	0	h ⁻¹	LT Study
Natural ventilation open	0	h ⁻¹	LT Study
Natural ventilation closed	0	h ⁻¹	LT Study
Infiltration	0.5	h ⁻¹	Standard
Heating curve low outside	10	°C	Standard
Heating curve low inside	19	°C	Standard
Heating curve high outside	18	°C	Standard
Heating curve high inside	14	°C	Standard
AHU heat recovery present	Yes	Yes/No	LT Study
AHU heating present	Yes	Yes/No	LT Study
AHU cooling present	Yes	Yes/No	LT Study
AHU post heating present	No	Yes/No	LT Study
AHU mechanical ventilation present	Yes	Yes/No	LT Study
AHU humidification present	No	Yes/No	LT Study
AHU heat recovery efficiency	0.3	-	LT Study
Solar blinds Solar Gain Factor	0.19	-	Standard
Solar blinds Light Gain Factor	0.43	-	Standard
Solar blinds convection factor	0.05	-	Standard
Solar blinds switch on value	150	W/m ²	Standard
Solar blinds switch off value	125	W/m ²	Standard